

**Base isolation system with negative stiffness for
displacement mitigation under long-period and
near-fault ground motions**

(負剛性ばねを利用した変位抑制効果を有する免震シ
ステム)

2019 年 12 月

埼玉大学大学院理工学研究科 (博士後期課程)

理工学専攻 (主指導教員 齊藤正人)

Sandhya Nepal

Base isolation system with negative stiffness for displacement mitigation under long-period and near-fault ground motions

負剛性ばねを利用した変位抑制効果を有する免震システム

A dissertation submitted in partial fulfillment of the requirements for the degree of

Doctor of Philosophy

by

Sandhya Nepal

Supervisor

Prof. Masato Saitoh



Department of Civil and Environmental Engineering

Graduate School of Science and Engineering

Saitama University

Japan

December 2019

ABSTRACT

Base isolation technique is one of the most widely accepted design philosophy for earthquake resistant design of both the large-scale structures and small-scale structures such as sensitive instruments, cultural assets, furniture, and art monuments. Base isolation detaches the structures/objects to impede the seismic wave propagation from the ground or floor on which they are supported. However, the long-period ground motion anticipated from the near-fault ground motion greatly influence the conventional base isolation systems. Such long-period ground motion has the intensity to resonant the base-isolated object with a long fundamental natural period, generating the large lateral displacement which might cause catastrophic damage to the isolated object due to damage in the components of the base isolation system. Conventional base isolation systems are effective mainly for earthquakes with the high-frequency components. Only a few studies of the earthquakes with the long-period components can be found but even in these earthquakes, the frequency range of long-period component is limited to 2-3 s as compared to earthquakes anticipated in Japan with fundamental period 5-10 s. Mitigating the displacement due to both the near-fault and the long-period ground motions is important from a seismic resistant design point of view. Very few studies have done for the displacement mitigation of the isolated objects subjected to both types of earthquake excitations. Those studies show the presence of the residual displacement due to use of friction device to control displacement. There have been no reported studies on the development of an elastic linear system for displacement mitigation, which is necessary for seismic-resistant design due to both types of ground motions. In these recent years, use

of negative stiffness and variable stiffness for base isolation have been increased rapidly. Despite, till date, the performance of negative stiffness with variable stiffness is unknown. This study mainly focuses on displacement mitigation of base-isolated objects or the target objects such as sensitive instruments, critical computer servers, and furniture. Thus, the objectives of this study have been: (1) to study the performance of isolation systems with variable negative stiffness, (2) to develop new device comprising a unit of negative and positive springs (NP unit) arranged in series for displacement mitigation of conventional base isolation system for both near-fault and long-period ground motions simultaneously, and (3) to verify the performance of the proposed model when subjected to observed and simulated earthquake.

In this study first, a comparative study is performed to determine the performance of base isolation systems with variable negative stiffness. For this negative stiffness is varied parametrically using different functions in terms of the displacement response of the isolated objects. To study the performance of base-isolated objects subjected to near-fault and long-period ground motions, equations of motions are constructed. The numerical studies show that varying the stiffness with high-order power, elliptical and exponential functions, effectively mitigate the displacement response. However, with an increase in the order of the power function acceleration response subjected to near-fault ground motion increase appreciably. An optimal order of power function satisfying the allowable limits of both the displacement and acceleration responses in practical use is proposed.

From a practical viewpoint, varying negative stiffness is complicated in comparison with varying positive stiffness because negative stiffness itself is unstable so, stability should also be taken into account. Therefore, a system with varying positive stiffness satisfying the performance of varying negative stiffness with the optimal order of power function is proposed which is also useful for retrofitting of the existing conventional base isolation

system.

An external device using NP unit is proposed to fulfill the second objective. This device consists of NP unit arranged in parallel with positive spring and a damper. The positive stiffness of the NP unit is varied linearly in term of displacement response of the base isolated object. The performance of the proposed model is investigated by comparing it with the conventional base isolation model.

Time history analysis is performed by numerical integration using Newmark's method to verify the performance of the proposed systems. Kobe NS 1995, Ojiya EW 2004, Shin-Tokai EW, and Tomakomai EW 2003 earthquakes are used for applying ground acceleration \ddot{u}_g to the systems. Through the numerical analysis, this study verifies the improvement in the performance of base isolation system by using negative-positive springs unit with variable stiffness. The results show that the proposed device markedly reduces the lateral displacement response of the system against both near-fault and long-period ground motions. The proposed model, exhibits a significant decrease in relative displacement of the object with respect to the base for both types of earthquake excitations. An optimal range of damping values and slope, satisfying the allowable limits of both the displacement and acceleration responses when subjected to near-fault and long-period for practical use is proposed.

For realization of the system, first the variable positive spring of NP unit is to be realized practically. Hence, in this study, approximation of negative-positive stiffness in practical has been discussed using discontinuous stiffness-displacement (K-D) relationship. From the numerical analysis, this study verifies that both the acceleration and displacement responses can be limit to allowable ranges using discontinuous K-D relationship.

ACKNOWLEDGEMENTS

Firstly, I would like to express my deep gratitude to my advisor, Prof. Masato Saitoh for his valuable guidance, patience and encouragement throughout this study. Without his enthusiastic support, suggestions and critical comments this study would not have been possible to finish.

Besides my advisor, I would like to thank the rest of my doctoral co-supervisor and examination committee Prof. Takeshi Maki, Prof. Yasunao Matsumoto, Assoc. Prof. Hidenori Mogi, and Assoc. Prof. Taro Uchimura for their encouragement and the critical comments which motivated me to widen my research from various perspectives.

I am thankful to Assistant Professor Chandra Shekhar Goit for his help and suggestions to improve my dissertation.

I would like to thank the Government of Japan for providing Monbukagakusho scholarship to pursue the degree of Ph.D. at Saitama University.

I would also like to thank all the members of Earthquake Disaster Prevention and Mitigation Laboratory for their support. I would also like to thank all my friends who supported me in writing and providing strong incentive to strive towards my goal.

I am immensely grateful to my parents and other family members for their support and encouragement throughout this study. Your prayer for me was what sustained me thus far.

Finally, my special thanks to my beloved husband Gyanendra for his eternal support, encouragement, and understanding throughout this study. It was impossible to implement this endeavor without his unfailing support, patience and good humor. I dedicate this dissertation to my parents and my husband.

For my parents and my husband

SUMMARY OF CONTENTS

| CHAPTER | TITLE | PAGE |
|---------|---|------|
| 1 | INTRODUCTION | 1-1 |
| 2 | BASE ISOLATION SYSTEM WITH VARIABLE NEGATIVE STIFFNESS | 2-1 |
| 3 | BASE ISOLATION SYSTEM WITH NEGATIVE- VARIABLE POSITIVE MECHANICAL UNIT | 3-1 |
| 4 | APPROXIMATION OF NEGATIVE-POSITIVE VARIABLE STIFFNESS IN PRATICE | 4-1 |
| 5 | CONCLUSIONS AND RECOMMENDATIONS FOR FUTURE RESEARCH | 5-1 |
| | REFERENCES | R-1 |

TABLE OF CONTENTS

| | |
|--|--------------|
| ABSTRACT | v |
| ACKNOWLEDGEMENTS..... | ix |
| SUMMARY OF CONTENTS | xiii |
| TABLE OF CONTENTS | xv |
| LIST OF FIGURES..... | xix |
| LIST OF TABLES..... | xxvii |
| LIST OF NOTATIONS..... | xxix |
| CHAPTER 1 INTRODUCTION | 1-1 |
| 1.1 Background..... | 1-1 |
| 1.2 Approach to overcome issue associated with near-fault ground motions | 1-4 |
| 1.3 Approach to overcome issue associated with long-period ground motions | 1-6 |
| 1.4 Approach to overcome issue associated with both types of ground excitations..... | 1-6 |
| 1.5 Research objective..... | 1-7 |
| 1.6 Thesis organization..... | 1-8 |
| CHAPTER 2 BASE ISOLATION SYSTEM WITH VARIABLE NEGATIVE STIFFNESS | 2-1 |
| 2.1 Background and objectives | 2-1 |
| 2.2 Base isolations models..... | 2-2 |
| 2.2.1 Conventional base isolation model..... | 2-2 |
| 2.2.2 Proposed model | 2-3 |
| 2.2.2.1 Power functions..... | 2-4 |

| | |
|--|------|
| 2.2.2.2 Elliptical function..... | 2-4 |
| 2.2.2.3 Exponential function | 2-5 |
| 2.2.3 Fundamental parameters of proposed systems..... | 2-5 |
| 2.3 Ground motions | 2-8 |
| 2.3.1 Near-fault ground motions | 2-8 |
| 2.3.2 Long-period ground motions | 2-8 |
| 2.4 Effectiveness of parameter T_{to} , κ , h_t , Δk , and α | 2-9 |
| 2.5 Numerical Simulation | 2-23 |
| 2.5.1 Time history responses due to near-fault ground motion | 2-26 |
| 2.5.2 Time history responses due to long period ground motion | 2-31 |
| 2.6 Discussion..... | 2-36 |
| 2.7 Conclusions | 2-37 |

CHAPTER 3 BASE ISOLATION SYSTEM WITH NEGATIVE-VARIABLE

| | |
|--|------------|
| POSITIVE MECHANICAL UNIT | 3-1 |
| 3.1 Background and objectives..... | 3-1 |
| 3.2 Negative-positive spring systems | 3-2 |
| 3.2.1 Stiffness variation of Negative-positive spring unit..... | 3-2 |
| 3.2.2 Configuration of base isolation systems with a negative-positive spring unit.. | 3-4 |
| 3.3 Base isolation models..... | 3-5 |
| 3.3.1 Conventional base isolation model..... | 3-5 |
| 3.3.2 Proposed Models | 3-6 |
| 3.4 Basic properties, parameters and principle of isolation system with proposed external device | 3-8 |
| 3.4.1 Fundamental parameters of proposed systems..... | 3-8 |
| 3.4.2 Functioning and principle for production of proposed device | 3-10 |

| | |
|---|------------|
| 3.4.3 Input motions and model properties | 3-12 |
| 3.4.4 Effectiveness of parameter α_0 , h_t and κ | 3-13 |
| 3.5 Numerical analysis and results..... | 3-21 |
| 3.5.1 Time history responses subjected to near-fault ground motion..... | 3-21 |
| 3.5.2 Time history responses subjected to long-period ground motion..... | 3-24 |
| 3.5.3 Time history responses for different earthquake ground motions..... | 3-30 |
| 3.5.4 Response spectra of proposed model for general ground motions | 3-31 |
| 3.6 Discussion..... | 3-34 |
| 3.6.1 Setting up of natural period of the system with proposed device..... | 3-35 |
| 3.6.2 Discussion on the significant change in the total stiffness of the system | 3-36 |
| 3.6.3 Comparison of Model I with variable negative stiffness system | 3-37 |
| 3.7 Conclusions..... | 3-43 |
| CHAPTER 4 APPROXIMATION OF NEGATIVE-POSITIVE VARIABLE | |
| STIFFNESS IN PRACTICE | 4-1 |
| 4.1 Approximation of the system using step function for varying stiffness..... | 4-1 |
| 4.1.1 Numerical Analysis and Result | 4-3 |
| 4.1.2 Practical Implementations | 4-13 |
| CHAPTER 5 CONCLUSIONS AND RECOMMENDATIONS FOR FUTURE | |
| RESEARCH | 5-1 |
| 5.1 General conclusions | 5-2 |
| 5.2 Recommendations for future research..... | 5-4 |
| REFERENCES | R-1 |

LIST OF FIGURES

| | |
|---|------|
| Fig. 1-1: Floating roofs sunk during Tokachi-oki earthquake (http://nrifd.fdma.go.jp/english/research/protect_oiltanks/02/index.html)..... | 1-3 |
| Fig. 2-1: Models of base isolation systems: (a) Conventional base isolation system; (b) Proposed Model..... | 2-3 |
| Fig. 2-2: Time histories of the earthquake waves used for time history analyses: (a) Kobe NS 1995, (b) Ojiya EW 2004, (c) Shin-Tokai EW, and (d) Tomakomai EW 2003 . | 2-6 |
| Fig. 2-3: (a) Displacement response spectra, (b) Acceleration response spectra, and (c) velocity response spectra for both types of earthquake ground motions | 2-7 |
| Fig. 2-4: Maximum amplitudes of the response of the relative displacement for the proposed model using Eq. (2.5) for stiffness variation (a) $T_{to} = 1.789$ s, (b) $T_{to} = 2.828$ s, and (c) $T_{to} = 3.328$ s. | 2-10 |
| Fig. 2-5: Maximum amplitudes of the response of the absolute acceleration for the proposed model using Eq. (2.5) for stiffness variation (a) $T_{to} = 1.789$ s, (b) $T_{to} = 2.828$ s, and (c) $T_{to} = 3.328$ s. | 2-11 |
| Fig. 2-6: Maximum amplitudes of the response of relative displacement for the proposed model using Eq. (2.6) for stiffness variation (a) $T_{to} = 1.789$ s, (b) $T_{to} = 2.828$ s, and (c) $T_{to} = 3.328$ s..... | 2-12 |
| Fig. 2-7: Maximum amplitudes of the response of absolute acceleration for the proposed model using Eq. (2.6) for stiffness variation (a) $T_{to} = 1.789$ s, (b) $T_{to} = 2.828$ s, and (c) $T_{to} = 3.328$ s..... | 2-13 |
| Fig. 2-8: Maximum amplitudes of the response of relative displacement for the proposed model using Eq. (2.6) for stiffness variation (a) $T_{to} = 1.789$ s, (b) $T_{to} = 2.828$ s, and | |

(c) $T_{tO} = 3.328$ s. 2-14

Fig. 2-9: Maximum amplitudes of the response of absolute acceleration for the proposed model using Eq. (2.7) for stiffness variation (a) $T_{tO} = 1.789$ s, (b) $T_{tO} = 2.828$ s, and (c) $T_{tO} = 3.328$ s. 2-15

Fig. 2-10: Maximum amplitudes of the response of relative displacement for the proposed system using Eq. (2.5) for varying stiffness (a) total damping ratio $h_t = 5\%$, (b) total damping ratio $h_t = 10\%$, (c) total damping ratio $h_t = 15\%$ 2-16

Fig. 2-11: Maximum amplitudes of the response of absolute acceleration for the proposed system using Eq. (2.5) for varying stiffness (a) total damping ratio $h_t = 5\%$, (b) total damping ratio $h_t = 10\%$, (c) total damping ratio $h_t = 15\%$ 2-17

Fig. 2-12: Maximum amplitudes of the response of relative displacement for the proposed system using Eq. (2.6) for varying stiffness (a) total damping ratio $h_t = 5\%$, (b) total damping ratio $h_t = 10\%$, (c) total damping ratio $h_t = 15\%$ 2-19

Fig. 2-13: Maximum amplitudes of the response of absolute acceleration for the proposed system using Eq. (2.6) for varying stiffness (a) total damping ratio $h_t = 5\%$, (b) total damping ratio $h_t = 10\%$, (c) total damping ratio $h_t = 15\%$ 2-20

Fig. 2-14: Maximum amplitudes of the response of relative displacement for the proposed system using Eq. (2.7) for varying stiffness (a) total damping ratio $h_t = 5\%$, (b) total damping ratio $h_t = 10\%$, (c) total damping ratio $h_t = 15\%$ 2-21

Fig. 2-15: Maximum amplitudes of the response of absolute acceleration for the proposed system using Eq. (2.7) for varying stiffness (a) total damping ratio $h_t = 5\%$, (b) total damping ratio $h_t = 10\%$, (c) total damping ratio $h_t = 15\%$ 2-22

Fig. 2-16: Time history response comparison between the conventional base isolation and the proposed systems excited by Kobe for varying negative stiffness: (a) relative displacement (b) absolute acceleration..... 2-24

Fig. 2-17: Time history response comparison between the conventional base isolation and the proposed systems excited by Ojiya for varying negative stiffness: (a) relative displacement (b) absolute acceleration 2-25

Fig. 2-18: Relationship between (a) total stiffness, (b) negative stiffness, and (c) period of the system with relative displacement for different variation of negative stiffness excited by Kobe. 2-28

Fig. 2-19: Relationship between (a) total stiffness, (b) negative stiffness, and (c) period of the system with relative displacement for different variation of negative stiffness excited by Ojiya. 2-29

Fig. 2-20: Relationship between (a) relative displacement, (b) absolute acceleration of the system for different variation of negative stiffness compared with conventional (conv.) base isolation excited by both near-fault and long-period ground motions. 2-30

Fig. 2-21: Time history response comparison between the conventional base isolation and the proposed systems excited by Shin-Tokai for varying negative stiffness: (a) relative displacement (b) absolute acceleration 2-32

Fig. 2-22: Time history response comparison between the conventional base isolation and the proposed systems excited by Tomakomai for varying negative stiffness: (a) relative displacement (b) absolute acceleration 2-33

Fig. 2-23: Relationship between (a) total stiffness, (b) negative stiffness, and (c) period of the system with relative displacement for different variation of negative stiffness excited by Shin-Tokai. 2-34

Fig. 2-24: Relationship between (a) total stiffness, (b) negative stiffness, and (c) period of the system with relative displacement for different variation of negative stiffness excited by Tomakomai. 2-35

Fig. 3-1: Negative-Positive spring unit (NP unit). 3-3

Fig. 3-2: Relationship between stiffness of NP unit and parameter α 3-3

Fig. 3-3: Models of base isolation systems: (a) Conventional base isolation system; (b) Model I. 3-4

Fig. 3-4: Relationship between transmitting force due to proposed external device $F_n - p - a$ and displacement of an isolated object compared with and without varying

| | |
|---|------|
| stiffness..... | 3-11 |
| Fig. 3-5: Potential energy function of the proposed external device..... | 3-12 |
| Fig. 3-6: (a) Maximum absolute acceleration (b) Maximum relative displacement and (c) Node displacement for various α_0 when $\dot{h} = 15\%$ | 3-14 |
| Fig. 3-7: Maximum amplitudes of the response of relative displacement for Model I (a) total damping ratio $\dot{h} = 5\%$, (b) total damping ratio $\dot{h} = 10\%$, (c) total damping ratio $\dot{h} = 15\%$ | 3-15 |
| Fig. 3-8: Maximum amplitudes of the response of absolute acceleration of Model I (a) total damping ratio $\dot{h} = 5\%$, (b) total damping ratio $\dot{h} = 10\%$, (c) total damping ratio $\dot{h} = 15\%$ | 3-16 |
| Fig. 3-9: Potential energy function of the proposed system various κ values when excited by Oijya..... | 3-17 |
| Fig. 3-10: Maximum amplitudes of (a) relative displacement and (b) absolute acceleration responses for Model II for various κ | 3-18 |
| Fig. 3-11: Comparison of time history responses of (a) relative displacements and (b) response accelerations between the conventional base isolation system and the proposed models excited by Kobe NS 1995..... | 3-19 |
| Fig. 3-12: Relationship between (a) restoring force by mass of isolated object, (b) period of the proposed device, (c) period of the system and (d) damping ratio of the system with relative displacement for Model I, Model II and Model III excited by Kobe. 3-20 | |
| Fig. 3-13: Comparison of time history responses of (a) relative displacements and (b) response accelerations between the conventional base isolation system and the proposed models excited by Ojiya EW 2004..... | 3-22 |
| Fig. 3-14: Relationship between (a) restoring force by mass of isolated object, (b) period of the proposed device, (c) period of the system and (d) damping ratio of the system with relative displacement for Model I, Model II and Model III excited by Ojiya 3-23 | |
| Fig. 3-15: Comparison of time history responses of (a) relative displacements and (b) response accelerations between the conventional base isolation system and the | |

| | |
|---|------|
| proposed models excited by Shin-Tokai EW..... | 3-25 |
| Fig. 3-16: Relationship between (a) restoring force by mass of isolated object, (b) period of the proposed device, (c) period of the system and (d) damping ratio of the system with relative displacement for Model I, Model II and Model III excited by Shin-Tokai. | 3-26 |
| Fig. 3-17: Comparison of time history responses of (a) relative displacements and (b) response accelerations between the conventional base isolation system and the proposed models excited by Tomakomai EW 2003. | 3-27 |
| Fig. 3-18: Relationship between (a) restoring force by mass of isolated object, (b) period of the proposed device, (c) period of the system and (d) damping ratio of the system with relative displacement for Model I, Model II and Model III excited by Tomakomai..... | 3-28 |
| Fig. 3-19: (a) Relative displacement response, (b) Absolute acceleration response for Kobe, Ojiya, Shin-Tokai, and Tomakomai earthquake excitations..... | 3-29 |
| Fig. 3-20: Maximum amplitudes of (a) response of relative displacement, and (b) response of absolute acceleration of the conventional base isolation system (Conv.) and proposed models..... | 3-30 |
| Fig. 3-21: Displacement, velocity and acceleration response spectra of Model I, Model III and Conventional (Conv.) base isolation systems using (a) Type-A, (b) Type-B and (c) Type-C pulse. | 3-33 |
| Fig. 3-22: Maximum amplitudes of (a) response of relative displacement, and (b) response of absolute acceleration of the conventional base isolation system (Conv.) and proposed models..... | 3-34 |
| Fig. 3-23: Relationship between (a) total stiffness, (b) negative stiffness, and (c) period of the system with relative displacement Model I and variable negative stiffness system with power function ($u^{1.5}$) when excited by Kobe. | 3-39 |
| Fig. 3-24: Relationship between (a) total stiffness, (b) negative stiffness, and (c) period of the system with relative displacement Model I and variable negative stiffness system with power function ($u^{1.5}$) when excited by Ojiya. | 3-40 |
| Fig. 3-25: Relationship between (a) total stiffness, (b) negative stiffness, and (c) period of | |

| | |
|---|------|
| the system with relative displacement Model I and variable negative stiffness system with power function ($u^{1.5}$) when excited by Shin-Tokai..... | 3-41 |
| Fig. 3-26: Relationship between (a) total stiffness, (b) negative stiffness, and (c) period of the system with relative displacement Model I and variable negative stiffness system with power function ($u^{1.5}$) when excited by Tomakomai. | 3-42 |
| Fig. 4-1: Stiffness-displacement relationship..... | 4-2 |
| Fig. 4-2: Relationship between (a) positive stiffness, (b) total stiffness of the system, (c) total period of the system and (d) restoring force by mass of the isolated object with relative displacement for Model I, Model with Step function variation of stiffness using two springs excited by Kobe..... | 4-4 |
| Fig. 4-3: Relationship between a) positive stiffness, (b) total stiffness of the system, (c) total period of the system and (d) restoring force by mass of the isolated object with relative displacement for Model I, Model with Step function variation of stiffness using two springs excited by Ojiya. | 4-5 |
| Fig. 4-4: Relationship between a) positive stiffness, (b) total stiffness of the system, (c) total period of the system and (d) restoring force by mass of the isolated object with relative displacement for Model I, Model with Step function variation of stiffness using two springs excited by Shin-Tokai | 4-6 |
| Fig. 4-5: Relationship between (a) positive stiffness, (b) total stiffness of the system, (c) total period of the system and (d) restoring force by mass of the isolated object with relative displacement for Model I, Model with Step function variation of stiffness using two springs excited by Tomakomai | 4-7 |
| Fig. 4-6: Relationship between (a) positive stiffness, (b) total stiffness of the system, (c) total period of the system and (d) restoring force by mass of the isolated object with relative displacement for Model I, Model with Step function variation of stiffness using three springs excited by Kobe..... | 4-9 |
| Fig. 4-7: Relationship between (a) positive stiffness, (b) total stiffness of the system, (c) total period of the system and (d) restoring force by mass of the isolated object with relative displacement for Model I, Model with Step function variation of stiffness using three springs excited by Ojiya. | 4-10 |
| Fig. 4-8: Relationship between (a) positive stiffness, (b) total stiffness of the system, (c) | |

total period of the system and **(d)** restoring force by mass of the isolated object with relative displacement for Model I, Model with Step function variation of stiffness using three springs excited by Shin-Tokai 4-11

Fig. 4-9: Relationship between **(a)** positive stiffness, **(b)** total stiffness of the system, **(c)** total period of the system and **(d)** restoring force by mass of the isolated object with relative displacement for Model I, Model with Step function variation of stiffness using three springs excited by Tomakomai..... 4-12

LIST OF TABLES

| | |
|--|------|
| Table 2-1: Maximum amplitude of responses for all cases | 2-27 |
| Table 3-1 Maximum amplitudes of displacement and acceleration responses of base isolation systems (Conv., Model I and Model with variable negative stiffness) | 3-38 |
| Table 4-1 Comparison of relative displacement and absolute acceleration of base isolation systems (Model I (smooth line K-D curve) and isolation system with a discontinuous K-D curve) using two springs and conventional base isolation system | 4-2 |
| Table 4-2 Comparison of relative displacement and absolute acceleration of base isolation systems (Model I (smooth line K-D curve) and isolation system with a discontinuous K-D curve) using three springs and conventional base isolation system..... | 4-8 |

LIST OF NOTATIONS

Chapter 2

| | |
|------------|--|
| a | parameter for variation of negative stiffness |
| c | damping coefficient of conventional isolation system |
| c_s | damping coefficient of spring/damper unit |
| c_t | critical damping coefficient of the system |
| h_s | damping constant of spring/damper unit |
| h | damping constant of conventional isolation system |
| h_t | total damping constant of base isolation system |
| k_s | spring coefficient of a spring/damper unit |
| k | stiffness of conventional isolation system |
| k_n | stiffness of negative spring |
| k_{no} | initial stiffness of negative spring |
| k_t | total stiffness of the system |
| κ | slope for changing k_n |
| Δk | change in stiffness of negative stiffness |

| | |
|--------------|--|
| m_s | mass of base-isolated object |
| T_i | natural period of the proposed system |
| u | displacement response of base-isolated object with respect to base |
| \ddot{u}_g | ground acceleration |
| u_{\max} | maximum allowable displacement |
| ω | natural circular frequency of conventional isolation system |
| ω_s | natural circular frequency of spring/damper unit |
| ω_n | natural circular frequency of negative spring |

Chapter 3

| | |
|----------|--|
| α | parameter defining value of positive spring of NP unit |
| c_a | damping coefficient of additional spring/damper unit |
| c_s | damping coefficient of conventional isolation system |
| f_s | natural frequency of conventional isolation system |
| h_s | damping constant of conventional isolation system |
| h_t | total damping constant of base isolation system |
| k_a | stiffness of additional spring/damper unit |
| k_n | stiffness of negative spring of NP unit |
| k_s | stiffness of conventional isolation system |

| | |
|------------------|--|
| k_{n-p-a} | combine stiffness of NP unit with additional spring |
| k_p | stiffness of positive spring of NP unit |
| k_t | total stiffness of the system |
| k^* | total stiffness of NP unit |
| κ | slope for changing α |
| m_s | mass of base-isolated object |
| P | restoring force of the system |
| T_n | fundamental period of negative spring |
| T_{n-p-a} | fundamental period of the proposed device |
| T_{n-p} | fundamental period of the NP unit |
| T_t | natural period of the system |
| u | displacement response of base-isolated object with respect to base |
| \ddot{u}_g | ground acceleration |
| U_s | potential energy of the proposed system |
| ω_s | natural circular frequency of conventional isolation system |
| ω_a | natural circular frequency of additional spring |
| ω_n | natural circular frequency of negative spring |
| ω_{n-p-a} | natural circular frequency of the proposed device |

CHAPTER 1

INTRODUCTION

1.1 Background

The fixed base structures or objects are vulnerable to the ground movement produced by a strong earthquake. For the seismic resistance design, inventors and engineers proposed the concept known as base isolation or seismic isolation. Base isolation is one of the most widely accepted seismic protection system in earthquake susceptible areas. It is the separation of the objects from damaging effects of a seismic wave propagating from ground or floor on which they are supported. During the last few decades, various kind of base isolation systems have been proposed and applied in practice are summarized by Kelly [1] and Buckle and Mayes [2]. Sliding bearing [3–5] and laminated rubber bearings such as natural rubber bearing, lead rubber bearing [6, 7] and high damping rubber bearing is often used in the base isolated system.

From the past research it has been found that these bearings can significantly reduce the acceleration response of the base isolated objects at the expense of large lateral displacement of bearings for near-fault ground motion due to their low stiffness [8, 9]. On the other hand, due to such large lateral displacement large clearance must be provided around the base isolated objects, and this might be difficult if spaces are limited. It was also noted that the bearing displacement decreases with increase in the damping and there exist a certain value of damping where the acceleration of base-isolated objects can be minimized. In reality, the approach to reduce the relative displacement by increasing

damping, in turn, will result in a higher level of acceleration. This clashing interest in controlling increasing acceleration with an acceptable range of displacement, in essence, defines the limiting range of the effectiveness of seismic isolation systems.

Many researchers have conducted many research and studies for controlling the large lateral displacement of the bearing. Many studies were conducted for optimizing the appropriate parameters of bearings/dampers to reduce the bearing displacement [10–13]. Jangid [10, 11] perform a study for optimizing the parameters of friction pendulum system and lead-rubber isolation bearing to reduce the displacement of the bearing. It was found that friction pendulum system/lead-rubber bearing with the low friction coefficient/bearing yield strength produce a significantly large displacement in contrast with increasing the friction coefficient/bearing yield strength, the displacement reduced remarkably without considerably change in acceleration. Further, variable curvature had been used by many researchers for seismic isolation of near-fault ground motions [14, 15]. Studies had shown that the displacement and the acceleration responses may be amplified remarkably when a structure was isolated by a conventional FPS subjected to a ground motion with near-fault characteristics, due to the long-period pulse-like wave component possessed in most near-fault earthquakes. By varying the curvature of the sliding surface, it was expected that the isolation frequency will changes with the isolator displacement, so the resonant behavior exerted by the isolation frequency can be mitigated. The conventional base isolation systems are mainly effective for ground motions including mainly high-frequency components. Hence, many researchers are limited mainly to the near-fault ground motions.

Recently, earthquake waves with long-period components had been focused because of its intensity to resonant base isolated objects [16, 17]. In the aftermath of Tohoku earthquake in 2011, it was reported that long-period ground motions were induced in Tokyo, Nagoya,

and Osaka and had caused damage to non-structural elements. These cities are located near deep layers of sediment and such conditions can create long period ground motions of low frequency even when far from the epicenter of an earthquake. During 2003 Tokachi-Oki earthquake, oil storage tank had been damaged due to the resonant phenomenon, occurred due to the matching of the period of sloshing liquid and the long period component of ground motion, although the tank was located 200 km distance from the epicenter (the period of the sloshing mode ranges from 5 to 10 sec) [18, 19]. The effect of Tokachi-Oki earthquake can be seen in **Fig. 1.1**. During this earthquake, the floating roof of the oil tanks shook dramatically which damaged the floating roofs of the oil tanks and sinking into the tanks. The fire also took place because oil was exposed to the atmosphere.



Fig. 1-1: Floating roofs sunk during Tokachi-oki earthquake
(http://nrifd.fdma.go.jp/english/research/protect_oiltanks/02/index.html)

Ariga et al. [16] predicted that the long-period ground motion due to such earthquake has the capability to resonant the base-isolated objects with the long period component. In fact, the acceleration amplitude of such long-period ground motion is small, but the velocity amplitude is fairly large. It is expected that base isolated objects with long fundamental natural periods are greatly influenced by these long-period motions, generating the large lateral displacement which might cause catastrophic damage to the

isolated object due to damage in base isolation components such as bearings. Moreover, the existing base isolation systems cannot allow such large lateral displacement; therefore, it is important to investigate an effective method for mitigating displacement for both types of earthquake excitations in order to retrofit conventional base isolation system.

1.2 Approach to overcome issue associated with near-fault ground motions

A recent study for a near-fault earthquake with pulse-like waveform indicates that the bearing amplifies to produce the large displacement [8]. To overcome this issues associated with the pulse-like near-fault earthquake, researchers proposed isolation system with the variable curvature [14, 15], where the fundamental period of the base isolation objects was a function of the isolator displacement. In order to reduce the input energy from the ground motion by elongating the fundamental period of the object to avoid possible resonance phenomenon, Kobori et al. [20] proposed variable stiffness system. Nagarajaiah and Varadarajan [21] developed a short time Fourier transformation control algorithm for mitigating displacement with variable stiffness isolation system in near-fault earthquakes. This study showed that changing the angle of coil generate variable stiffness. It also showed the effectiveness of the controlled stiffness for reducing base displacement and interstory drifts. An experimental and numerical study shows the effectiveness of controlled stiffness for reducing base displacement of sliding base isolated building [22]. Lu et al. [23] proposed a semi-active stiffness controllable isolation system for near-fault ground motions. Here, the stiffness of the isolation system changed by varying the restoring force of the system and this restoring force was passive force induced by the base displacement. The restoring force provided by the system was controlled by the semi-active control method based on the active feedback control. Additionally, Liu et al. [24]

developed semi-active vibration isolation system with variable stiffness and damping. The stiffness of the system had been controlled by changing the damping coefficient. Leverage type stiffness controllable isolation system (LSCIS) with fuzzy logic control (FLC) was another system for variable stiffness proposed by Lin [25]. Only the information of velocity and displacement of isolation base was transmitted to FLC which control the LSCIS system. Lead-screw had been used to change the position of the pivot point which controls the isolation stiffness. The proposed system was able to mitigate displacement of the isolated object with tolerable acceleration response due to near-fault earthquakes. An adaptive system consisting of adaptive stiffness or damping devices were capable of changing stiffness or damping depending upon the displacement amplitudes [26, 27]. This device with the structure exhibits remarkable characteristics on the force-displacement relationship. Recently, Iemura et al. [28] and Iemura and Pradono [29] proposed negative stiffness damper capable of producing negative hysteretic loops which reduces the total force significantly. Consequently, the use of negative stiffness system increased during these recent years for seismic protection. Sarlis et al. [30] developed the true negative stiffness device consisting of pre-compressed springs and gap assembly for seismic protection of structure. Sun et al. [31] developed a negative stiffness system consisting of a novel negative stiffness device (NSD) and passive damper (PD) to emulate apparent yielding of structural system for response reduction to protect the base-isolated structure in a near-fault earthquake. For realizing an alternative approach of an adaptive stiffness, a concept of adaptive negative stiffness system [32] was proposed to achieve adaptive negative stiffness by combining negative stiffness device (NSD) [30] and a viscous damper for reducing structural responses.

1.3 Approach to overcome issue associated with long-period ground motions

Few studies have been conducted for the displacement mitigation due to long-period ground motions. Based on the study by Takawaki [33], Takawaki et al. [34] it is well understood that building with passive energy dissipating systems were effective for displacement mitigation of long-period ground motions. But they are not effective for near-fault ground motions [35] because the passive system cannot respond effectively to impulsive loadings. Xiang and Nishitani [36] used non-traditional tuned mass dampers (TMD) to mitigate resonances due to long-period ground motions. But the conventional base isolation systems were not necessarily resistant long-period ground motions with the characteristic period of 5-8 s [16, 37]. So, it is important to investigate an effective way to mitigate displacement for both the near-fault and the long-period earthquake waves.

1.4 Approach to overcome issue associated with both types of ground excitations

New developments on base isolation technology are still active and the recently developed triple friction pendulum isolators [38, 39] provides large displacement capacity. For the large displacement of isolators larger clearance around the isolation object is required. Thus, even though the recently developed isolators are capable to resist large displacement, if the spaces are limited, installation of such isolators becomes an issue. Moreover, the conventional base isolation systems cannot allow the large displacement. Practically, retrofitting of the conventional base isolation systems might be challenging because of necessity to move isolated objects under service to incorporate new devices in the system. Addition to this, the constraint space to fit the new system might be another challenging task. Further, the target objects of the current study are small structures such

as computer servers, sensitive instruments and machinery which are placed closed to each other. The damage of these structures might cause economic losses, data losses (due damage of computer servers), etc. Therefore, one of the best ways to mitigate displacement response subjected to both types of earthquakes for conventional base isolation system might be using external devices allowing two directional movements. Very few external devices had been proposed till date which was applicable for retrofitting. Saitoh [40] proposed an external rotary friction device to mitigate lateral displacement to both near-fault and long-period ground motions. The rotary friction device consists of a rotary plate with the shaft, coil spring and ratchet switch. The proposed system sufficiently decreases the displacement response but friction in the system always contains a residual displacement. Due to which, this system lacks the self-centering mechanism and after an earthquake, there will be the possibility of permanent offset of friction device which is a drawback of this system. So, developing a linear system will be very beneficial for overcoming such drawback.

1.5 Research objective

As described in the previous section, long-period ground motions generated large lateral displacement of the base-isolated objects. Due to the large displacement of the isolated objects, bearings might be destroyed causing catastrophic damage to the structure or the objects. So, it is important to study various ways to mitigate displacement of the isolated objects (i.e., target objects such as sensitive instruments, critical computer servers, and furniture) subjected to both near-fault and long-period ground motions. In practice, for retrofitting the conventional base isolation systems that have already been installed, difficulties might be encountered due to the fact that the isolated objects under service are needed to be moved to install a new device to the system. Therefore, one of the possible

option to retrofit the existing conventional base isolation system is by applying the external device to the isolation systems. Generally, base isolation systems are free to move in a plane, therefore it is necessary the external devices allow a two-directional movement. Moreover, the system must be elastic linear, so that the system does not contain the residual displacement after an earthquake. Therefore, an innovative technique is required to overcome all the issues.

Based on the above background, negative stiffness has been found to be used frequently for response reductions. Hence, to solve these above-mentioned problems the objectives of this study have been:

- to propose base isolation system with negative and positive springs with variable stiffness to mitigate displacement of base-isolated objects.
- to optimize parameters of proposed systems for obtaining displacement and acceleration responses within acceptable limits considering both the displacement and acceleration responses of the target objects and the stability condition in practice.
- to study the performance of the proposed model when subjected to an observed and simulated earthquake.

1.6 Thesis organization

This thesis is organized into five chapters. Chapter 1 provides introduction and literature survey to this effort. The objectives of this study are also listed in the chapter.

Chapter 2 presents the comparative study of the base isolation systems for varying stiffness using different equations (power functions, exponential function and elliptical function). It also includes the information of the extremes near-fault and long-period

ground motions used for the numerical simulation in this study. Two near-fault (Kobe and Ojiya) and two long-period (Shin-Tokai and Tomakomai) earthquakes have been taken for the analysis. A parametric study was conducted in order to fix the values of various parameters of the proposed base isolation system. Numerical analysis was performed and results were compared with conventional base isolation system and to others different variation in the stiffness.

Chapter 3 proposed the negative-variable positive mechanical unit to vary total negative stiffness. This unit was proposed due to the fact that negative stiffness itself is unstable thus, cannot stay under solitary state and moreover, varying negative stiffness itself is a challenging job. In this study also, a parametric study was conducted in order to fix the values of various parameters of the proposed base isolation models. Numerical analysis was performed, and results were compared with conventional base isolation system and models itself. Also, the comparison of the performance of base isolation system with proposed device against base isolation with variable negative stiffness and the previous existing systems were presented.

Chapter 4 is about the approximation of negative-positive variable stiffness in practice and in chapter 5 conclusions and recommendations for future research are presented.

CHAPTER 2

BASE ISOLATION SYSTEM WITH VARIABLE NEGATIVE STIFFNESS

2.1 Background and objectives

Stiffness is the properties of the material to counteract the external force. In case of positive stiffness, the direction of both the deformation and the applied external force are in the same direction and the corresponding reaction force returns the deformed body to its neutral position. On the other hand, negative stiffness generates a force on a body that acts in the same direction in which the body is displaced and generates larger forces with increasing displacement. Hence, negative stiffness itself is unstable. Many types of research about the behavior, property and stability conditions of negative stiffness have been reported [41–44]. Negative stiffness in stable condition shows better vibration control performance. Therefore, the concept of negative stiffness in vibration isolation might be relevant. In these recent years, negative stiffness spring/systems have been proposed and applied by many researchers for vibration isolation. For the several proposals of vibration isolation systems, Molyneaux in 1957 [45] introduce the concept of negative stiffness for the first time. Mizuno [46] studied active vibration control using zero-power magnetic suspension. They found that zero-power system behaves as negative stiffness and when combined with normal spring it generates infinite stiffness. The negative stiffness was obtained by hydraulic damping device which is controlled actively or semi-actively to reduce structural responses [28], [47]. Sarlis [30] proposed the negative

stiffness device for seismic protection of structure consisting of pre-compressed spring and two gap spring assembly (GSA). When the device deforms in one direction, the pre-compressed spring rotates and generates a force that facilitates the motion, thus creating the negative stiffness. In a recent study by Nakagawa [48], the combination of negative and positive stiffness characteristics was used for obtaining constant repulsive force. For realizing negative stiffness coil spring, and mechanical linkage has been employed.

The above background indicates that use of the negative stiffness in recent years has been accelerated. To the best of the author's knowledge, very few studies have been conducted for variable negative stiffness till date. Thus, this study presents the comparative study on the performance of base isolation systems with variable negative stiffness. The current study proposes a new base isolation system employing variable negative stiffness with different equations: (i) power functions in terms of displacement response of the isolated objects, (ii) elliptical, and (iii) exponential for displacement mitigation. The performance of the proposed system is verified analytically by comparing against the conventional base isolation systems. An optimal order of power function to satisfy the acceptable limits of both the displacement and the acceleration responses of an isolated object subjected to near-fault and long-period ground motions is proposed.

2.2 Base isolations models

2.2.1 Conventional base isolation model

Fig. 2-1(a) shows the conventional base isolation system with lateral stiffness k and damping coefficient c . The base-isolated object is assumed to have a lumped mass m_s . The relative displacement of the mass m_s is denoted as u . The response of the system when excited by ground acceleration \ddot{u}_g can be represented by the following equation:

$$m_s (\ddot{u} + \ddot{u}_g) + c\dot{u} + k u = 0 \quad (2.1)$$

Eq. (2.1) can be rewritten as follows:

$$\ddot{u} + 2h\omega\dot{u} + \omega^2 u = -\ddot{u}_g \quad (2.2)$$

where, $\omega = \sqrt{k/m_s}$ is the natural circular frequency of the base isolation system and $h = c/2\sqrt{m_s k}$ is the damping constant of the system.

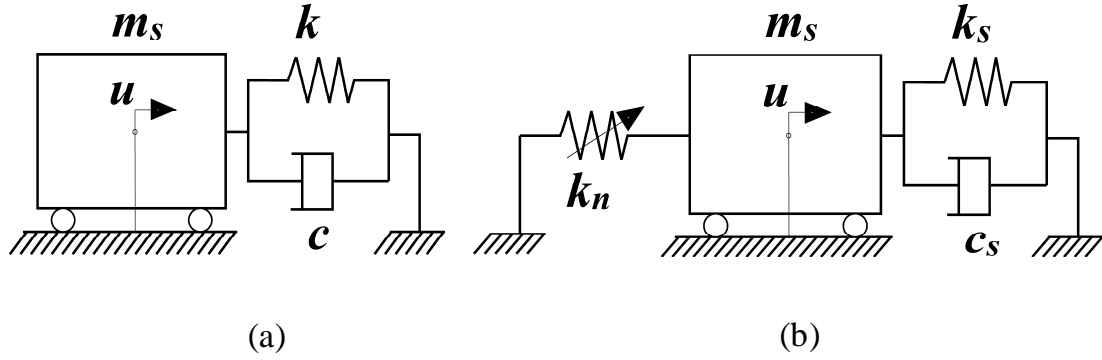


Fig. 2-1: Models of base isolation systems: **(a)** Conventional base isolation system; **(b)** Proposed Model

2.2.2 Proposed model

Fig. 2-1(b) shows a base isolation system with varying negative spring stiffness. The response of the proposed system when excited by ground acceleration \ddot{u}_g is represented by the following equation:

$$m_s (\ddot{u} + \ddot{u}_g) + c_s\dot{u} + (k_s + k_n) u \quad (2.3)$$

where, k_s and c_s are the damping coefficient and spring coefficient of the spring and the damper unit, respectively. k_n is the stiffness of the negative spring. Eq. (2.3) can be rewritten as follows:

$$\ddot{u} + 2h_s\omega_s\dot{u} + (\omega_s^2 - \omega_n^2)u = -\ddot{u}_g \quad (2.4)$$

where, $\omega_s = \sqrt{k_s/m_s}$ and $h_s = c_s/2\sqrt{m_s k_s}$ are the natural circular frequency and the damping constant of the spring and damper unit, respectively, and, $\omega_n = \sqrt{|k_n|/m_s}$ is the natural circular frequency of the negative spring. The stiffness of the negative spring is varied with different equations as follows:

2.2.2.1 Power functions

The following power functions are used for varying negative stiffness:

$$k_n = k_{no} - \kappa|u|^{1.5} \quad (2.5)$$

$$k_n = k_{no} - \kappa|u| \quad (2.6)$$

$$k_n = k_{no} - \kappa|u|^{0.5} \quad (2.7)$$

where, k_{no} is the initial stiffness of the negative spring, $\kappa (\geq 0)$ is the slope for changing k_n and $|u|$ is the relative displacement of the base-isolated object with respect to the ground. Slope κ for different mathematical functions as shown above were fixed based on the results of the parametric study.

2.2.2.2 Elliptical function

$$k_n = \frac{\Delta k}{u_{max}} \sqrt{u_{max}^2 - |u|^2} - |k_{no}| - \Delta k \quad (2.8)$$

where, Δk is change in stiffness of negative stiffness and u_{max} is maximum allowable displacement (± 0.3 m).

2.2.2.3 Exponential function

$$k_n = k_{no}e^{a|u|} \quad (2.9)$$

where, a is a parameter for variation of negative stiffness.

2.2.3 Fundamental parameters of proposed systems

The fundamental parameters of the proposed isolation model are summarized below. The total stiffness of the system k_t is given by:

$$k_t = k_s + k_n \quad (2.10)$$

Eq. (2.10) can be rewritten as:

$$T_t = \frac{2\pi}{\sqrt{\omega_s^2 - \omega_n^2}} \quad (2.11)$$

where, T_t is the natural period of the proposed system.

The total damping ratio h_t is given by:

$$h_t = \frac{c_s}{c_t} = h_s \sqrt{\frac{k_s}{k_t}} \quad (2.12)$$

where, c_t is the critical damping coefficient.

To enhance the performance of the proposed model, choosing the parameters κ , Δk , and a for power, elliptical and exponential functions respectively, h_t and T_t is eminently important.

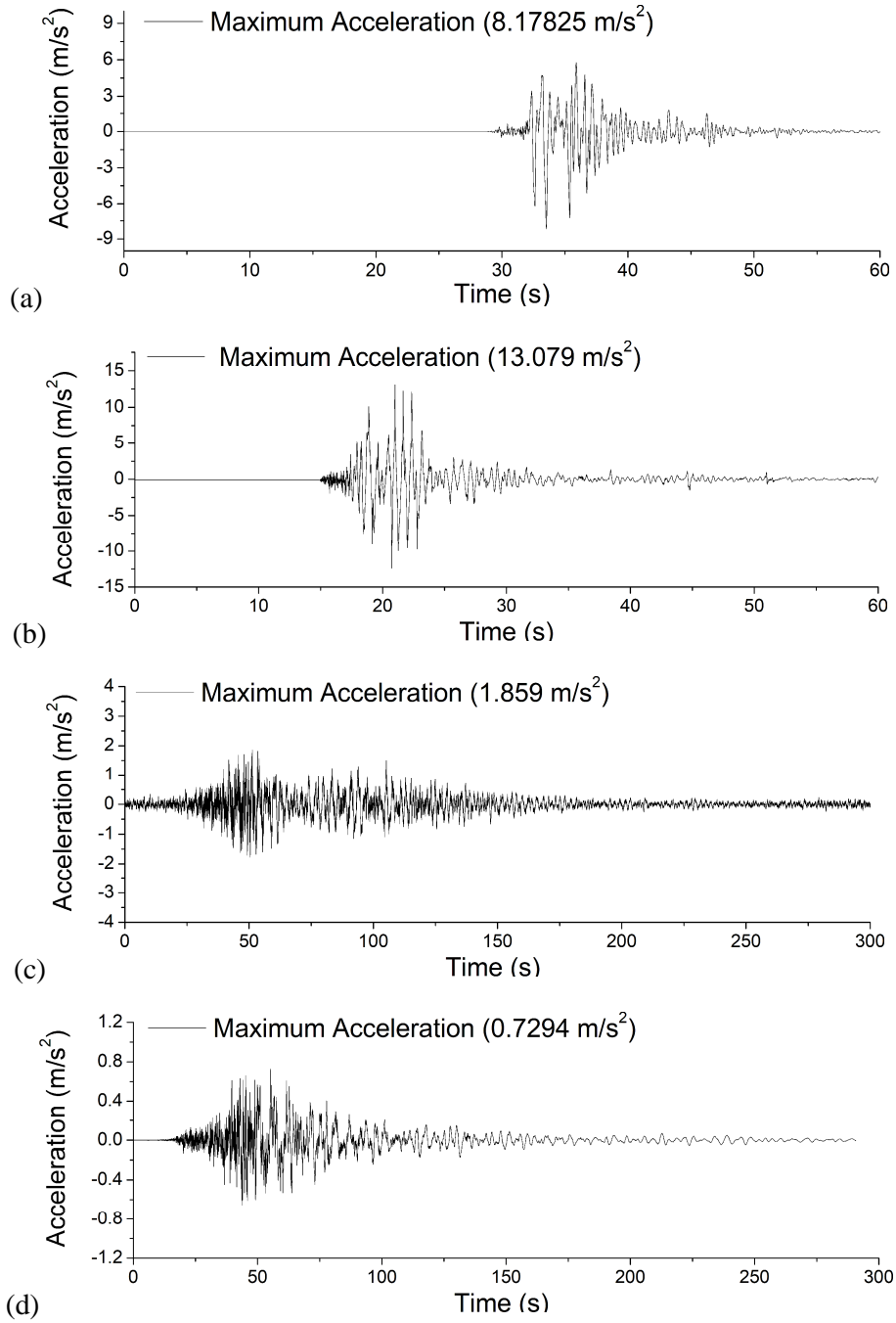


Fig. 2-2: Time histories of the earthquake waves used for time history analyses: (a) Kobe NS 1995, (b) Ojiya EW 2004, (c) Shin-Tokai EW, and (d) Tomakomai EW 2003

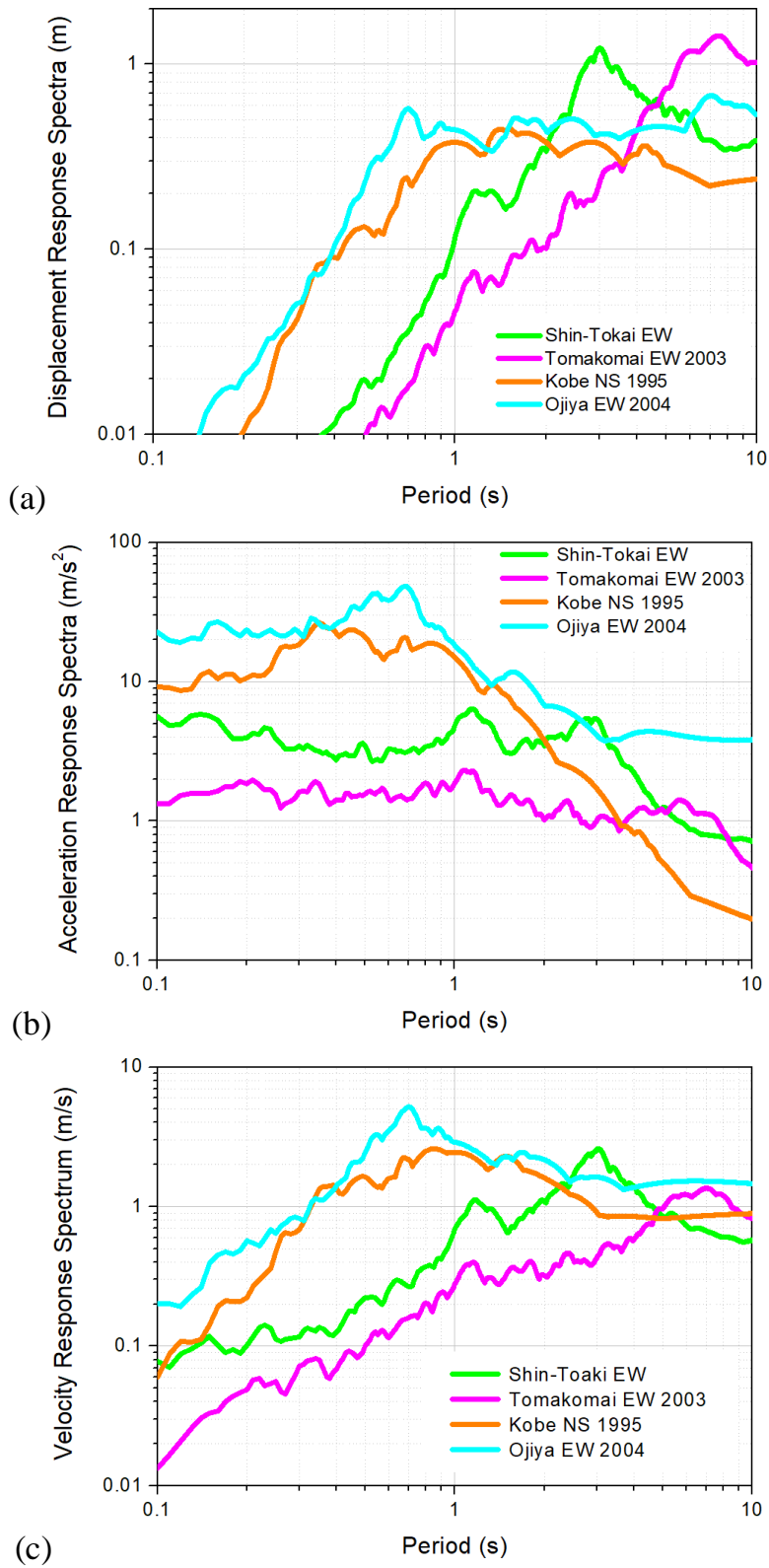


Fig. 2-3: (a) Displacement response spectra, (b) Acceleration response spectra, and (c) velocity response spectra for both types of earthquake ground motions

2.3 Ground motions

The time history analysis is performed by numerical integration using Newmark's method with $\beta = 1/6$, and a time interval Δt of 0.001 s. Newton Rapson method is implemented for obtaining converged responses. The following two types of earthquake records are used for applying the ground acceleration \ddot{u}_g to the systems: (i) Near-fault ground motions, and (ii) Long-period ground motions. For the conventional base isolation system (i.e., **Fig. 2-1(a)**), the natural frequency is assumed to be $f(= \omega/2\pi) = 0.25$ Hz while the damping constant as $h = 0.05$.

2.3.1 Near-fault ground motions

The following two near-fault earthquake records are used: (i) Kobe NS 1995 (referred as Kobe), (ii) Ojiya EW 2004 (referred as Ojiya). The time histories of the earthquake records are shown in **Fig. 2-2**. The elastic acceleration, velocity and displacement response spectra of the earthquakes for 5% damping are shown in **Fig. 2-3**. Kobe earthquake data was recorded at the JMA station in Kobe city in 1995 and has the largest maximum acceleration amplitudes. Ojiya earthquake data was recorded in the near-fault site and contains a wide range of frequency components with sharp maxima and minima in acceleration record. Response spectra shows that Ojiya has the largest maximum acceleration and velocity amplitudes.

2.3.2 Long-period ground motions

For the long-period ground motion, few earthquake ground motions are available which are: (i) Shin-Tokai EW (referred as Shin-Tokai), and (ii) Tomakomai EW 2003 (referred as Tomakomai). The time histories of the earthquake records are shown in **Fig. 2-2**. The elastic acceleration, velocity and displacement response spectra of the earthquakes for 5%

damping are shown in **Fig. 2-3**. Tomakomai was recorded at Tomakomai city during 2003 Tokachi-Oki earthquake located 200 km away from the epicenter. The response spectra of the earthquake ground motion show peaks ranging from 4 to 10 s with a maximum around 7 s. The Shin-Tokai is an artificial earthquake ground motion simulated for a scenario of the Tokai-Tonankai earthquake by the Chubu Regional Bureau, Aichi Prefecture, and Nagoya City, Japan [49]. Shin-Tokai shows a response peak at 3 s in both velocity and displacement response spectra.

2.4 Effectiveness of parameter T_{to} , κ , h_t , Δk , and α

For the effectiveness of the proposed model, appropriate selection of the parameters is of great importance. In the following section, therefore, the effect of these parameters upon the responses will be contemplated.

To investigate the behavior of T_{to} , $h_t = 0.15$ is chosen. **Figs. 2-4 and 2-5** show the effect of the natural period of the proposed system (T_t) using power function with Eq. (2.5) for varying stiffness. **Fig. 2-4** shows the response of relative displacement. It indicates that the proposed system with a higher natural period of the system, increases the displacement response without varying the slope κ . However, the system with varying the stiffness reduces the displacement response above the allowable limit ($u < 0.3 m$) except for the system with a lower natural period which reduces the displacement response with an increase in the slope κ of the power function. **Fig. 2-5** shows the response of absolute acceleration. This figure indicates that the proposed system with higher natural period shows the acceleration response within the allowable limit ($\ddot{u} < 3.0 m/s^2$) and also with an increase in slope κ acceleration response decrease further. In the case, with $T_{to} = 1.789 s$, acceleration response decrease with increase in slope κ to the allowable limit.

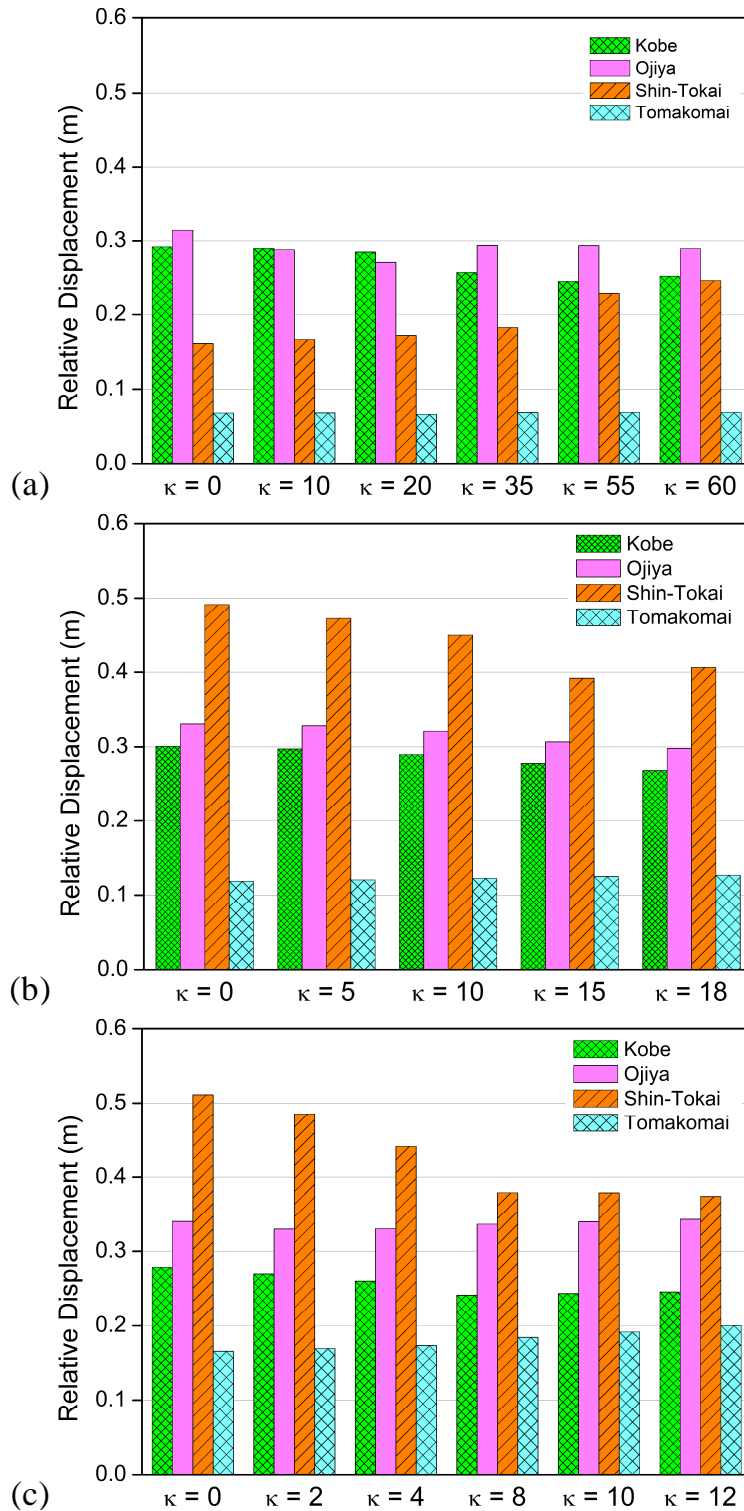


Fig. 2-4: Maximum amplitudes of the response of the relative displacement for the proposed model using Eq. (2.5) for stiffness variation (a) $T_{to} = 1.789$ s, (b) $T_{to} = 2.828$ s, and (c) $T_{to} = 3.328$ s.

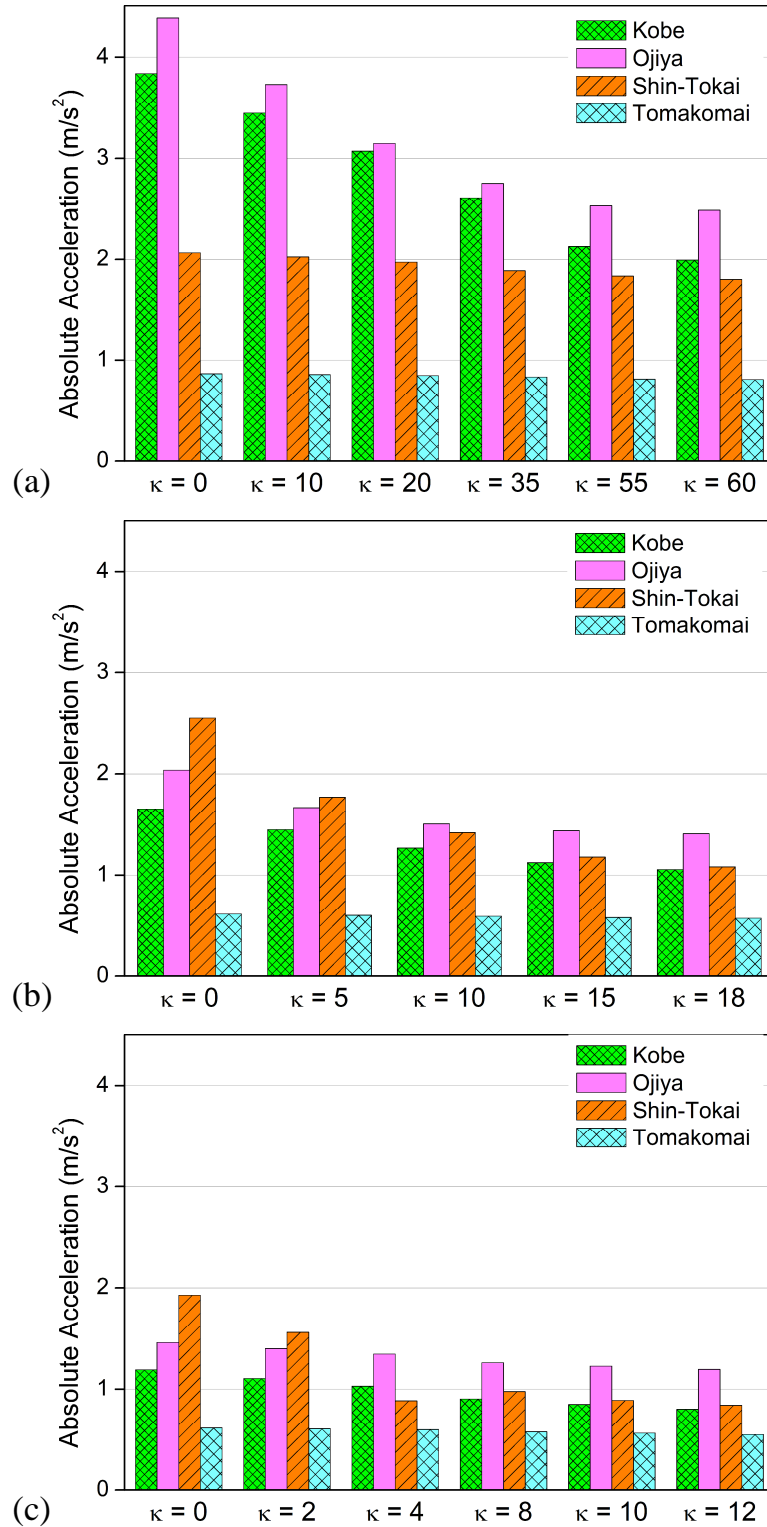


Fig. 2-5: Maximum amplitudes of the response of the absolute acceleration for the proposed model using Eq. (2.5) for stiffness variation (a) $T_{to} = 1.789$ s, (b) $T_{to} = 2.828$ s, and (c) $T_{to} = 3.328$ s.

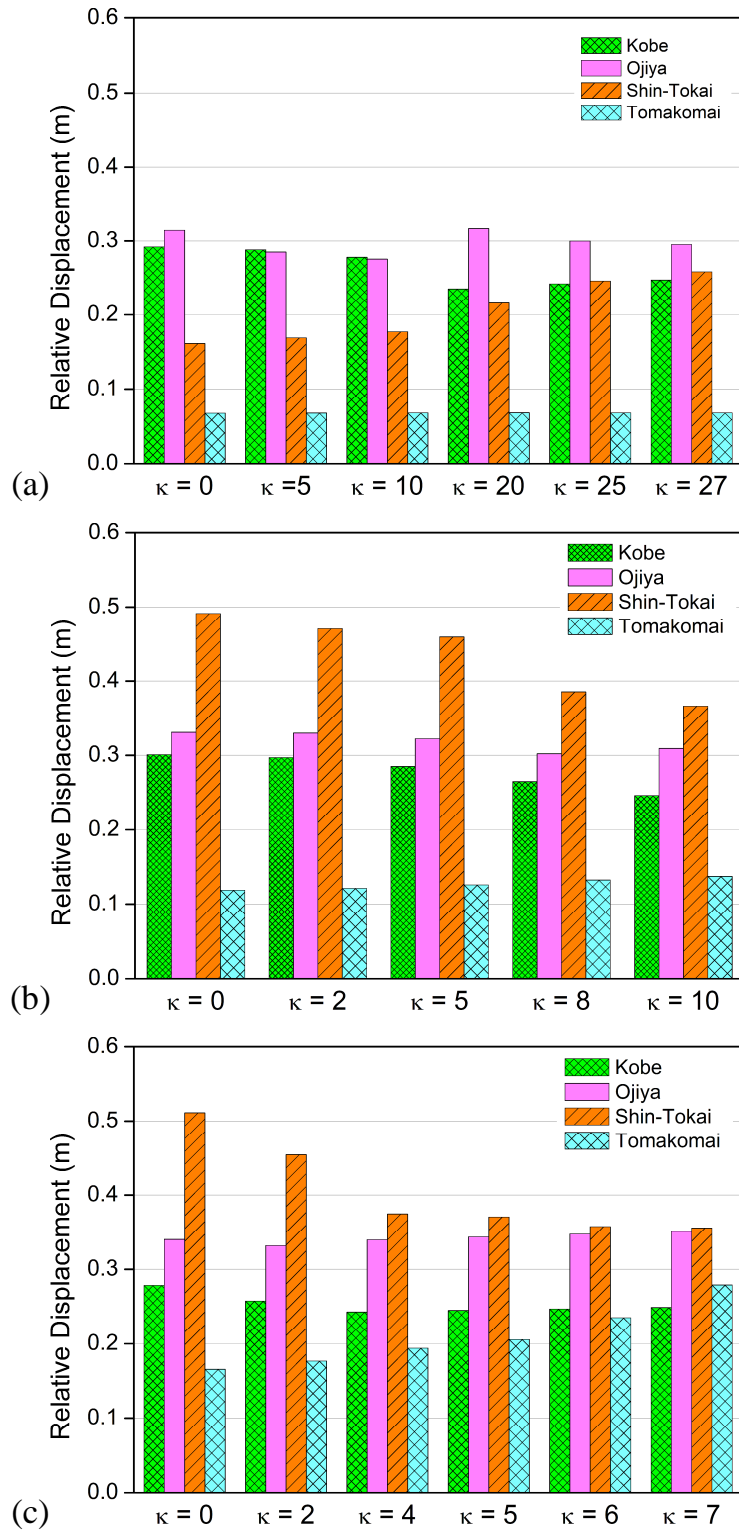


Fig. 2-6: Maximum amplitudes of the response of relative displacement for the proposed model using Eq. (2.6) for stiffness variation (a) $T_{to} = 1.789$ s, (b) $T_{to} = 2.828$ s, and (c)

$$T_{to} = 3.328 \text{ s.}$$

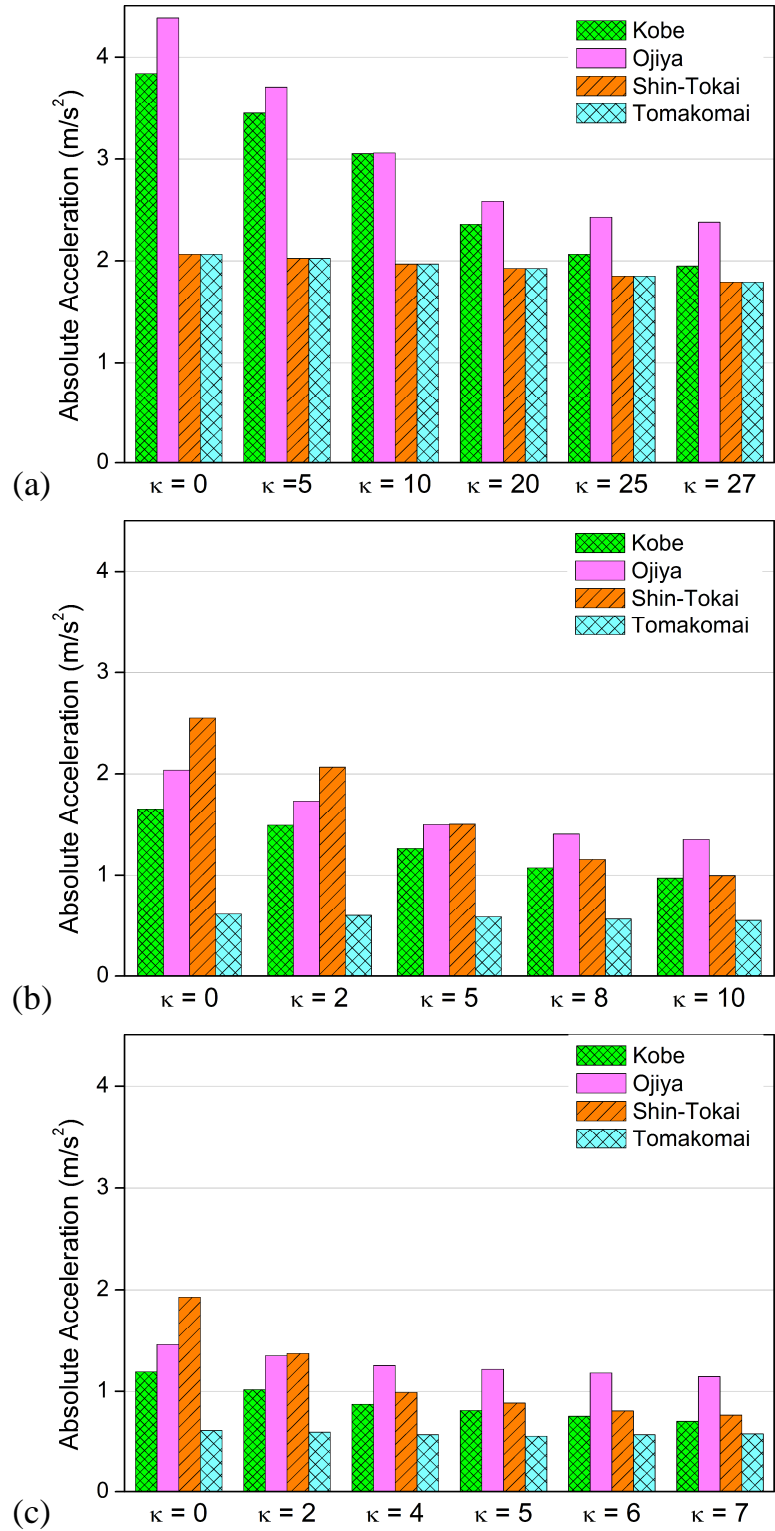


Fig. 2-7: Maximum amplitudes of the response of absolute acceleration for the proposed model using Eq. (2.6) for stiffness variation (a) $T_{to} = 1.789$ s, (b) $T_{to} = 2.828$ s, and (c)

$$T_{to} = 3.328 \text{ s.}$$

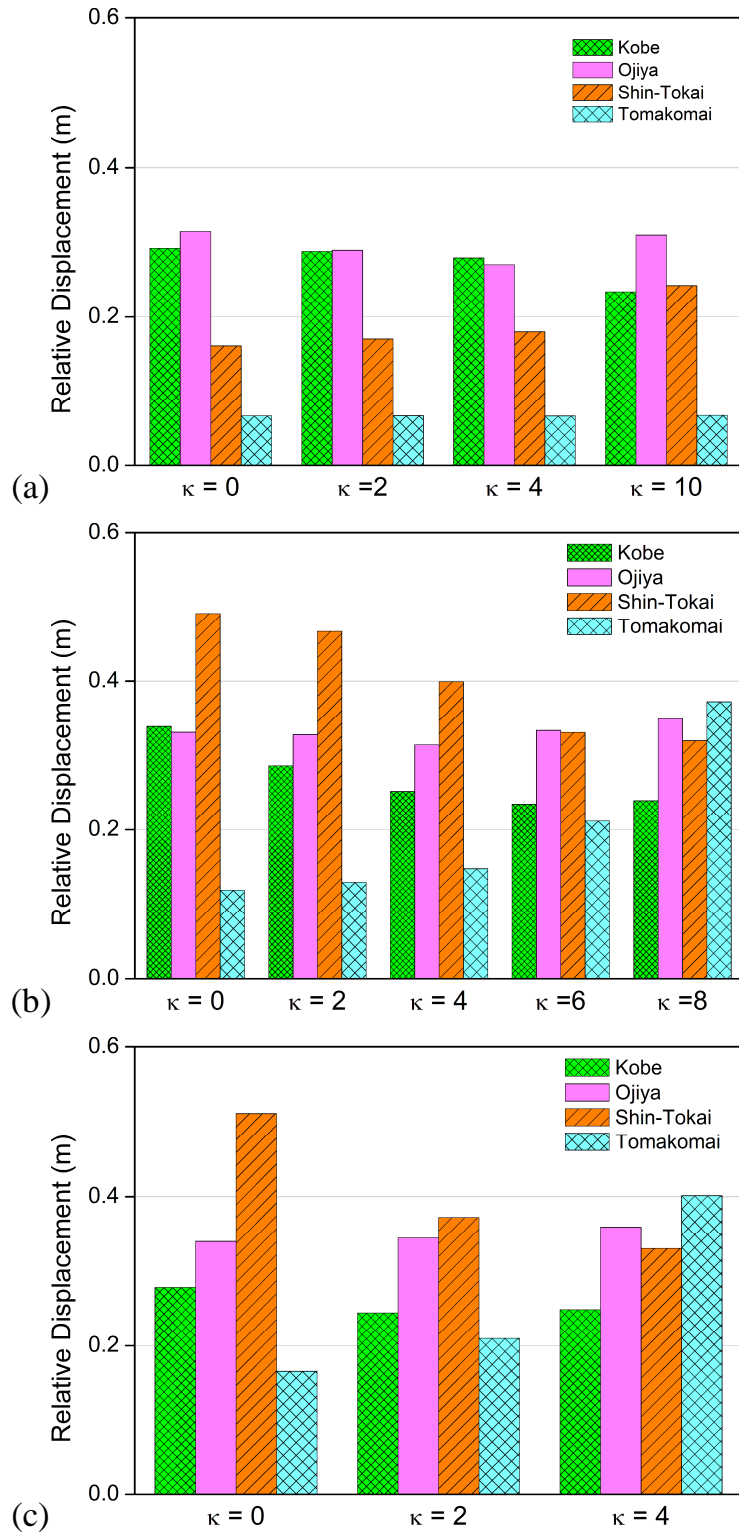


Fig. 2-8: Maximum amplitudes of the response of relative displacement for the proposed model using Eq. (2.6) for stiffness variation (a) $T_{to} = 1.789$ s, (b) $T_{to} = 2.828$ s, and (c)

$$T_{to} = 3.328 \text{ s.}$$

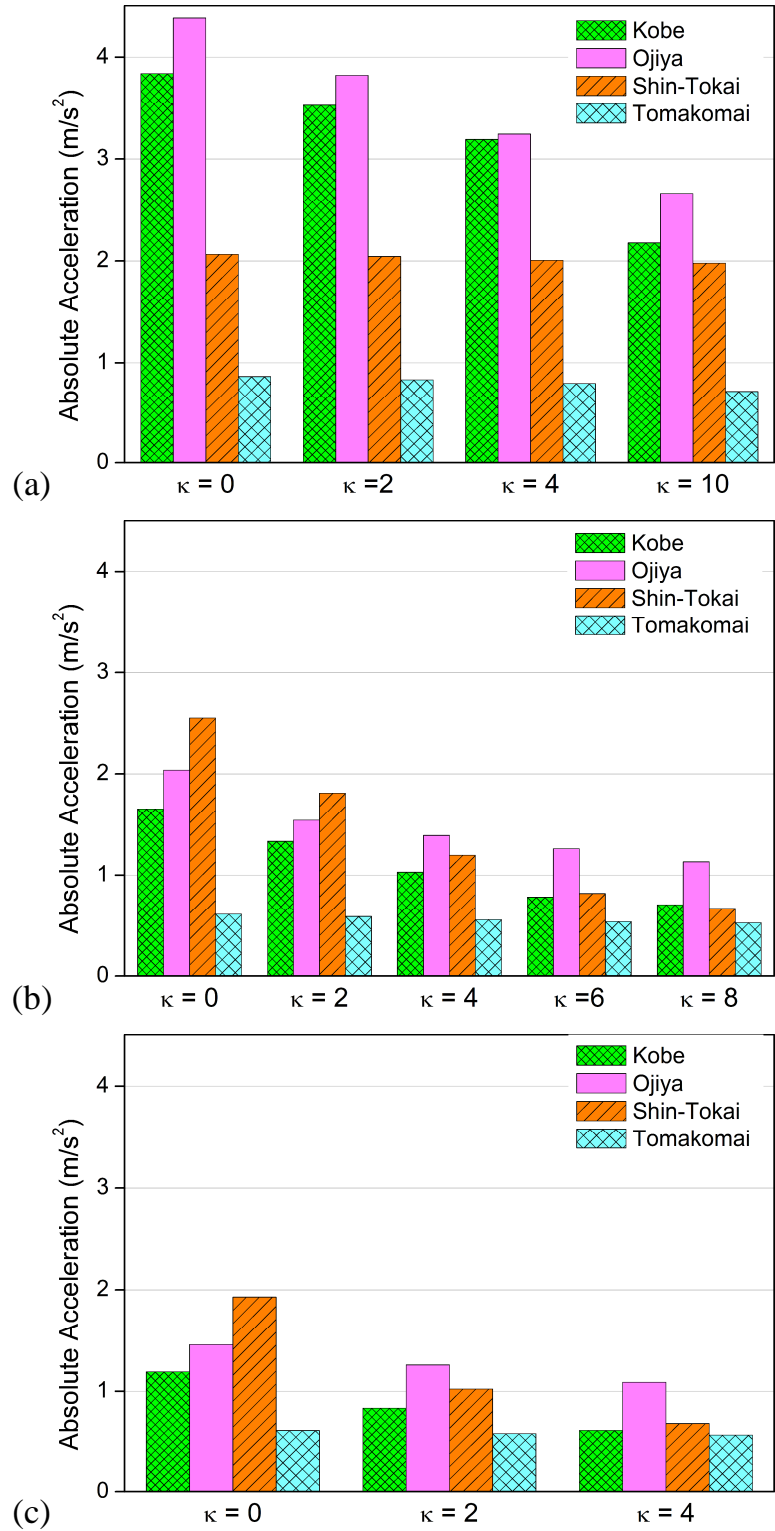


Fig. 2-9: Maximum amplitudes of the response of absolute acceleration for the proposed model using Eq. (2.7) for stiffness variation (a) $T_{to}=1.789$ s, (b) $T_{to}=2.828$ s, and (c)

$$T_{to}=3.328 \text{ s.}$$

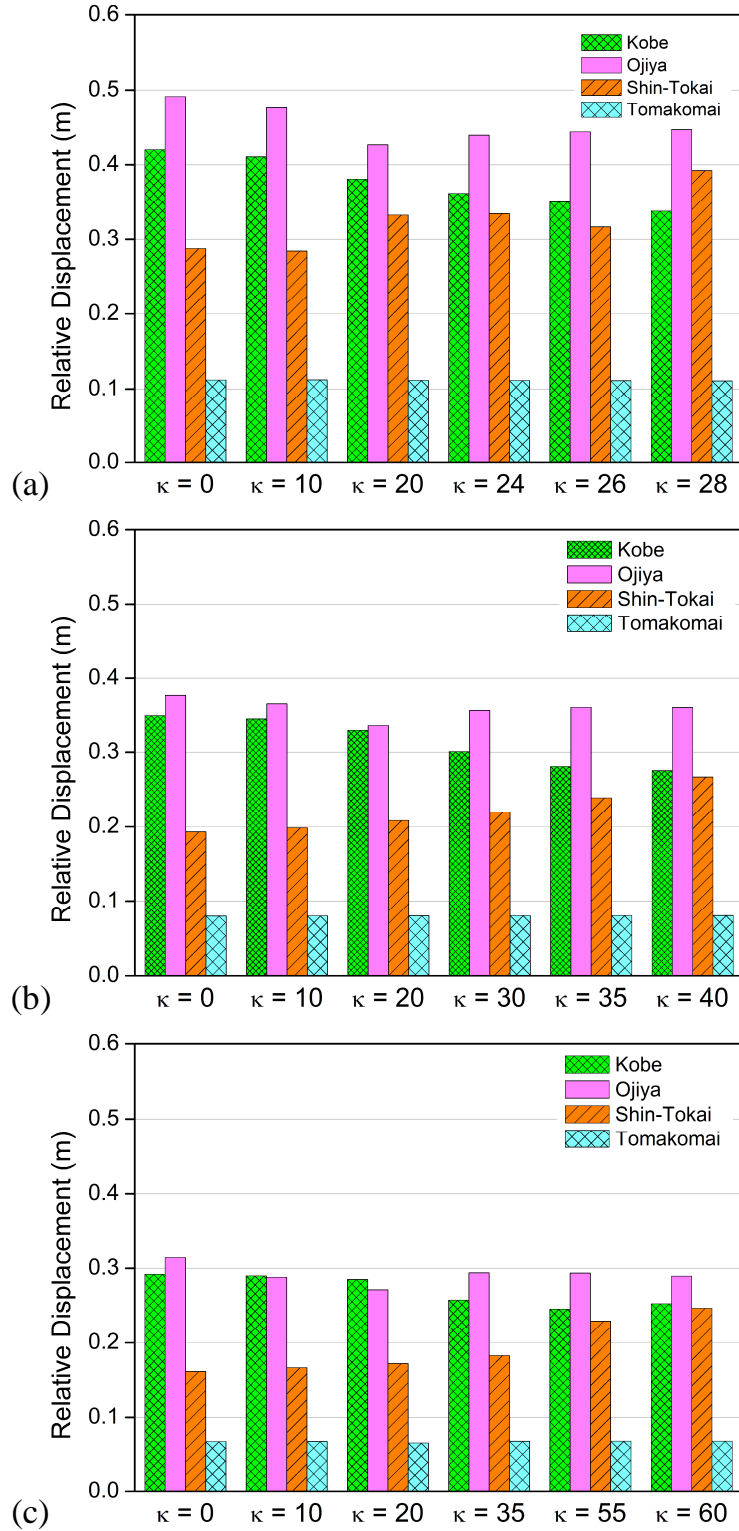


Fig. 2-10: Maximum amplitudes of the response of relative displacement for the proposed system using Eq. (2.5) for varying stiffness (a) total damping ratio $h_t = 5\%$, (b) total damping ratio $h_t = 10\%$, (c) total damping ratio $h_t = 15\%$.

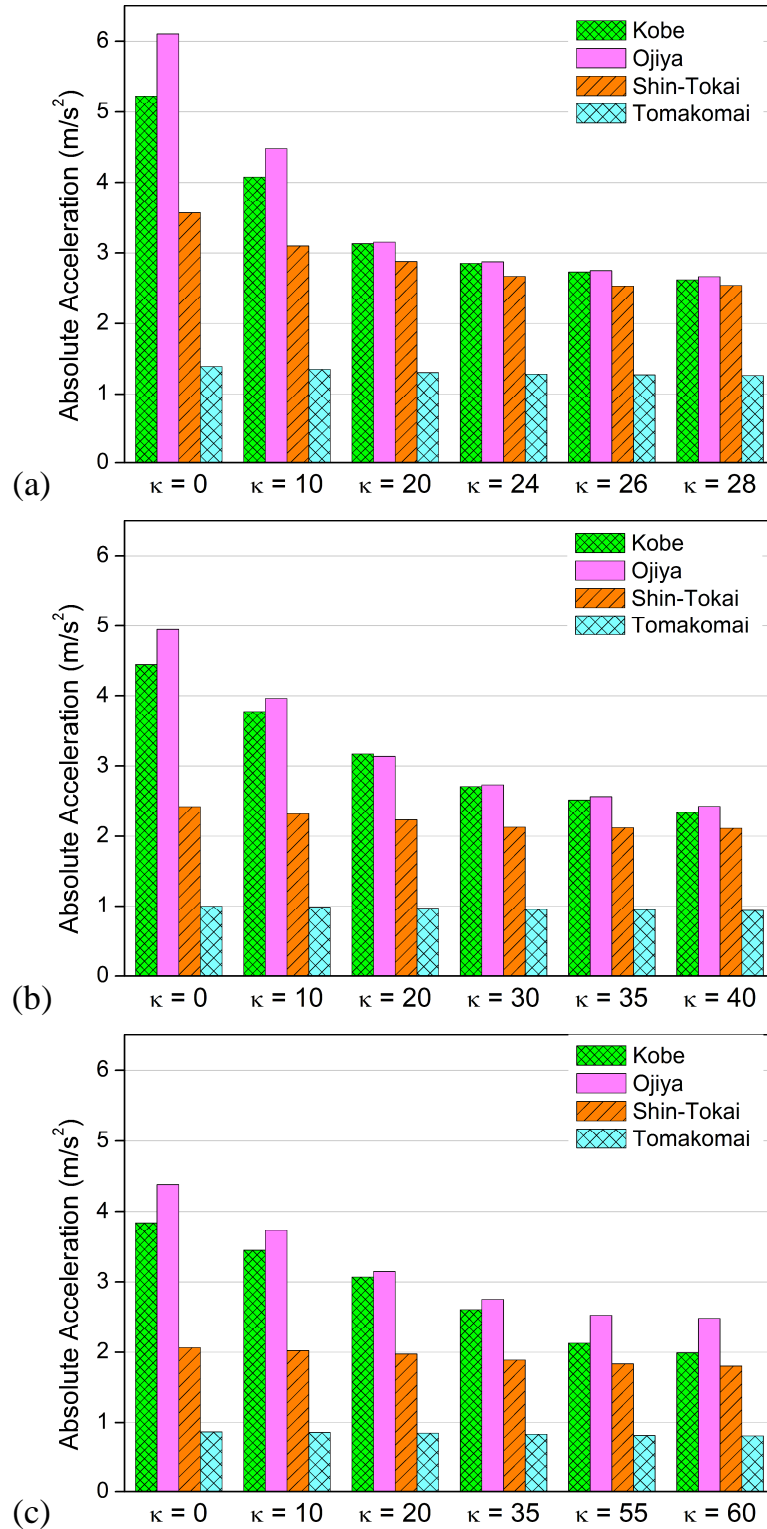


Fig. 2-11: Maximum amplitudes of the response of absolute acceleration for the proposed system using Eq. (2.5) for varying stiffness (a) total damping ratio $h_t = 5\%$, (b) total damping ratio $h_t = 10\%$, (c) total damping ratio $h_t = 15\%$.

Figs. 2-6 and 2-7 show the effect of the natural period of the proposed system (T_t) using power function with Eq. (2.6) for varying stiffness. And **Figs. 2-8 and 2-9** show the effect of the natural period of the proposed system (T_t) using power function with Eq. (2.7) for varying stiffness. These figures indicate that for a lower natural period of the system displacement shows small value, but acceleration shows larger value in comparison to the higher value of the natural period of the system. Thus, for obtaining allowable limits of the displacement and the acceleration responses of the isolated object when subjected to both near-fault and long-period ground motions $T_{to} = 1.789$ s is chosen.

Total damping ratio h_t and slope κ are also important parameters which enhance the performance of the proposed system. **Figs. 2-10 and 2-11** show the relative displacement and absolute acceleration of the isolated mass for the proposed system with varying slope κ using Eq. (2.5) and total damping ratio h_t . Increase in total damping ratio h_t decreases the displacement and acceleration responses for both types of earthquake excitations. These figures show that for varying the stiffness with $h_t = 0.05$, both displacement and acceleration responses decrease but still above the allowable limits. And for $h_t = 0.1$, acceleration response decreases within allowable limit but although displacement response decreases, it is still above the allowable limit in case of Ojiya. Further, **Figs 2-10(c) and 2-11(c)** ($h_t = 0.15$) show that with an increase in slope (κ), displacement and acceleration responses decrease in case of near-fault ground motions while in case of long-period ground motions, displacement response tends to increase steadily but acceleration response is almost the same. The change in the displacement in case of near-fault ground motions is not noticeable but the decrease in the acceleration response with an increase in slope (κ) for near-fault is almost half that of $\kappa = 0$ in comparison with $\kappa = 55$ which is the parameter that defines the effectiveness of the proposed system.

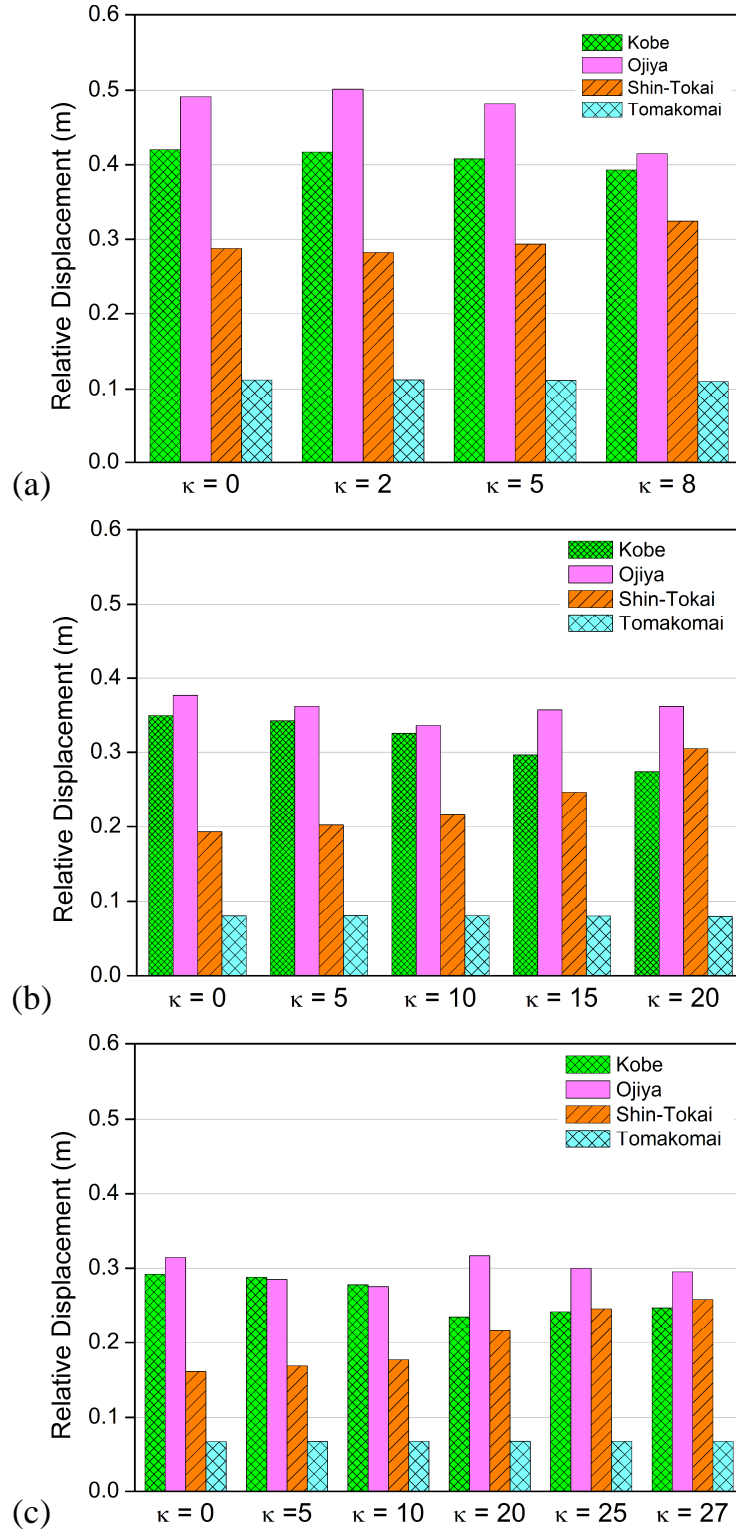


Fig. 2-12: Maximum amplitudes of the response of relative displacement for the proposed system using Eq. (2.6) for varying stiffness (a) total damping ratio $h_t = 5\%$, (b) total damping ratio $h_t = 10\%$, (c) total damping ratio $h_t = 15\%$.

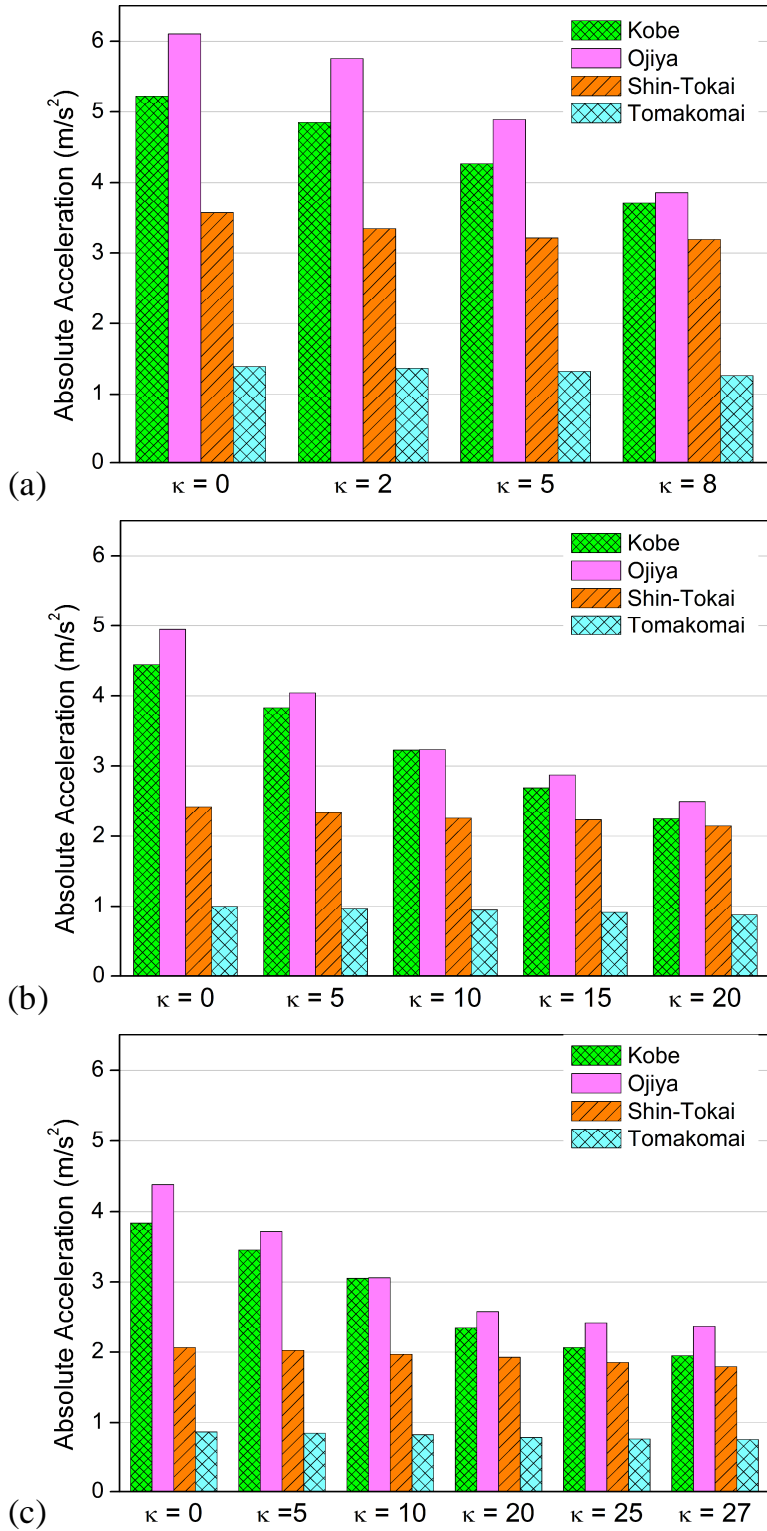


Fig. 2-13: Maximum amplitudes of the response of absolute acceleration for the proposed system using Eq. (2.6) for varying stiffness (a) total damping ratio $h_t = 5\%$, (b) total damping ratio $h_t = 10\%$, (c) total damping ratio $h_t = 15\%$.

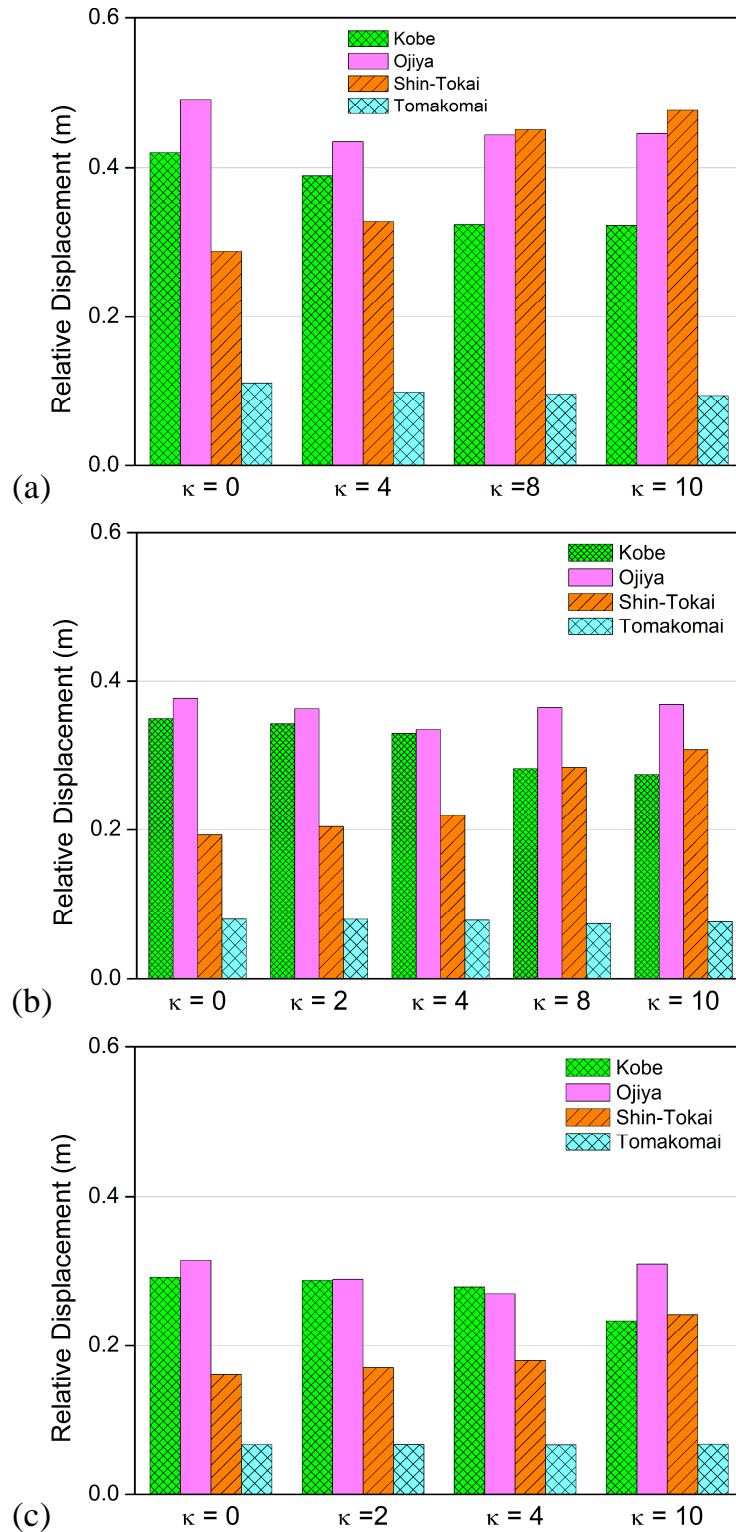


Fig. 2-14: Maximum amplitudes of the response of relative displacement for the proposed system using Eq. (2.7) for varying stiffness (a) total damping ratio $h_t = 5\%$, (b) total damping ratio $h_t = 10\%$, (c) total damping ratio $h_t = 15\%$.

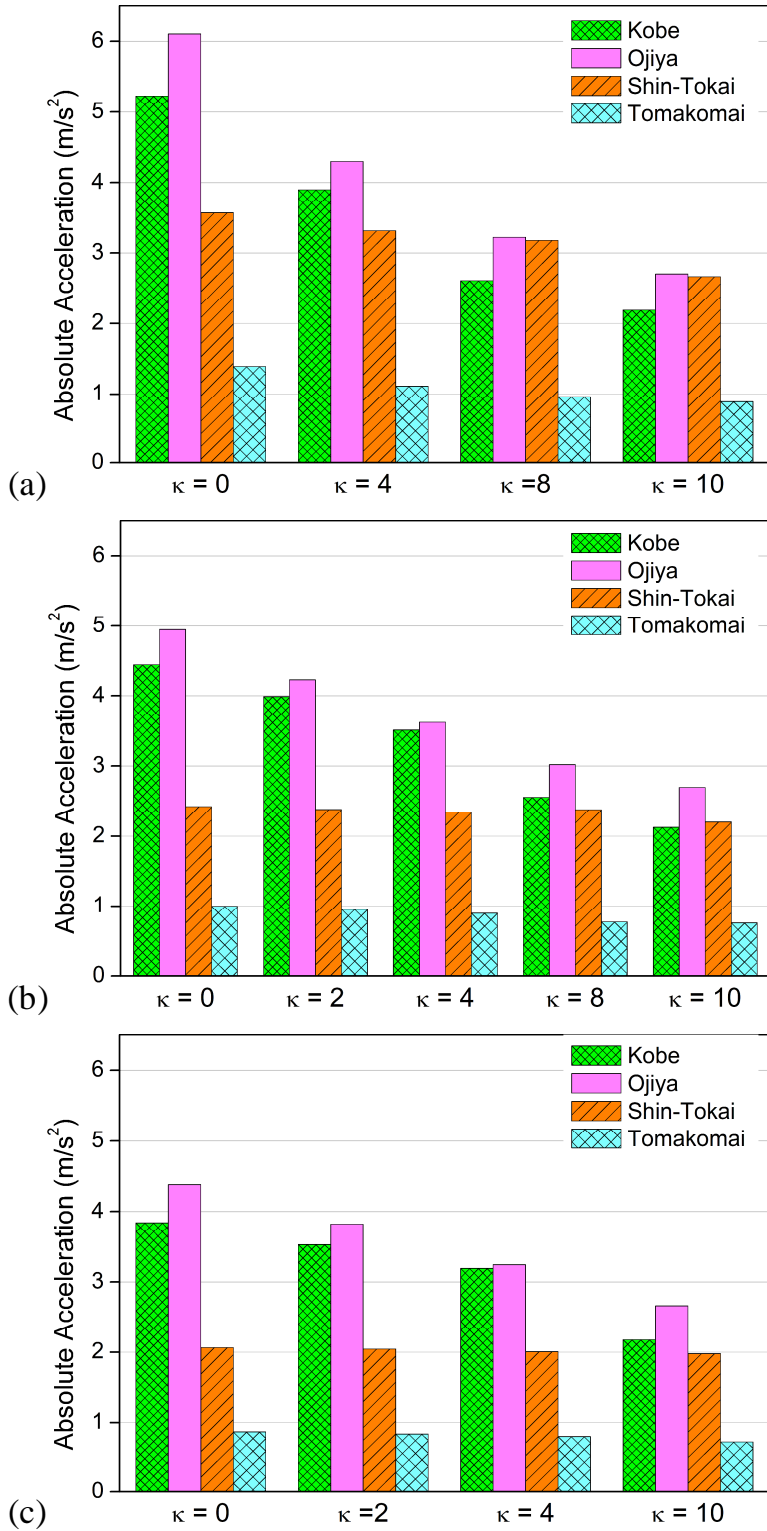


Fig. 2-15: Maximum amplitudes of the response of absolute acceleration for the proposed system using Eq. (2.7) for varying stiffness (a) total damping ratio $h_t = 5\%$, (b) total damping ratio $h_t = 10\%$, (c) total damping ratio $h_t = 15\%$.

Similarly, **Figs. 2-12** and **2-13** show the relative displacement and absolute acceleration of the isolated mass with the proposed system with varying slope κ using Eq. (2.6) and **Figs. 2-14** and **2-15** show the relative displacement and absolute acceleration of the isolated mass with the proposed system with varying slope κ using Eq. (2.7). Based on these results $\kappa = 25$ and 10 are chosen for Eqs. (2.6) and (2.7) respectively.

For Eq. (2.8), Δk is chosen based on the value of stiffness needed to limit both displacement and acceleration within allowable limits. And in this study, $\Delta k = 20$ is chosen. Further, for Eq. (2.9) it is found that with an increase in a , isolated objects subjected to long-period ground resonant. Therefore, in this study $a = 0.1$ is chosen.

Following parametric studies, optimal values of the following parameters are found to satisfy both the allowable displacement and the acceleration responses ($u < 0.3$ m and $\ddot{u} < 3.0$ m/s²): total damping ratio $h_t = 0.15$, natural frequency $f_s (= \omega_s/2\pi) = 2.015$ Hz, and initial natural period of the system $T_{to} = 1.789$ s. Values of slope (κ) = 55, 25 and 10 are chosen for Eqs. (2.5), (2.6) and (2.7), respectively. Change in stiffness of negative stiffness $\Delta k = 20$ and parameter $a = 0.1$ are chosen for Eqs. (2.8) and (2.9), respectively.

2.5 Numerical Simulation

In this section, the time history responses of the base isolation systems presented in the preceding section are calculated for the various earthquakes discussed in section 2.3. The performance of the proposed model with varying negative stiffness using different equations is compared with the conventional base isolation system. For the conventional base isolation system (i.e., **Fig. 2-1(a)**), the natural frequency is assumed to be $f (= \omega/2\pi) = 0.25$ Hz while the damping constant as $h = 0.05$. Following parametric studies,

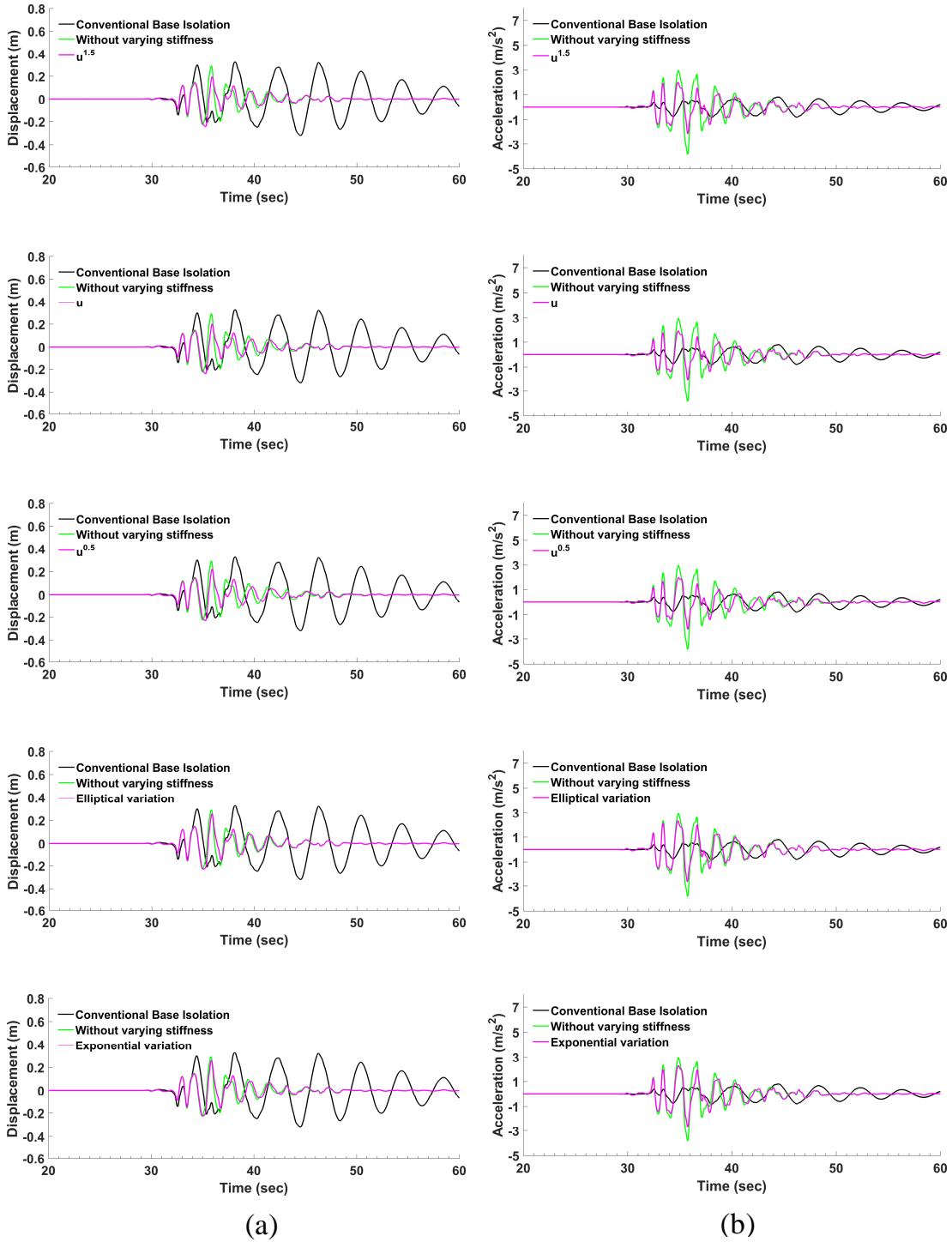


Fig. 2-16: Time history response comparison between the conventional base isolation and the proposed systems excited by Kobe for varying negative stiffness: **(a)** relative displacement **(b)** absolute acceleration

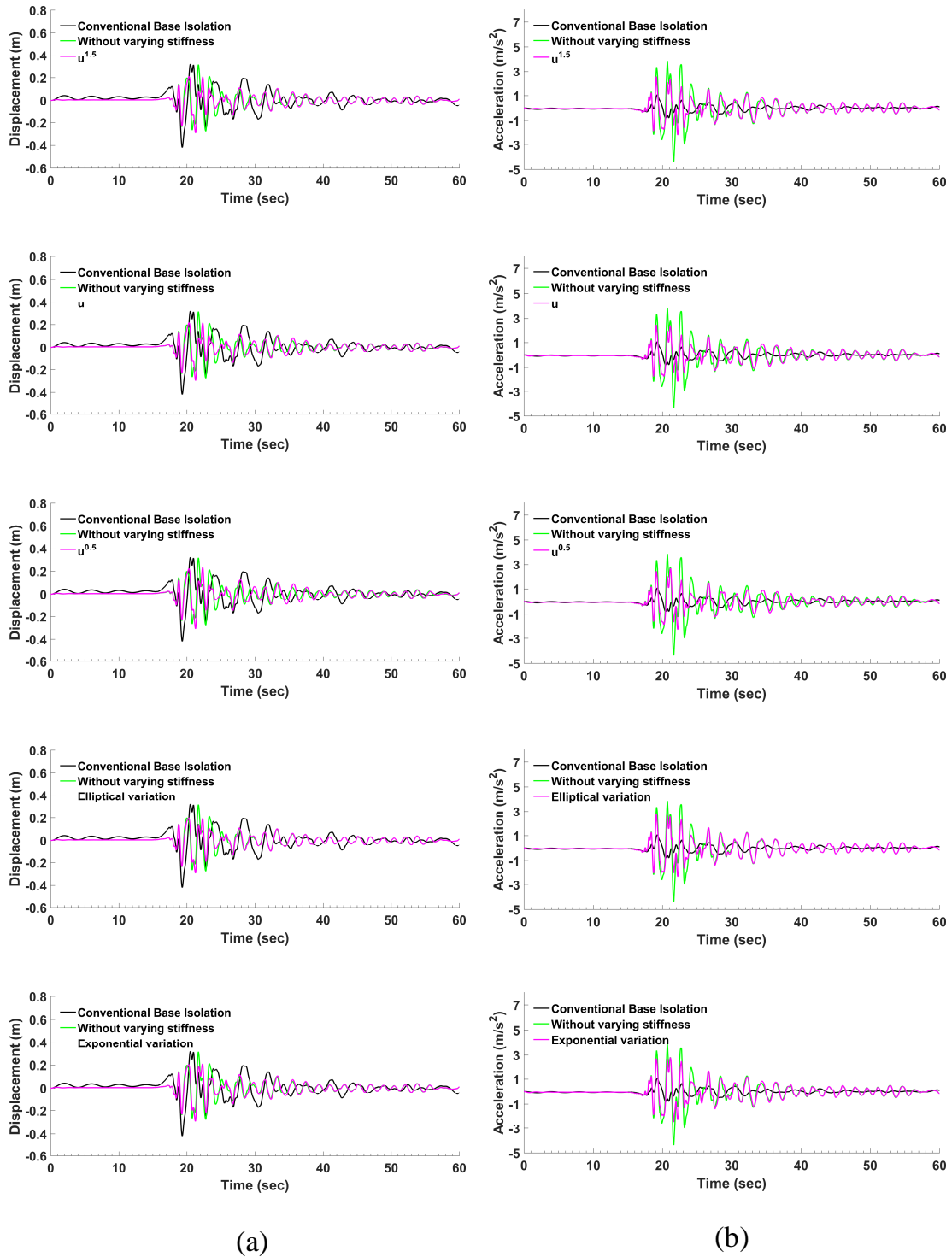


Fig. 2-17: Time history response comparison between the conventional base isolation and the proposed systems excited by Ojjiya for varying negative stiffness: (a) relative displacement (b) absolute acceleration

optimal values of the following parameters are found to satisfy both the allowable displacement and the acceleration responses ($u < 0.3$ m and $\ddot{u} < 3.0$ m/s²): total damping ratio $h_t = 0.15$, natural frequency $f_s (= \omega_s/2\pi) = 2.015$ Hz, damping constant $h_s = 0.042$, and initial natural frequency of negative stiffness $f_{no} (= \omega_{no}/2\pi) = 1.936$ Hz. Values of slope (κ) = 55, 25 and 10 are assumed for Eqs. (2.5), (2.6) and (2.7), respectively. Change in stiffness of negative stiffness $\Delta k = 20$ and parameter $a = 0.1$ are chosen for Eqs. (2.8) and (2.9), respectively.

2.5.1 Time history responses due to near-fault ground motion

Figs. 2-16 and **2-17** show the time history of the relative displacements u (with respect to the ground) and the absolute acceleration $\ddot{u} + \ddot{u}_g$ of the isolated object when excited by Kobe and Ojiya respectively using Eqs. (2.5), (2.6), (2.7), (2.8) and (2.9) for varying stiffness compared against the response of the conventional base isolation system. The maximum response amplitudes are indicated in the **Table 2-1**. The maximum displacement response decreases by 28% on average relative to the conventional base isolation system using Eqs. (2.5), (2.6), and (2.7) for both Kobe and Ojiya. Varying stiffness using Eqs. (2.8) and (2.9), displacement response decreases by 20% for Kobe and 30% for Ojiya.

When comparing with the conventional base isolation system, the acceleration response increases markedly without the variation in the stiffness. The acceleration response, however, remains within the allowable range with the variation in the stiffness. In the case of stiffness variation, the acceleration response decreases noticeably while compared to the case without any variation of the stiffness.

Table 2-1: Maximum amplitude of responses for all cases

| | Relative Displacement (m) | | | |
|------------------------------------|--|--------------|-------------------|------------------|
| | Kobe | Ojiya | Shin-Tokai | Tomakomai |
| Conv. | 0.326 | 0.420 | 0.675 | 0.438 |
| No variation | 0.292 | 0.314 | 0.162 | 0.067 |
| Power function $u^{1.5}$ (Eq. 2.5) | 0.246 | 0.294 | 0.230 | 0.068 |
| Power function u (Eq. 2.6) | 0.242 | 0.300 | 0.246 | 0.068 |
| Power function $u^{0.5}$ (Eq. 2.7) | 0.234 | 0.310 | 0.242 | 0.068 |
| Elliptical (Eq. 2.8) | 0.256 | 0.295 | 0.175 | 0.068 |
| Exponential (Eq. 2.9) | 0.261 | 0.294 | 0.192 | 0.068 |
| | | | | |
| | Absolute Acceleration (m/s²) | | | |
| | Kobe | Ojiya | Shin-Tokai | Tomakomai |
| Conv. | 0.815 | 1.073 | 1.677 | 1.084 |
| No variation | 3.840 | 4.381 | 2.065 | 0.865 |
| Power function $u^{1.5}$ (Eq. 2.5) | 2.128 | 2.530 | 1.835 | 0.812 |
| Power function u (Eq. 2.6) | 2.065 | 2.425 | 1.851 | 0.763 |
| Power function $u^{0.5}$ (Eq. 2.7) | 2.177 | 2.664 | 1.978 | 0.718 |
| Elliptical (Eq. 2.8) | 2.612 | 2.833 | 1.902 | 0.850 |
| Exponential (Eq. 2.9) | 2.684 | 2.805 | 1.934 | 0.806 |

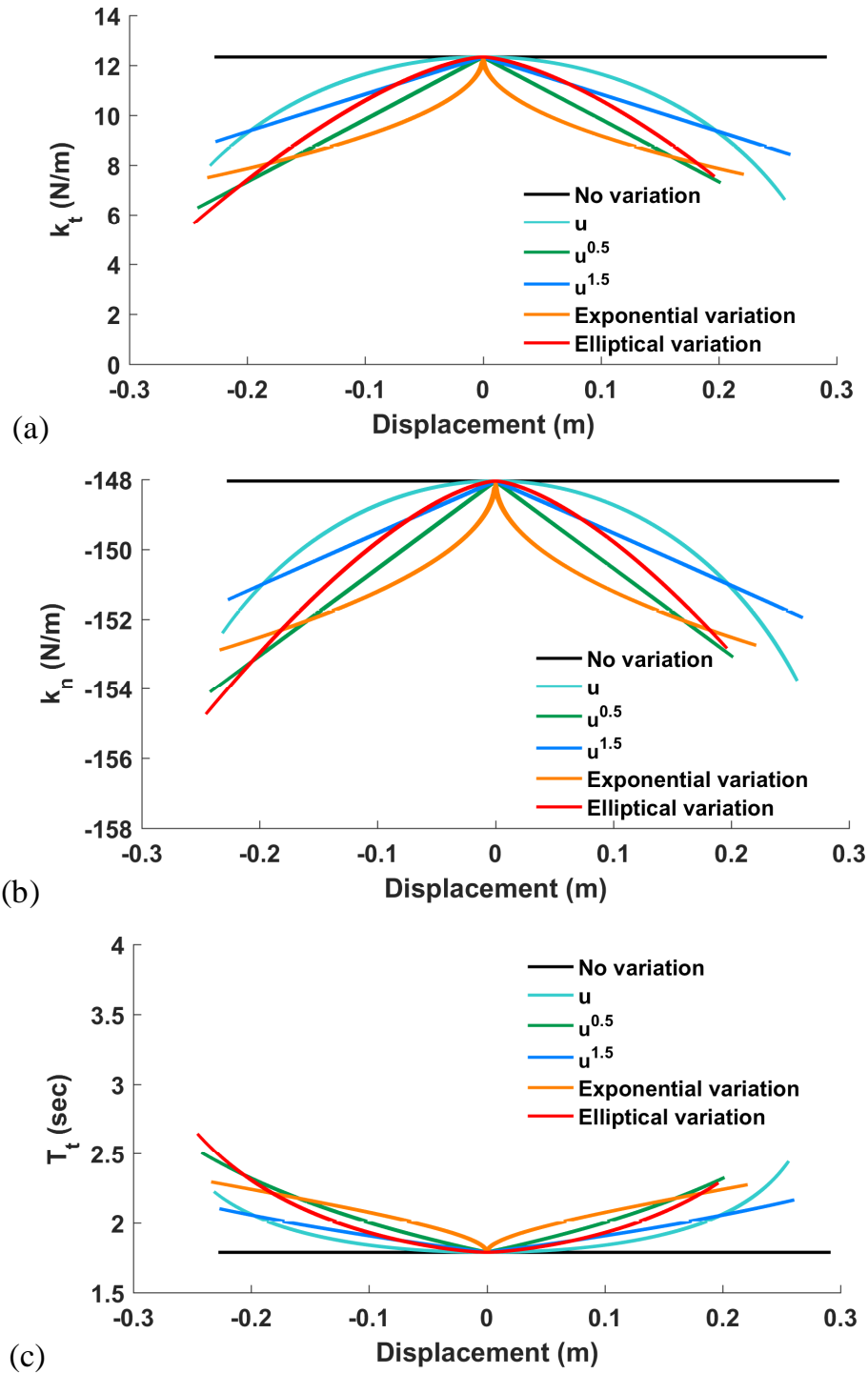


Fig. 2-18: Relationship between (a) total stiffness, (b) negative stiffness, and (c) period of the system with relative displacement for different variation of negative stiffness excited by Kobe.

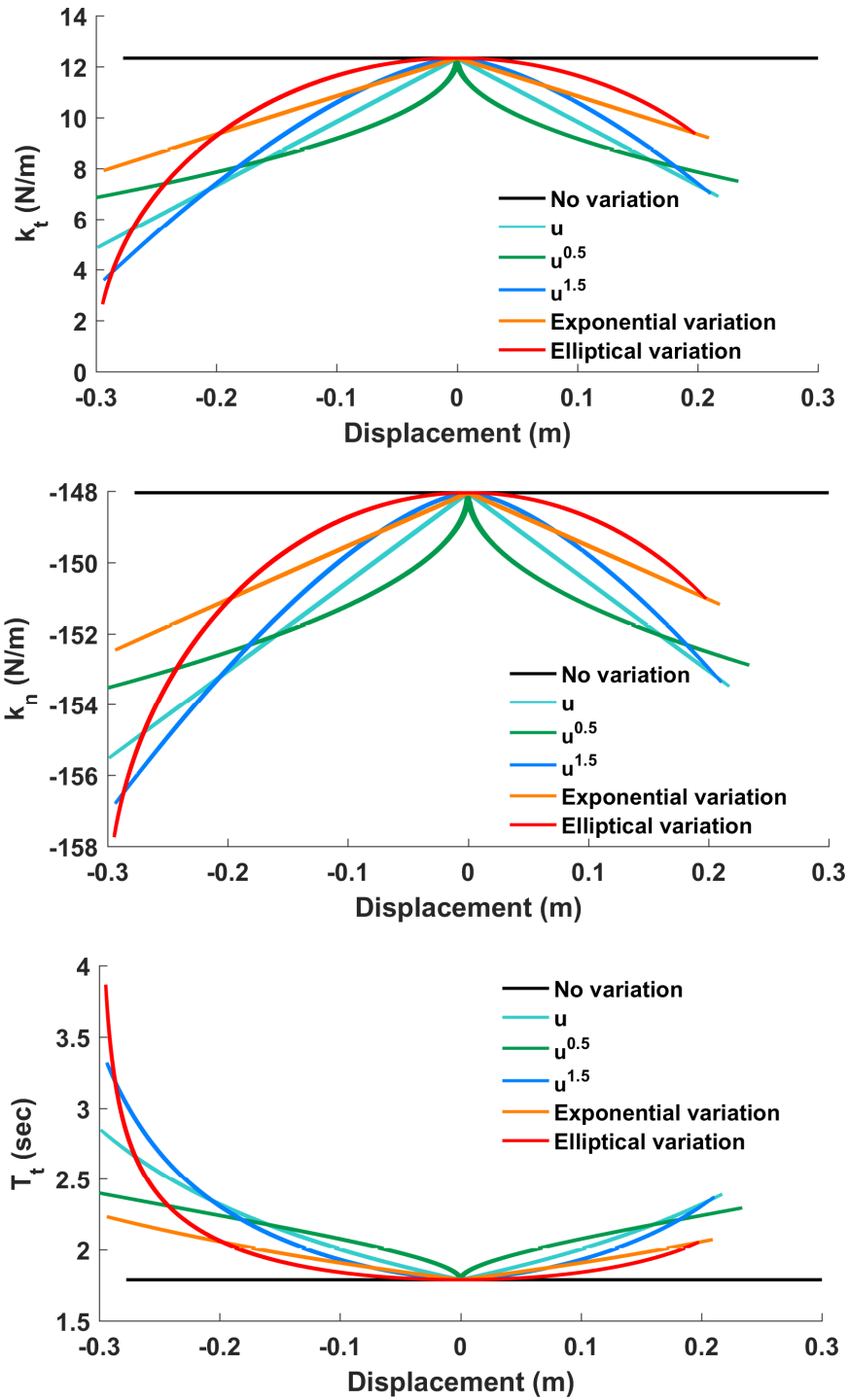


Fig. 2-19: Relationship between (a) total stiffness, (b) negative stiffness, and (c) period of the system with relative displacement for different variation of negative stiffness excited by Ojiya.

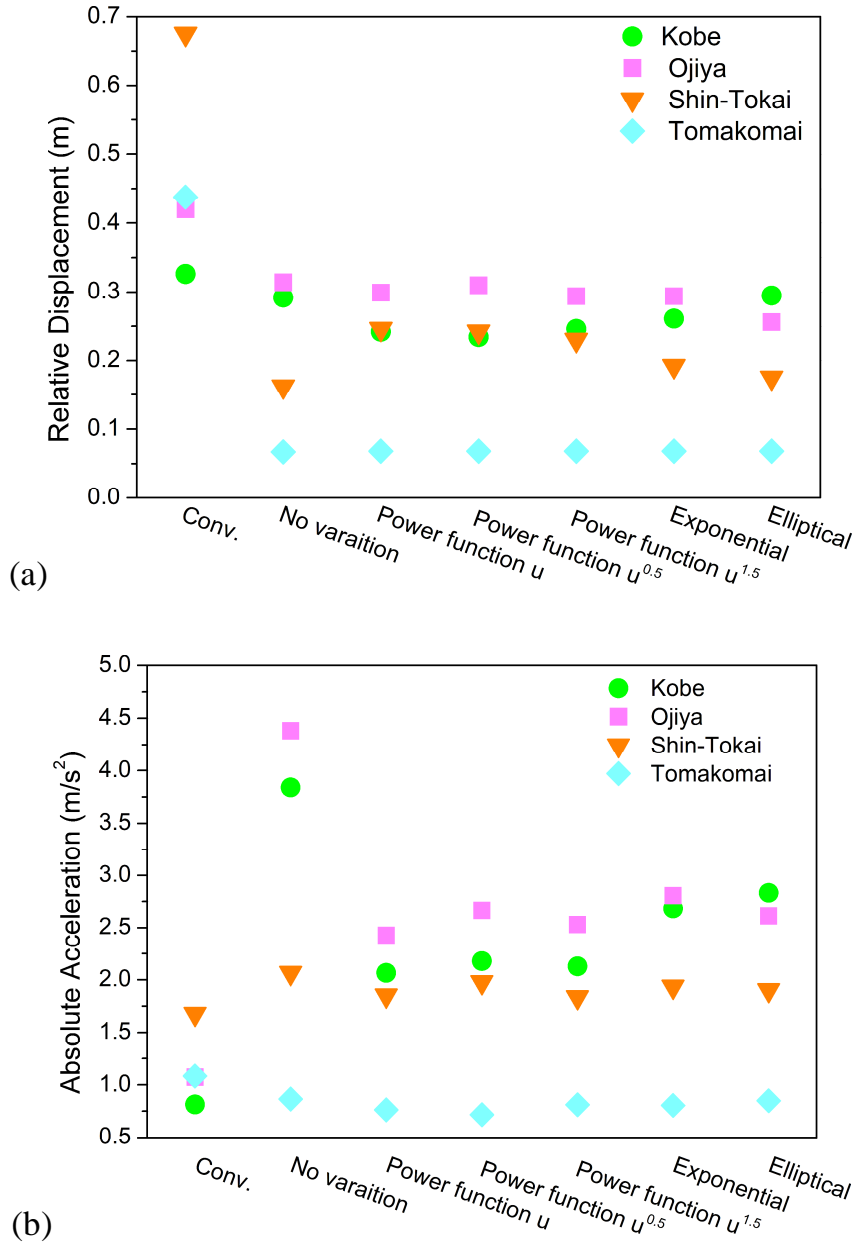


Fig. 2-20: Relationship between (a) relative displacement, (b) absolute acceleration of the system for different variation of negative stiffness compared with conventional (conv.) base isolation excited by both near-fault and long-period ground motions.

Figs. 2-18 and **2-19** show the relationship between the total stiffness of the system, the negative stiffness, and the period of the system with the relative displacement u of the base-isolated object (having unit mass) for Kobe and Ojiya respectively. **Figs. 2-18(a)** and

2-19(a) show that the total stiffness of the system decreases by 60% of the initial stiffness on average, increasing the period of the system to 2.5 s and 3.5 s for Kobe and Ojiya respectively (**Figs. 2-18(c)** and **2-19(c)**) for varying stiffness with higher order power function (Eq. (2.5)). The maximum amplitudes of the response are shown in **Fig. 2-20** compared with the conventional base isolation system. **Fig. 2-20** indicates that for the proposed system with no variation in the stiffness, the maximum acceleration response increase for Kobe and Ojiya, respectively, as compared to the other cases. With varying the stiffness using Eqs. (2.5), (2.6) and (2.7) the displacement responses decreases for the near-fault ground motions except for the case of Ojiya using Eq. (2.7) ($u^{0.5}$) as compared with no variation of the stiffness. Similarly, using Eqs. (2.8) and (2.9) displacement responses for near-fault ground motions increases compared to using other equations. In addition, the maximum absolute acceleration decreases for the proposed model using all equations as compared to without any variation.

2.5.2 Time history responses due to long period ground motion

Figs. 2-21 and **2-22** show the time histories of the isolated object when excited by Shin-Tokai and Tomakomai respectively using Eqs. (2.5), (2.6), (2.7), (2.8) and (2.9) for varying stiffness compared against the response of the conventional base isolation system. The maximum response amplitudes are indicated in **Table 2-1**. It shows that the displacement response reduces by 75% on average and the acceleration response increases slightly for all cases for Shin-Tokai and decreases for Tomakomai while compared to the conventional base isolation system. With varying the stiffness, the acceleration response decreases, and the displacement response tends to increase for Shin-Tokai and same for Tomakomai when compared to the case with no variation in the stiffness for all equations of variation.

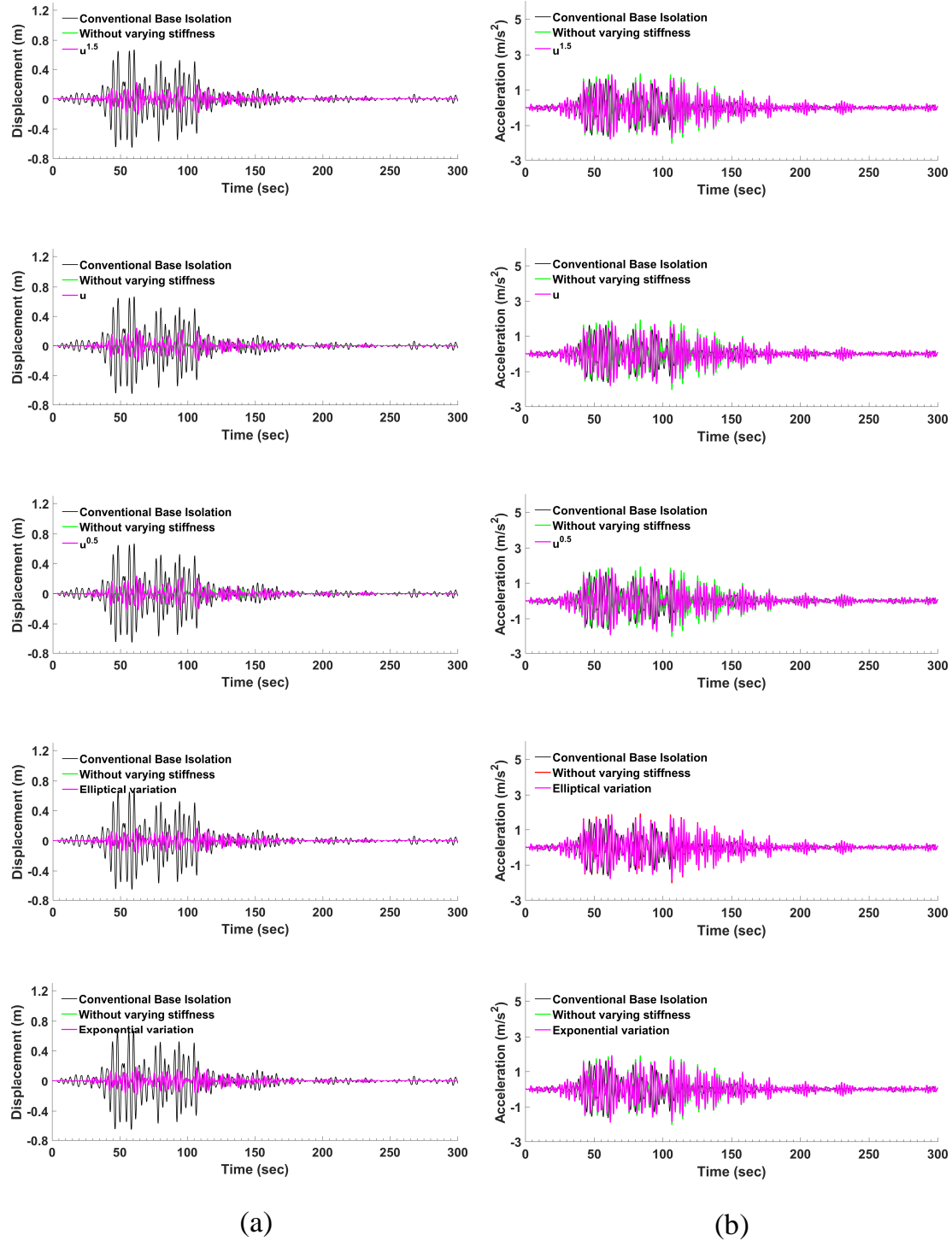


Fig. 2-21: Time history response comparison between the conventional base isolation and the proposed systems excited by Shin-Tokai for varying negative stiffness: (a) relative displacement (b) absolute acceleration

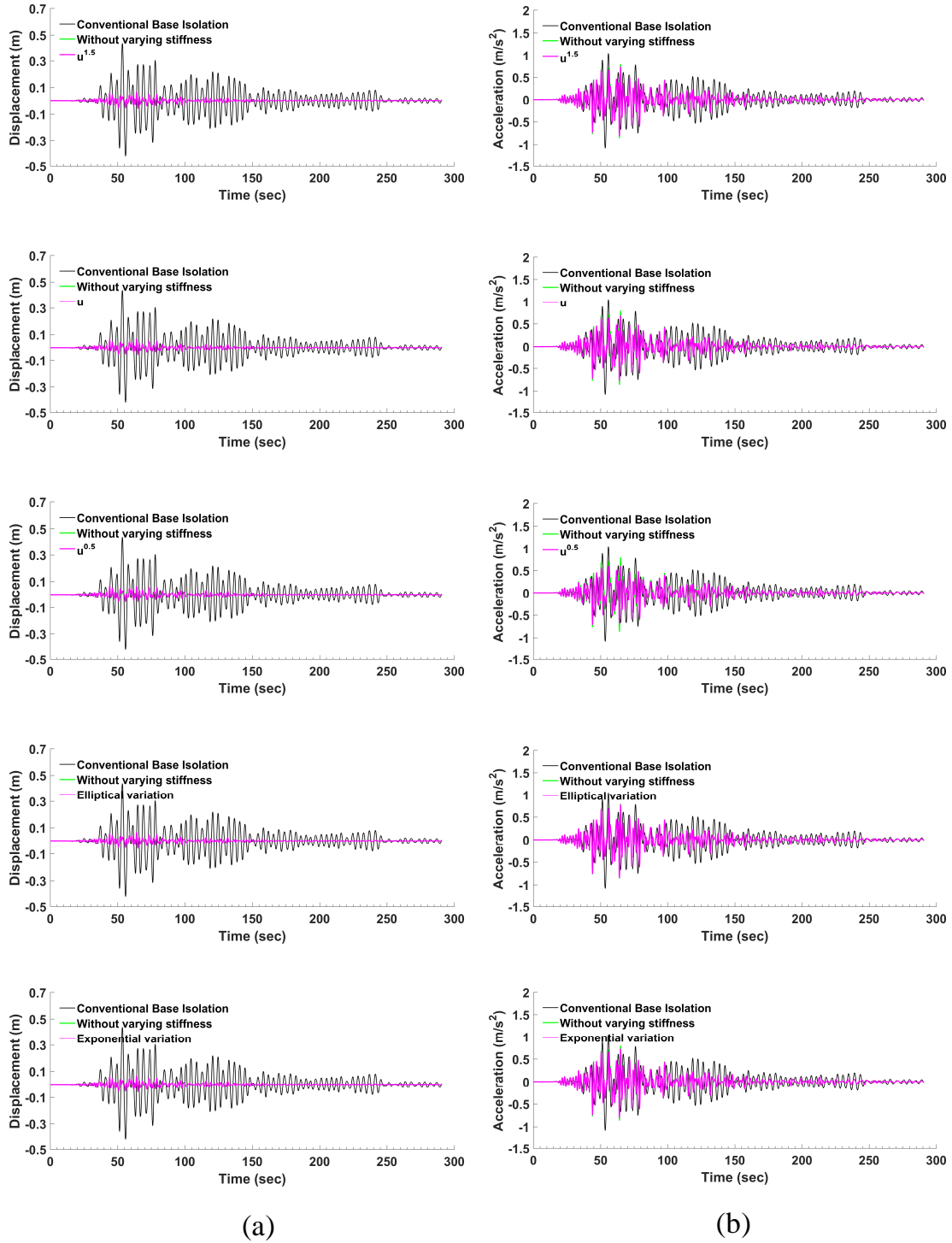


Fig. 2-22: Time history response comparison between the conventional base isolation and the proposed systems excited by Tomakomai for varying negative stiffness: **(a)** relative displacement **(b)** absolute acceleration

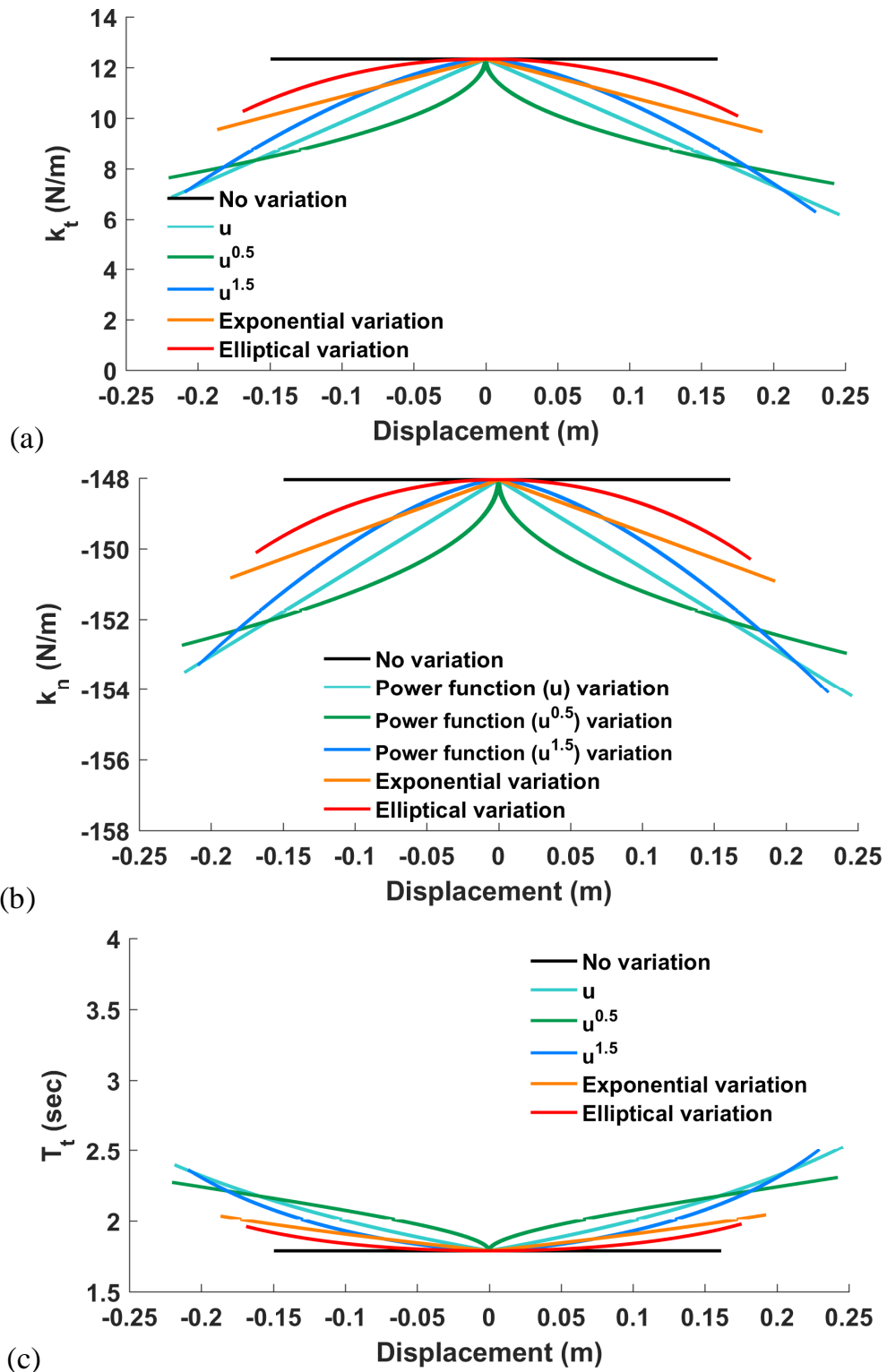


Fig. 2-23: Relationship between (a) total stiffness, (b) negative stiffness, and (c) period of the system with relative displacement for different variation of negative stiffness excited by Shin-Tokai.

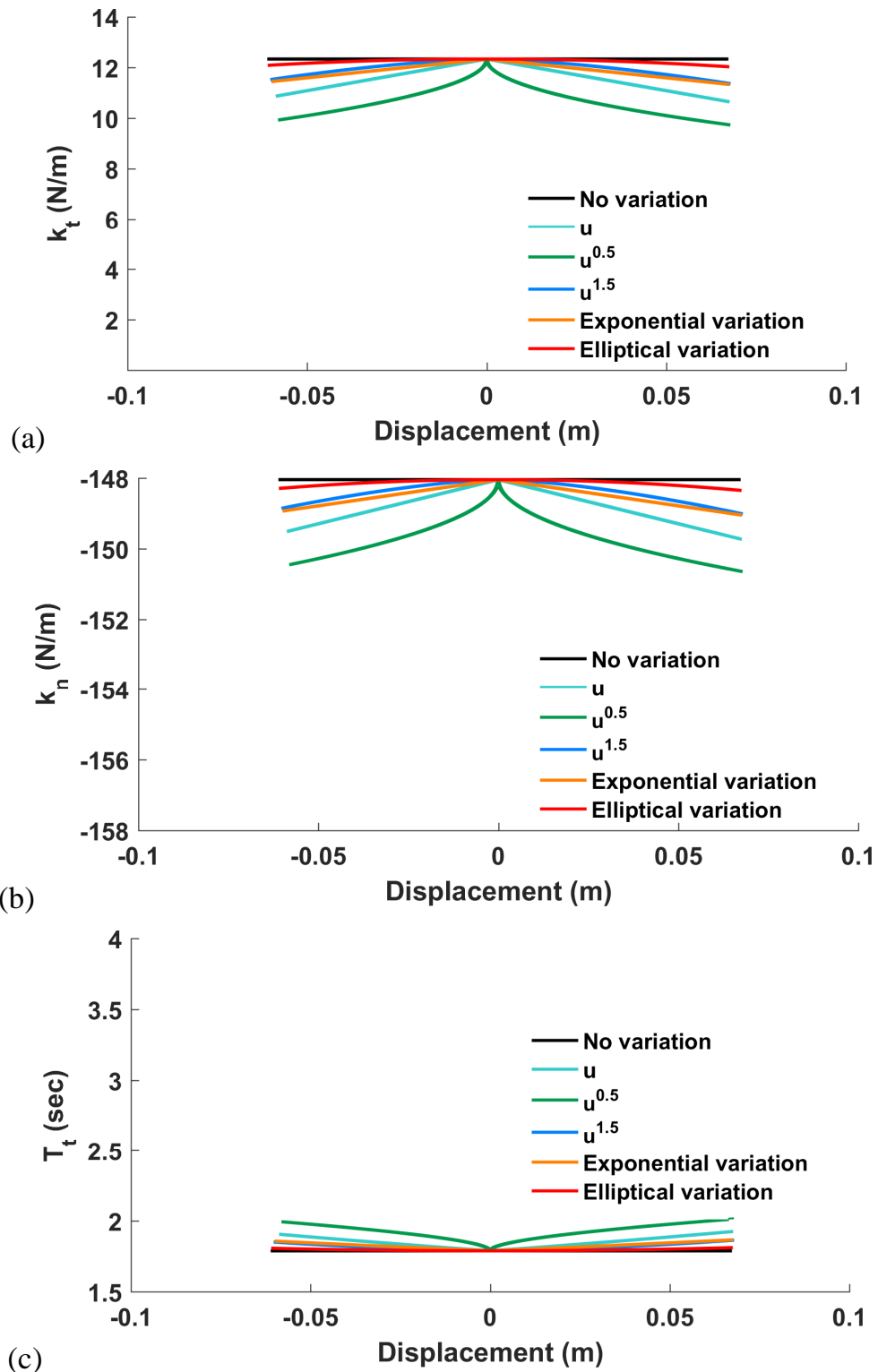


Fig. 2-24: Relationship between (a) total stiffness, (b) negative stiffness, and (c) period of the system with relative displacement for different variation of negative stiffness excited by Tomakomai.

Figs. 2-23 and **2-24** show the relationship between the total stiffness of the system, the negative stiffness, and the period of the system with the relative displacement u of the base-isolated object (having unit mass) for Shin-Tokai and Tomakomai respectively. **Fig. 2-23(a)** shows that the stiffness of the system is half of the initial stiffness, increasing the period of the system to around 2.5 s (**Fig. 2-23(c)**) for varying stiffness with higher order power function (Eq. (2.5)) when exciting base-isolated object by Shin-Tokai. In addition, maximum amplitudes of the response compared with the conventional base isolation system are shown in **Fig. 2-20**. This figure indicates that for the proposed system with no variation in the stiffness, the maximum displacement response decreases by 75% and 85% compared to the conventional base isolation system when excited by Shin-Tokai and Tomakomai, respectively. Accordingly, the maximum acceleration response increases for Shin-Tokai and decreases for Tomakomai as compared to the conventional base isolation system. When stiffness varies, the displacement response increases within allowable limit and the acceleration response decreases slightly for the proposed system using all the equations used in this study.

2.6 Discussion

Based on the carried out numerical analyses, it can be inferred that by using the proposed system without varying the stiffness, even though the displacement response reduces markedly, the acceleration response increases above the allowable limit ($\ddot{u} < 3.0 \text{ m/s}^2$) for the near-fault ground motions due to its large stiffness while compared to the conventional base isolation system. Varying the stiffness (increase in the period) of the system plays an important role in reducing the acceleration response of the base-isolated objects subjected to near-fault ground motion. The decrease in the stiffness of the system leads to decrease in the critical damping coefficient which increases the damping ratio of

the system. Thus, a further decrease in displacement response occurs due to the increase in damping. **Fig. 2-20** and **Table 2-1** shows that in contrast to the conventional base isolation system, a considerable decrease in the displacement response and an increase in the acceleration response within allowable limits can be expected when the negative stiffness is varied with Eqs. (2.5), (2.8) and (2.9) for both the near-fault and the long-period ground motions.

2.7 Conclusions

Based on the carried-out study, the following conclusions can be drawn:

- the conventional base isolation system, in general, shows a small acceleration response while an unacceptably large displacement response during earthquakes. This study proposes a base isolation system incorporating negative variable stiffness for reducing the displacement response under both the near-fault and the long-period ground motions. Negative stiffness is varied using different power functions in terms of the displacement response of the isolated objects.
- time history responses of the proposed model with and without varying the stiffness subjected to both types of ground motions are compared. Without any variation of the negative stiffness, the model shows a small displacement response besides the large acceleration response. In order to reduce the acceleration response, variation in the stiffness is required. The decrease in the stiffness increases the period of the system, thereby decreasing the acceleration response.
- while compared to conventional base isolation system, using high order power of u ($u^{1.5}$), elliptical and exponential functions in the proposed model, the maximum displacement of the isolated object reduced by 25% under the near-fault

ground motion while by 65% under the long-period ground motion.

- the maximum achieved absolute acceleration of the base-isolated object with the proposed system is less than 3.0 m/s^2 while the relative displacement is less than 0.3 m for both types of the earthquake ground motions.

CHAPTER 3

BASE ISOLATION SYSTEM WITH NEGATIVE-VARIABLE POSITIVE MECHANICAL UNIT

3.1 Background and objectives

Above study mainly focuses on the performance of base isolation system using negative stiffness varying with different equations (such as power function, elliptical and exponential). In this study, to define the values of different parameters, parametric studies are conducted. It is found that varying negative stiffness with higher order power function Eq. (2.5), Exponential Eq. (2.8) and Elliptical Eq. (2.9) functions are effective in reducing displacement response of the base isolated object subjected to both near-fault and long-period ground motions. Furthermore, in the practical viewpoint varying negative stiffness is quite a difficult job. Therefore, this study focuses on the development of a new external device which can perform similar to varying negative stiffness with Eqs. (2.5), (2.8) and (2.9) for modifying the performance of existing base isolation systems.

This study proposes a new external device to mitigate both the displacement and acceleration responses of base-isolated objects subjected to both near-fault and long-period ground motions simultaneously at the same time. This device consists of a unit having a negative spring and a variable positive spring arranged in series, which varies its total negative stiffness. Since all springs comprising the unit are elastic linear, residual displacement never occurs after earthquakes at all. Thus, the objectives of this study are:

- 1) to propose a negative-variable positive mechanical unit for varying total negative

stiffness and to verify its performance; 2) to study the effectiveness of the different parameters (such as slope of linear function and damping ratio) in the unit incorporated on the isolation system and to find the appropriated parameters satisfying the allowable limits of both the displacement and acceleration responses for practical use; and 3) to verify the performance of the proposed systems by comparing with the conventional isolation systems.

3.2 Negative-positive spring systems

3.2.1 Stiffness variation of Negative-positive spring unit

Stiffness is the properties of the material to counteract the external force. In case of positive stiffness, the direction of both the deformation and the applied external force are in the same direction and the corresponding reaction force returns the deformed body to its neutral position. On the other hand, negative stiffness generates a force on a body that acts in the same direction in which the body is displaced and generates larger forces with increasing displacement. Hence, negative stiffness itself is unstable. If the positive and negative springs are arranged in series with the condition that the stiffness of the positive spring is greater than that of the absolute value of the negative spring, negative spring becomes stable and can generate a wide range of variation in the total stiffness which will be negative. To verify this performance, a negative spring and a positive spring arranged in series referred as “NP unit” hereafter is considered as shown in **Fig. 3-1**; the relation between the springs is given by:

$$k_p = \alpha |k_n| \quad (3.1)$$

where, k_n and k_p are stiffnesses of the negative and the positive springs, respectively, and

α is a parameter with a value greater than 1.

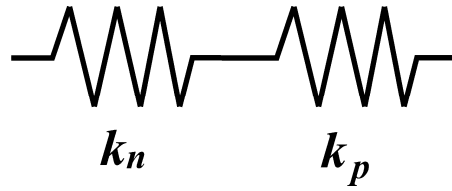


Fig. 3-1: Negative-Positive spring unit (NP unit).

The total stiffness (k^*) of the ‘NP unit’ can be written as:

$$k^* = \frac{1}{\frac{1}{k_n} + \frac{1}{k_p}} = \frac{k_n k_p}{k_p + k_n} = \frac{k_n \alpha |k_n|}{\alpha |k_n| + k_n}$$

$$k^* = \frac{\alpha}{1 - \alpha} |k_n| \tag{3.2}$$

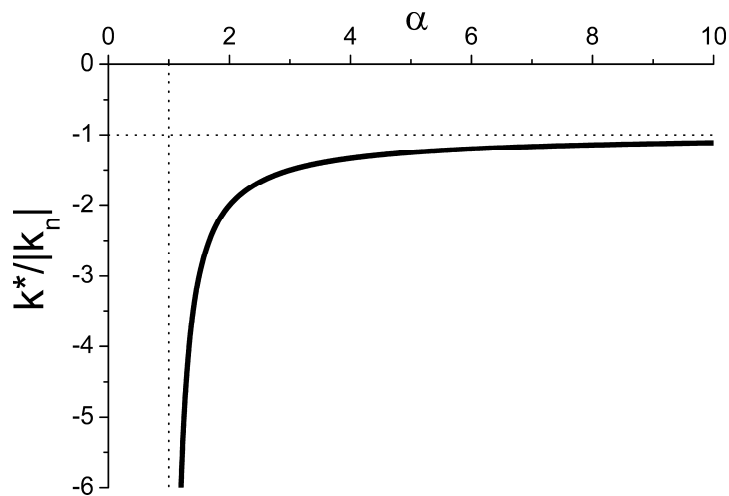


Fig. 3-2: Relationship between stiffness of NP unit and parameter α .

Eq. (3.2) shows that for every value of $\alpha (> 1)$, negative and positive springs arranged in series generate negative stiffness that is always less than k_n as seen in **Fig. 3-2**. The figure

shows that from the variation of the parameter α , a wide range of negative stiffness and a rapid change in stiffness of NP unit can be realized. This suggests that applying a conventional stiffness controllable system for varying the parameter α may result in a substantial variation in the total stiffness of the base isolation systems.

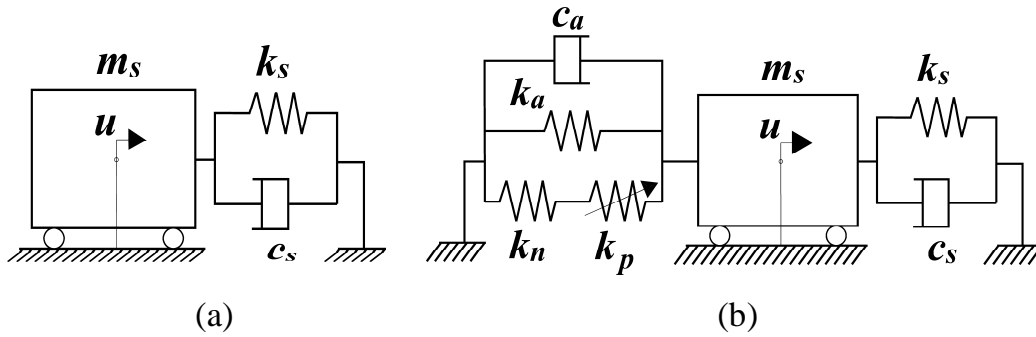


Fig. 3-3: Models of base isolation systems: **(a)** Conventional base isolation system; **(b)** Model I.

3.2.2 Configuration of base isolation systems with a negative-positive spring unit

In this section, an external device using NP unit is proposed. A conventional base isolation system is shown in **Fig. 3-3(a)**. The spring constant and damping coefficient of the base isolation system are denoted by k_s and c_s respectively. **Fig. 3-3(b)** shows a base isolation system incorporating the proposed device. This device consists of NP unit arranged in parallel with a positive spring and a damper. The positive spring stabilizes the proposed device under solitary state due to the fact that NP unit has negative stiffness and is not stable on its own. The damper indicates intrinsic damping such as friction in the mechanical components or additional damping for actively functioning of the system.

With the foregoing discussions that an NP unit shows a change in negative stiffness, it is enticing to speculate how the variation of the parameter α works for mitigating the

acceleration and displacement responses against various earthquake waves. In the current study, it is assumed that the variation of the parameter α is a function of the relative displacement of the isolated object with respect to the base. Reasons for this assumption are: (a) stiffness of a base isolation system is directly related to its natural period, which affects the acceleration and displacement responses at each position of the isolated object; (b) position of an isolated object can easily be captured in both active and passive control systems through electrical sensors or mechanical transmissions.

In the following sections, numerical simulation is used to verify the performance of base isolation system with the proposed device in response to near-fault and long-period ground motions. In the verification process, responses of the following base isolation systems are computed and compared: (i) a conventional base isolation system, as shown in **Fig. 3-3(a)**; and (ii) a base isolation system with the proposed device, as shown in **Fig. 3-3(b)** (referred to as ‘Model I’). To compare the performance of the proposed device without any additional damper and without varying stiffness of the system, two additional models are considered as follows: (i) a base isolation system with the proposed device without a damper arranged in parallel (referred to as ‘Model II’); and (ii) a base isolation system with the proposed device without the variation of the parameter α (referred to as ‘Model III’).

3.3 Base isolation models

3.3.1 Conventional base isolation model

The conventional base isolation system is represented by the model as shown in **Fig. 3-3(a)**. The base isolation system has lateral stiffness k_s and damping c_s where the base-isolated object is assumed to have a lumped mass m_s . The relative displacement of the

lumped mass m_s with respect to the base is denoted as u . The response of the conventional base isolation system, when excited by ground acceleration, \ddot{u}_g can be written as:

$$m_s (\ddot{u} + \ddot{u}_g) + c_s \dot{u} + k_s u = 0 \quad (3.3)$$

Eq. (3.3) can be rewritten as follows:

$$\ddot{u} + 2h_s \omega_s \dot{u} + \omega_s^2 u = -\ddot{u}_g \quad (3.4)$$

where, $\omega_s = \sqrt{k_s/m_s}$ is the natural circular frequency of the base isolation system and $h_s = c_s/2\sqrt{m_s k_s}$ is the damping constant of the system.

3.3.2 Proposed Models

Fig. 3-3(b) shows a base isolation system with the proposed device comprised of an NP unit (having variable positive spring stiffness) with an additional spring/damper element arranged in parallel. As per the assumptions, the variation of the parameter α is a function of the relative displacement u of the isolated object with respect to the base. The parameter α is expressed as:

$$\alpha = \alpha_o - \kappa |u| \quad (3.5)$$

where, α_o is a parameter which defines the initial value of k_p , $\kappa(\geq 0)$ is the slope for changing the value of the parameter α .

The total stiffness (k_{n-p-a}) of the proposed device is given by:

$$k_{n-p-a} = k_a + k^* \quad (3.6)$$

Eq. (3.6) can be rewritten as follows:

$$\omega_{n-p-a}^2 = \omega_a^2 - \omega_{n-p}^2 = \omega_a^2 + \frac{\alpha}{1-\alpha} \omega_n^2$$

$$T_{n-p-a} = \frac{1}{\sqrt{\frac{1}{T_a^2} - \frac{1}{T_{n-p}^2}}} = \frac{1}{\sqrt{\frac{1}{T_a^2} + \frac{\alpha}{1-\alpha} \frac{1}{T_n^2}}} \quad (3.7)$$

where, $\omega_{n-p} (= \sqrt{|k^*|/m_s})$ is the natural circular frequency of the NP unit, $\omega_n (= \sqrt{|k_n|/m_s})$ and $\omega_a (= \sqrt{k_a/m_s})$ are the natural circular frequencies of the negative spring and the additional spring, respectively and $k_a > |k^*|$ for stability the NP unit; T_{n-p} and T_{n-p-a} is a representative natural period of the NP unit and the proposed device respectively; $T_n = 2\pi/\omega_n$; and $T_a = 2\pi/\omega_a$.

The response of this isolation system, when excited by ground acceleration, \ddot{u}_g is derived from the following equation:

$$m_s (\ddot{u} + \ddot{u}_g) + (c_s + c_a) \dot{u} + k_{n-p-a} u + k_s u = 0 \quad (3.8)$$

Eq. (3.8) can be rewritten as follows:

$$\ddot{u} + (2h_s \omega_s + 2h_a \omega_s) \dot{u} + \left(\frac{\alpha_o - \kappa |u|}{1 - \alpha_o + \kappa |u|} \omega_n^2 + \omega_a^2 + \omega_s^2 \right) u = -\ddot{u}_g \quad (3.9)$$

where, $h_a = c_a / 2\sqrt{m_s k_s}$.

The equation of motion for Model II can be derived by substituting $h_a = 0$ in Eq. (3.9).

Similarly, the equation of motion for Model III can be derived by substituting $\kappa = 0$ in Eq.

(3.9).

The above Eq. (3.9) can be normalized as follows:

$$\begin{aligned} \frac{\ddot{u}}{\omega_{to}^2} + \left(2h_s \left(\frac{\omega_s}{\omega_{to}} \right) \left(\frac{1}{\omega_{to}} \right) + 2h_a \left(\frac{\omega_s}{\omega_{to}} \right) \left(\frac{1}{\omega_{to}} \right) \right) \dot{u} \\ + \frac{\omega_s^2}{\omega_{to}^2} \left(\frac{\alpha_o - \kappa|u|}{1 - \alpha_o + \kappa|u|} \frac{\omega_n^2}{\omega_s^2} + \frac{\omega_a^2}{\omega_s^2} + 1 \right) u = - \frac{\ddot{u}_g}{\omega_{to}^2} \end{aligned} \quad (3.10)$$

Eq. (3.10) shows that there are six parameters in this equation as shown below:

- ω_{to}
- h_s
- ω_s/ω_{to}
- h_a
- α_o
- κ

3.4 Basic properties, parameters and principle of isolation system with proposed external device

In this section, the fundamental properties of the proposed system are discussed in detail. In addition to this, the functioning of the proposed device based on the fundamental equations and important concepts need to account for those who deal with the production of the proposed device are also elaborated. Further, to enhance the performance of the proposed device, the parametric studies conducted are presented along with the input motions and model properties required for the time history analysis.

3.4.1 Fundamental parameters of proposed systems

The fundamental parameters of the proposed isolation systems are summarized in this section. The total stiffness k_t of the system as shown in **Fig. 3-3(b)** is given by:

$$k_t = k_s + k_{n-p-a} \quad (3.11)$$

The restoring force due to the spring components in the system is expressed as follows:

$$P = k_t u \quad (3.12)$$

And, the natural period of the proposed system (**Fig. 3-3(b)**) T_t can be written as:

$$T_t = \frac{2\pi}{\sqrt{\frac{\alpha_o - \kappa |u|}{1 - \alpha_o + \kappa |u|} \omega_n^2 + \omega_a^2 + \omega_s^2}} \quad (3.13)$$

Furthermore, the total damping ratio h_t of the proposed system (**Fig. 3-3(b)**) is

$$h_t = \frac{c_s + c_a}{c_t} = (h_s + h_a) \sqrt{\frac{k_s}{k_t}} \quad (3.14)$$

where, c_t is the critical damping coefficient.

Eq. (3.2) indicates that k^* is negative because $\alpha > 1$. For such, the term $\frac{\alpha}{1 - \alpha} \frac{1}{T_n^2}$ in Eq.

(3.7) is negative. Hence, for the validity of Eq. (3.7), following criteria should be met:

$$\frac{1}{T_a^2} > \left| \frac{\alpha}{1 - \alpha} \frac{1}{T_n^2} \right|$$

Now, substituting relationship of α from Eq. (3.5), above relation becomes:

$$\begin{aligned} \frac{1}{T_a^2} > \frac{\alpha_o - \kappa |u_{max}|}{\alpha_o - \kappa |u_{max}| - 1} \frac{1}{T_n^2} \\ \therefore \kappa |u_{max}| < \frac{\left[\frac{T_n^2}{T_a^2} - 1 \right] \alpha_o - \frac{T_n^2}{T_a^2}}{\left[\frac{T_n^2}{T_a^2} - 1 \right]} \end{aligned} \quad (3.15)$$

where, u_{max} is the maximum relative displacement response of the base-isolated object.

The limitation represented by Eq. (3.15) not only depends upon the parameter T_n, T_a ,

α_o and $|u_{max}|$ but also depends on the total damping ratio h_t . This is because the maximum displacement response u_{max} of the isolated object decreases with the increase in the damping ratio. Eq. (3.15) shows that the slope κ is inversely proportional to $|u_{max}|$ i.e., $\kappa \propto 1/|u_{max}|$. Therefore, with the variation in the values of the parameter h_t , the parameter κ also varies. Thus, to enhance the performance of the proposed device, choosing the parameters α_o , h_t , and κ is important.

3.4.2 Functioning and principle for production of proposed device

Based on the Eqs. (3.6) and (3.11), the performance of the proposed device deal with the change in stiffness of the base isolation system. The change on stiffness further depend upon the different parameters such as T_a and T_{n-p} . Thus, the behavior of the proposed device is enhanced by the assumption that T_{n-p} is close to and greater than T_a i.e., stiffnesses $|k^*|$ and k_a are very close to each other with $k_a > |k^*|$. Further, varying the positive spring stiffness (k_p), the stiffness of NP unit $|k^*|$ approaches to the stiffness k_a i.e., the stiffness of the proposed device decreases. With decreasing the stiffness, the period of the proposed device increases (Eq.(3.7)) and if the period of the proposed device increases further, the resisting force of the device decreases. Due to this reason, total stiffness of the system can decrease significantly although the variation of the stiffness of the NP unit is not significant with the variation of α .

In order to generate the significant change in total stiffness of the system, engineers who deal with the production of the proposed device needs to account following: (i) k_a should be greater and closer to the absolute value of the stiffness of NP unit ($|k^*|$), (ii) the stiffnesses $|k^*|$ and k_a should be much stiffer than the stiffness k_s because with the stiffer NP unit $|k^*|$ and k_a , the amount of difference in the stiffness ($k_a - |k^*|$) is much more

influenceable as compared to the stiffness k_s . Further, varying the stiffness of positive spring of NP unit, even though, the difference $(k_a - |k^*|)$ decreases by very small amount, the proposed device stiffness varies from stiffer range to softer range. And, even with a small amount of difference in the stiffness of the proposed device, very significant change in total stiffness is generated.

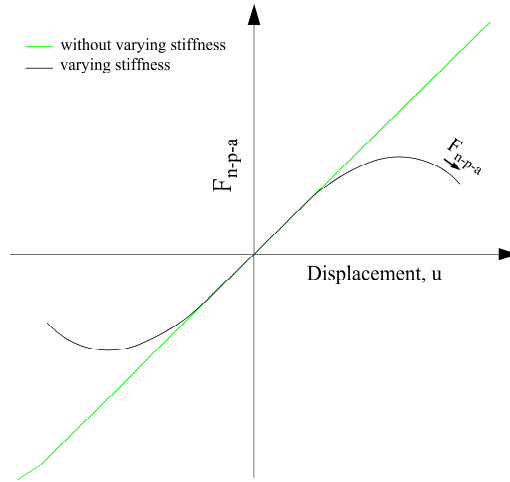


Fig. 3-4: Relationship between transmitting force due to proposed external device F_{n-p-a} and displacement of an isolated object compared with and without varying stiffness.

Fig. 3-4 shows the relationship between transmitting force to the system due to proposed external device F_{n-p-a} and displacement of isolated object compared with and without varying stiffness as explained above. It shows that with varying the stiffness k_p , force increases with an increase in the displacement of the isolated object up to certain value and then it decreases as the stiffness of the NP unit $|k^*|$ approaches to the stiffness k_a . The transmitting force due to external device with varying stiffness deviate from the transmitting force without varying stiffness. Increase in the transmitting force helps during long-period earthquakes as it makes isolated object difficult to move and the deviation of the transmitting force helps during near-fault ground motion as it reduces acceleration of isolated object by elongating period. The combination of negative and positive springs of

proposed external device, are the key elements for showing an above-described relationship, which is also the key feature of the proposed external device.

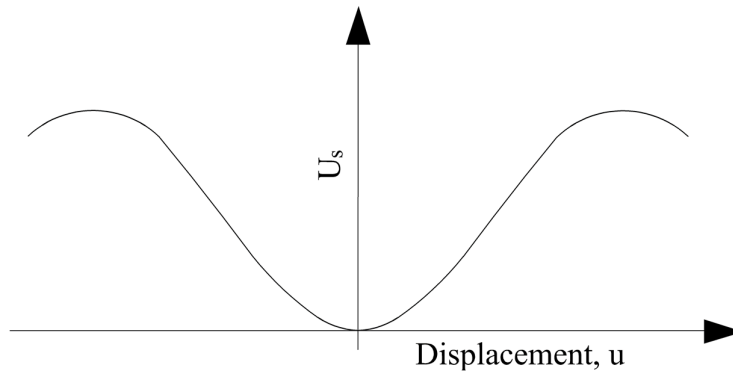


Fig. 3-5: Potential energy function of the proposed external device.

The stability of the proposed isolation system (external device incorporated to the conventional base isolation system) is also one of the key factors which is needed to be discussed. The stability of the mechanical system with springs can be judged by the potential energy. The potential energy function of the system for the force-displacement relationship as shown in **Fig. 3-4** might be represented by **Fig. 3-5**. The system is said to be in equilibrium when the system maintains the state of stable equilibrium. For the system to be in stable equilibrium, the derivative of the potential energy should be zero and potential energy should be minimum. **Fig. 3-5** shows that for large displacement, the potential energy might decrease. And for the displacement beyond the local maximum of the potential energy, the system is in unstable equilibrium. The system with varying stiffness tends to be unstable for the larger displacement so, to know the stability of the system for large displacement in the later part potential energy function of the system has also been discussed.

3.4.3 Input motions and model properties

The time history analysis of the proposed isolation models is carried out for different

earthquake records to verify the performance of the device. Both the proposed models and the conventional base isolation system are simply a single-degree-of-freedom system, as shown in Eqs. (3.4) and (3.9), respectively. Time history responses of the proposed models are performed by numerical integration using Newmark's method ($\beta = 1/6$), with a time interval Δt of 0.001 s. Newton-Rapson method is implemented for obtaining the converged responses. The following earthquake records: (i) Kobe NS 1995 (referred as Kobe), (ii) Ojiya EW 2004 (referred as Ojiya), (iii) Shin-Tokai EW (referred as Shin-Tokai), and (iv) Tomakomai EW 2003 (referred as Tomakomai) are employed as ground acceleration \ddot{u}_g to the systems which is described in detail in Chapter 2, Section 2.3. For the conventional base isolation system, natural frequency is assumed to be $f_s (= \omega_s/2\pi) = 0.25$ Hz, and damping constant to be $h_s = 0.05$ s. In the time history analysis for the proposed device, $f_a (= \omega_a/2\pi) = 2$ Hz and $T_{n-p-a} = 2$ s are assumed.

3.4.4 Effectiveness of parameter α_o , h_t and κ

The parameter α_o defines the displacement of the node between negative and positive springs. Damping is also one of the parameters which affect the responses of the isolated object. The effects of damping are conferred in succeeding paragraph. To investigate the behavior of α_o , $h_t=15\%$ is chosen. **Fig. 3-6** shows that for a small value of α_o , although the displacement and acceleration responses reduce to the allowable range for both types of earthquake excitations (i.e., near-fault and long-period), the node displacement is still unacceptable for the near-fault ground motion. On the other hand, for a larger value of α_o , the displacement and acceleration responses and the node displacement tend to decrease as shown in **Fig. 3-6(c)**. Based on the parametric study, α_o should be greater than 15 and for this study, $\alpha_o = 20$ is chosen.

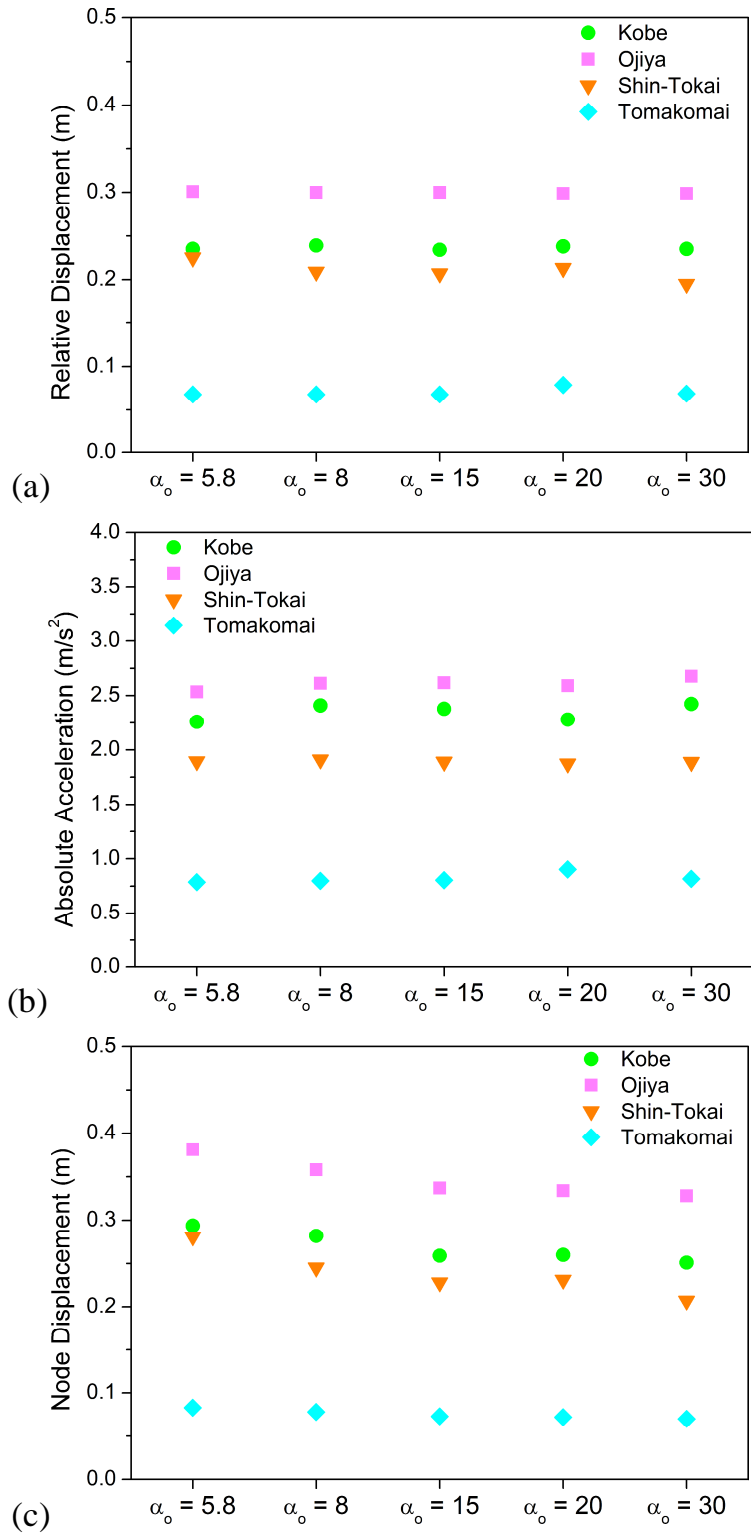


Fig. 3-6: (a) Maximum absolute acceleration (b) Maximum relative displacement and (c) Node displacement for various α_o when $\dot{h} = 15\%$.

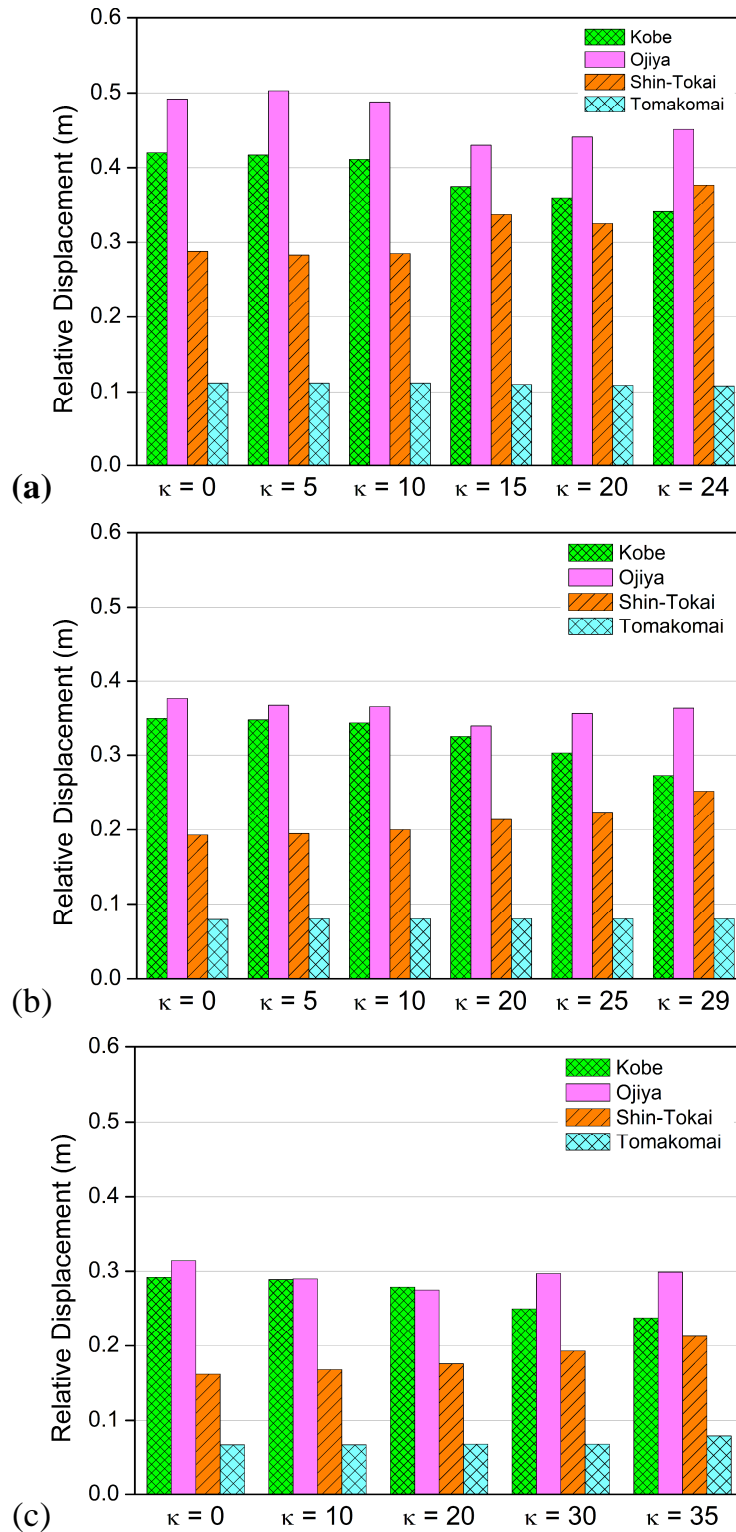


Fig. 3-7: Maximum amplitudes of the response of relative displacement for Model I **(a)** total damping ratio $\zeta = 5\%$, **(b)** total damping ratio $\zeta = 10\%$, **(c)** total damping ratio $\zeta = 15\%$.

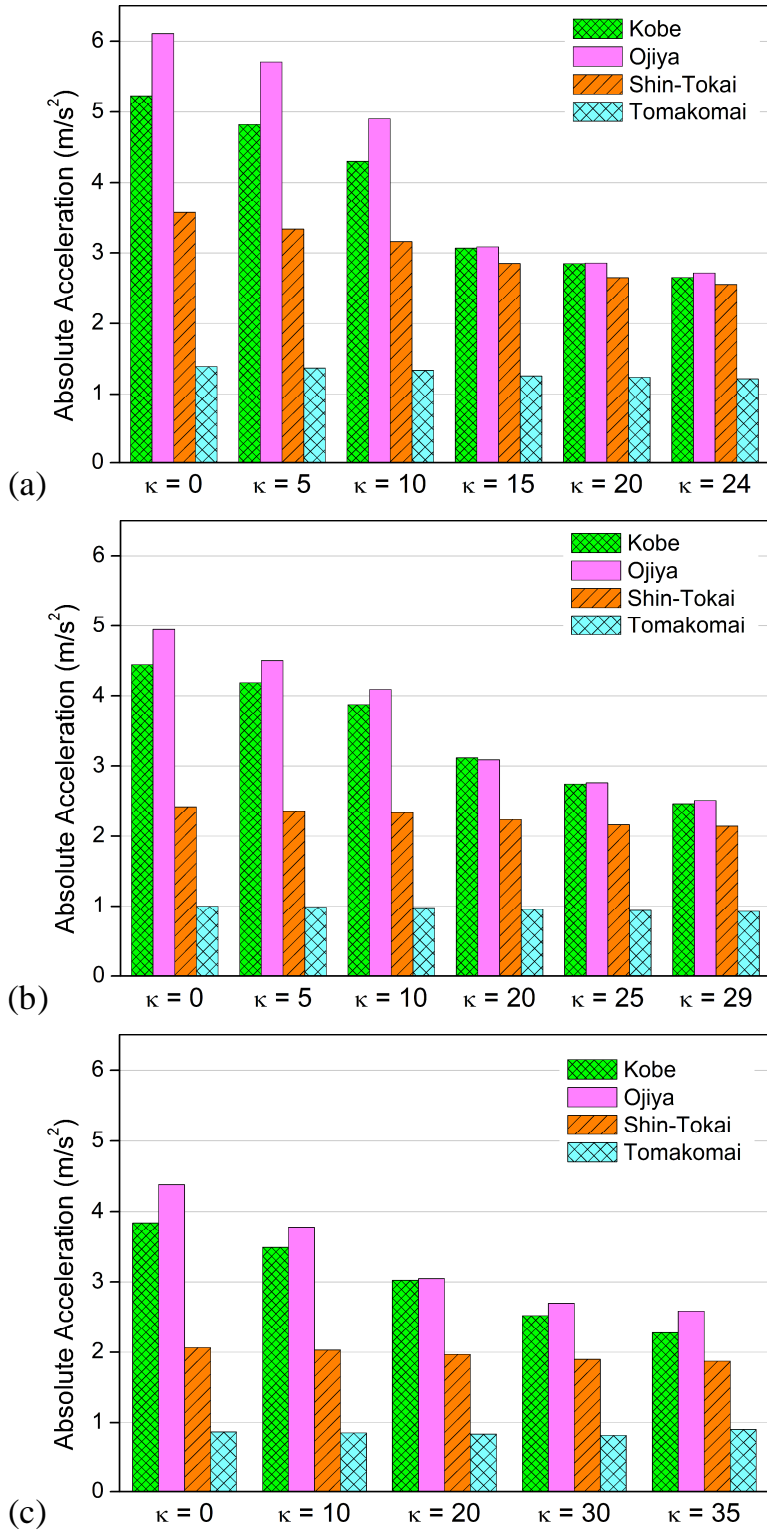


Fig. 3-8: Maximum amplitudes of the response of absolute acceleration of Model I (a) total damping ratio $\eta = 5\%$, (b) total damping ratio $\eta = 10\%$, (c) total damping ratio $\eta = 15\%$.

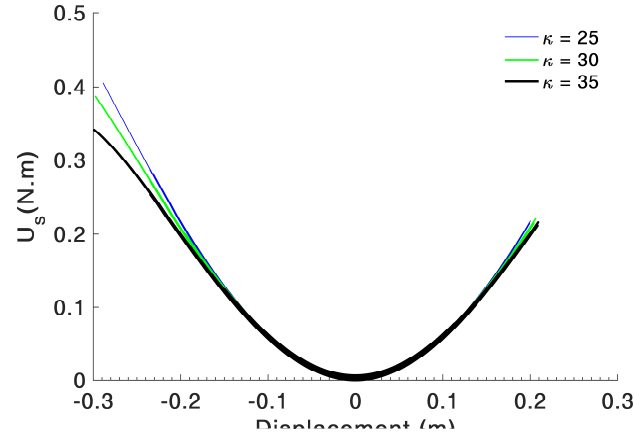


Fig. 3-9: Potential energy function of the proposed system various κ values when excited by Oijya.

Figs. 3-5 and **3-6** show the effect of parameter κ i.e., slope determining the value of α that enhance the performance of Model I. These figures show the relative displacement and absolute acceleration of the isolated object with Model I with varying slope κ and total damping ratio h_t . Increasing the total damping ratio h_t decreases the displacement and acceleration responses for both types of earthquake excitations. Further, **Figs. 3-5(c)** and **3-6(c)** ($h_t = 0.15$) show that with the increase in the slope (κ), displacement and acceleration responses decrease in the case of near-fault ground motion. In the case of long-period ground motion, displacement response tends to increase steadily but acceleration response is almost the same.

The change in the displacement is not noticeable but the decrease in the acceleration response with the increase in the slope (κ) for near-fault is almost half that of $\kappa = 0$ in comparison with $\kappa = 35$, which is the parameter that defines the effectiveness of Model I.

Figs. 3-7 and **3-8** indicate that for $\kappa > 20$ both the relative displacement and absolute acceleration are within the allowable ranges. Further, it is important to know the stability of the proposed isolation system. In order to confirm the stability of the system, potential energy U_s has been calculated. Potential energy of the system is obtained when the system

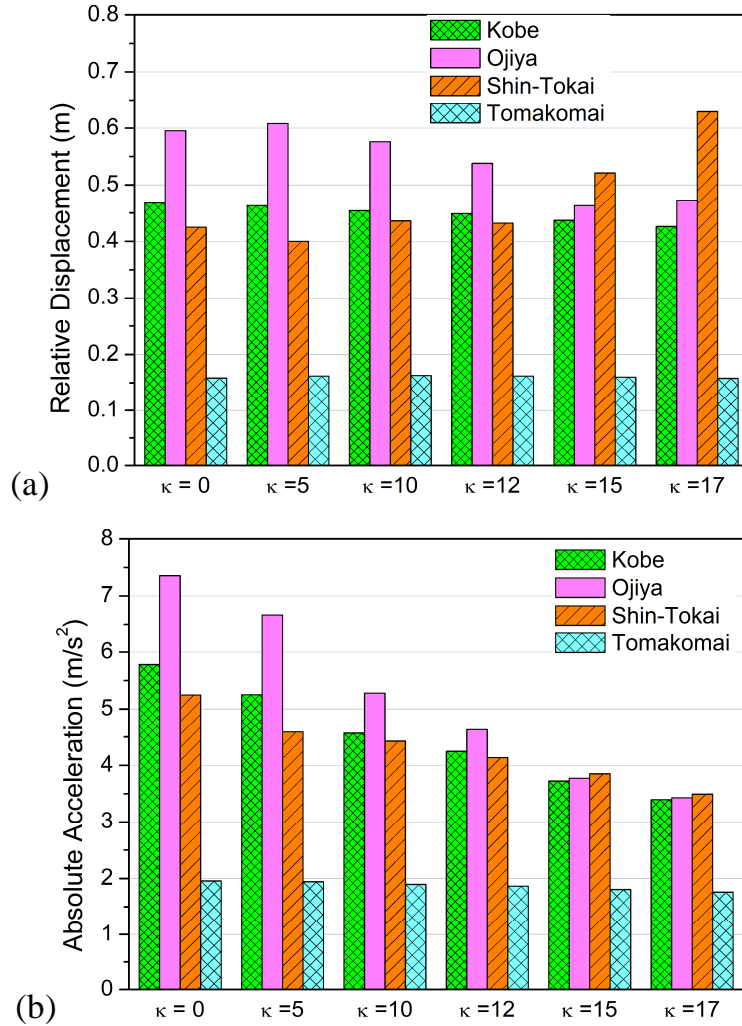


Fig. 3-10: Maximum amplitudes of (a) relative displacement and (b) absolute acceleration responses for Model II for various κ .

is excited only by Ojiya due to the fact that Ojiya has maximum displacement (**Fig. 3-7(c)**) and acceleration responses (**Fig. 3-8(c)**). **Fig. 3-9** shows the potential energy function of the system for various κ values when excited by Ojiya. It shows that potential energy (U_s) increases with increase in the displacement of isolated mass i.e., the stable equilibrium of the system is always maintained at $u = 0$ for all the values of κ . The figure also shows that, although with an increase in κ values potential energy tends to decrease, there is only one point of equilibrium (i.e., at $u = 0$) which is a point of stable equilibrium. Thus, the system is stable and in the current study, $\kappa=35$ is chosen. These parametric studies indicate

that Model I with $\alpha_o = 20$, $\kappa = 35$, and $h = 0.15$ achieves a significant reduction in the relative displacement and absolute acceleration.

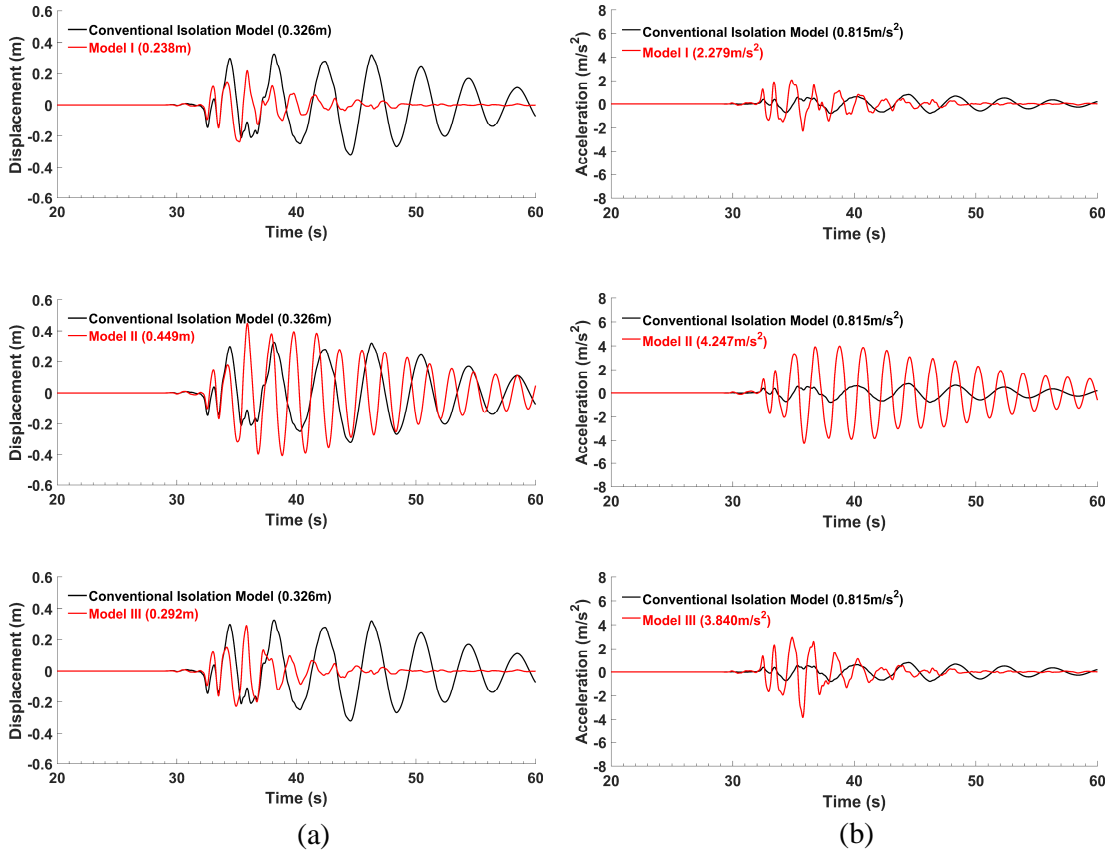


Fig. 3-11: Comparison of time history responses of (a) relative displacements and (b) response accelerations between the conventional base isolation system and the proposed models excited by Kobe NS 1995.

Fig. 3-10 shows the maximum displacement and acceleration responses for the variation of κ for Model II subjected to various earthquake waves. The figure shows that the acceleration response decreases with the increase in the slope κ while displacement response only slightly decreases, but after a certain value ($\kappa = 1.2$), response starts to increase mainly for long-period ground motion. Although, both the displacement and acceleration responses are above the allowable limits, $\kappa = 1.2$ is assumed for Model II to compare the performance of Proposed model (Model I) with other two models.

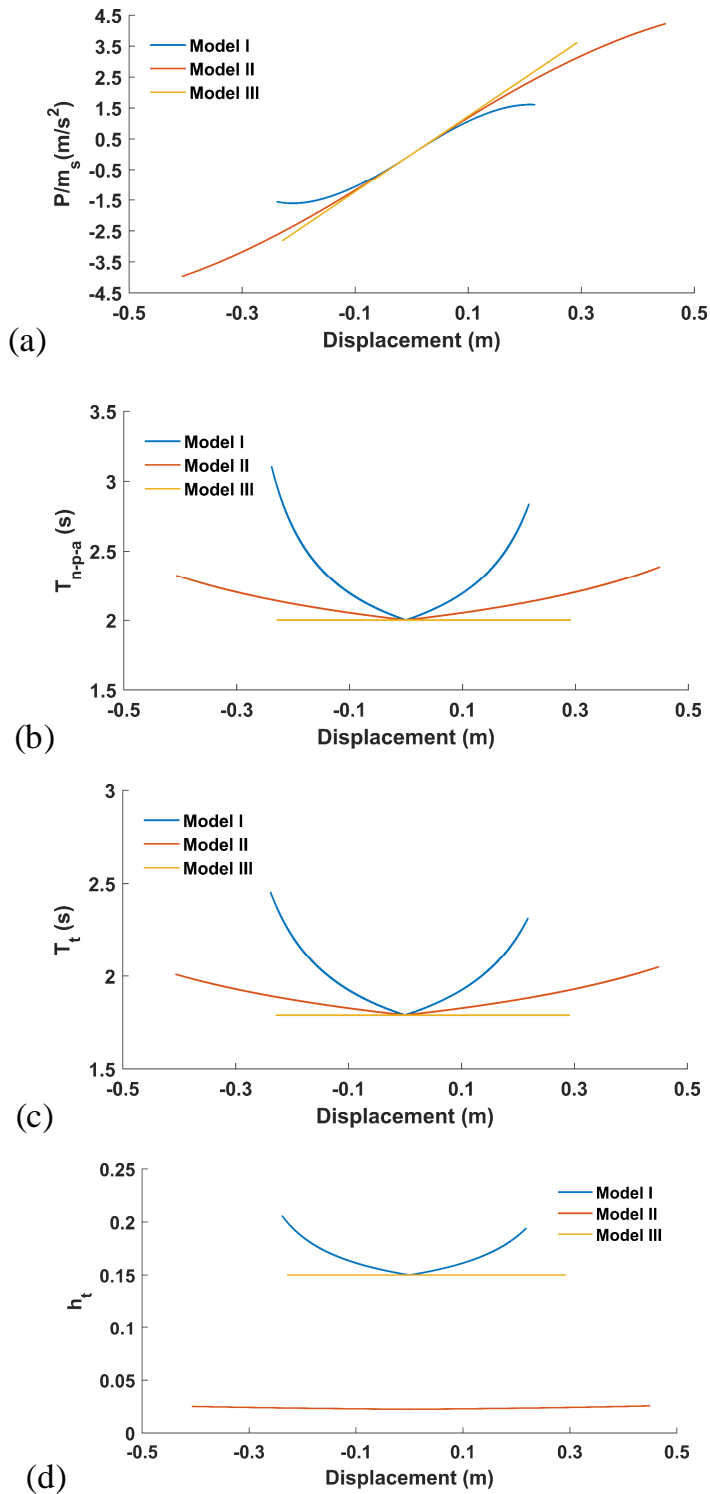


Fig. 3-12: Relationship between (a) restoring force by mass of isolated object, (b) period of the proposed device, (c) period of the system and (d) damping ratio of the system with relative displacement for Model I, Model II and Model III excited by Kobe

3.5 Numerical analysis and results

In this section, the time history responses of the base isolation systems are calculated for the observed and simulated ground motions. The performance of the base isolation systems with the proposed device (Model I) is compared with the conventional base isolation system, Model II, and Model III in order to verify the effectiveness of the proposed device. In the time history analysis, $f_s = 0.25$ Hz, $h_s = 0.05$, $f_a = 2$ Hz, $T_{n-p-a} = 2$ s, $h_t = 0.15$, $\alpha_o = 20$, $\kappa = 35$ (for Model I), and, $\kappa = 12$ (for Model II) are assumed to satisfy the allowable limits for both the displacement and the acceleration responses ($u < 0.3$ m and $\ddot{u} < 3.0$ m/s²) which are assumed based on the aspects of the allowable clearance and the safety of the target objects (sensitive instruments, cultural assets, art monuments and machinery etc.) against the acceleration.

3.5.1 Time history responses subjected to near-fault ground motion

The time histories of the relative displacement u with respect to the ground and the absolute acceleration $\ddot{u} + \ddot{u}_g$ of the base-isolated object are plotted for Kobe (**Fig. 3-11**) and Ojiya (**Fig. 3-13**). The response of the models (with the NP unit) are compared with the responses of the conventional base isolation system. The maximum amplitudes of the responses are indicated in the parenthesis. These figures show that both the maximum displacement and acceleration responses increase for the Model II as compared to the conventional base isolation system. This increase occurs due to the absence of damper in the proposed device which initially decreases the damping of the system which indicates that the damping might play an important role in mitigating the responses. The maximum displacement and acceleration responses of the Model III reduced by 38% (on average) of Model II. This decrease in responses of Model III is due to the presence of damping on the

proposed device which increases the damping of the system. Furthermore, although a notable degradation of maximum displacement response is achieved, the maximum acceleration response markedly increases in the model as compared to conventional base isolation system.

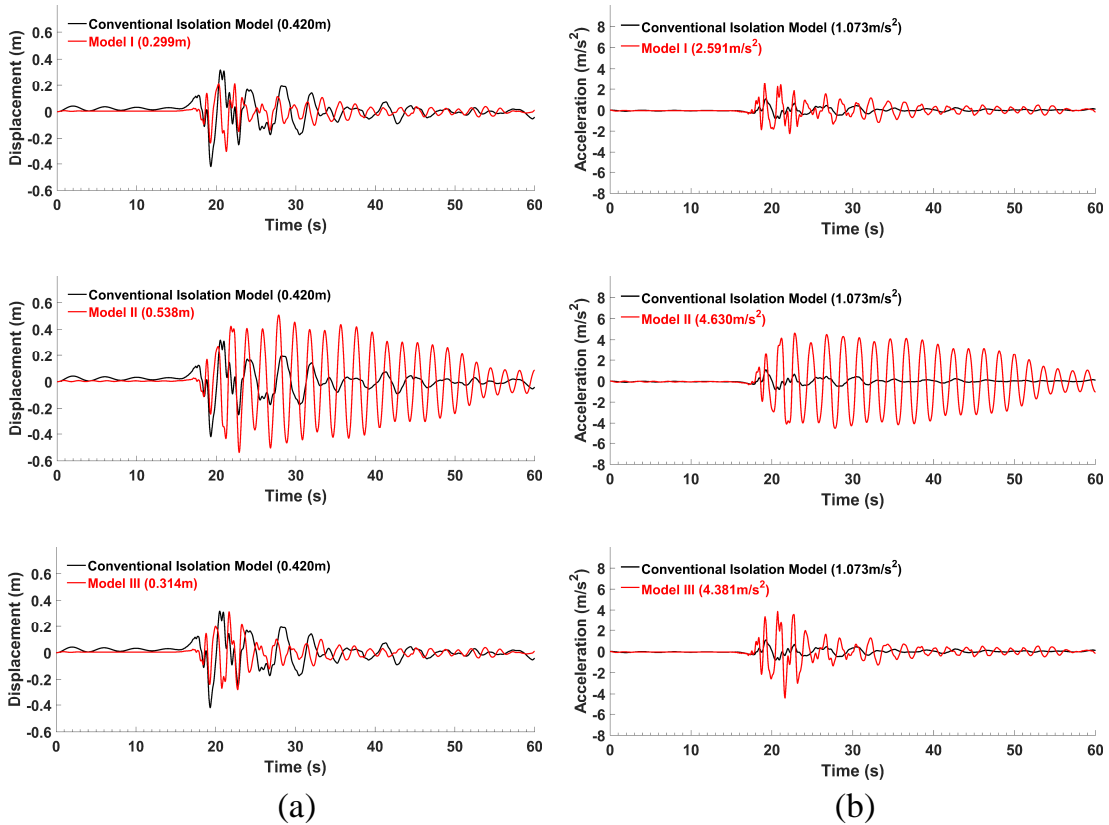


Fig. 3-13: Comparison of time history responses of (a) relative displacements and (b) response accelerations between the conventional base isolation system and the proposed models excited by Ojiya EW 2004.

The maximum displacement response decreases to almost 2/3rd compared to that achieved in the conventional base isolation system for Model I. Similarly, in comparison with Model II, Model I reduces the maximum acceleration response by 47% of Model II. Accordingly, the maximum acceleration response increases as compared to the conventional base isolation system, but the maximum acceleration is almost about 2.5 m/s² (0.25g) which is still within an allowable range in practice.

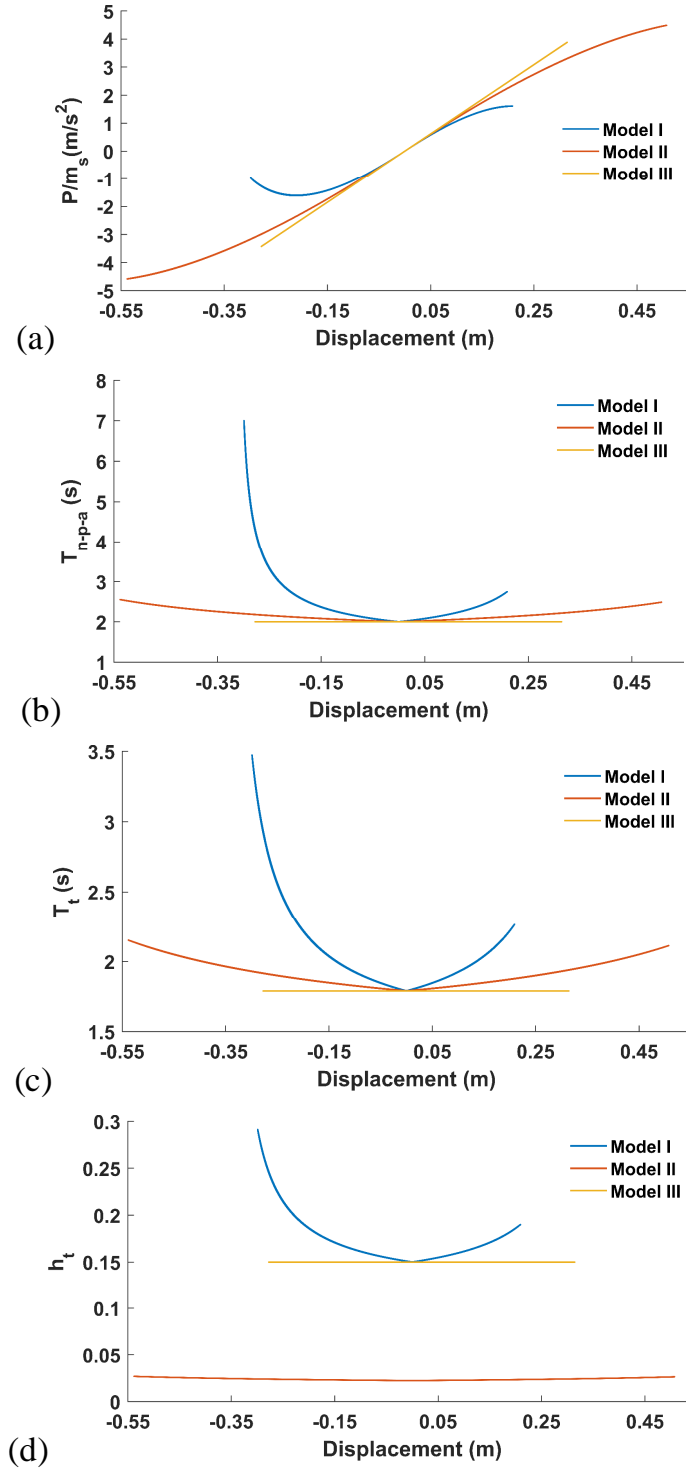


Fig. 3-14: Relationship between (a) restoring force by mass of isolated object, (b) period of the proposed device, (c) period of the system and (d) damping ratio of the system with relative displacement for Model I, Model II and Model III excited by Ojiya

Figs. 3-9(a) and **3-11(a)** shows the relationship between the ratio of the restoring force by mass of the isolated object (P/m_s) with the relative displacement response u of Model I, Model II and Model III when excited by Ojiya. **Figs. 3-9(b), (c)** and **3-11(b), (c)** shows the relationship between T_{n-p-a} and T_t with the relative displacement response u , respectively. **Figs. 3-9** and **3-11** indicates that although the maximum displacement response does not reduce sufficiently while comparing Model I and Model III, the acceleration response reduces (as shown in **Figs. 3-9(a)** and **3-11(a)**) significantly for Model I with the increase in the period of the system to 2.5 s and 3.5 s respectively for Kobe and Ojiya (as shown in **Figs. 3-9(c)** and **3-11(c)**). **Fig. 3-12(d)** shows the relationship between the total damping ratio with the displacement response when the Models are excited by Kobe. It shows that the decrease in the stiffness of the system leads to decrease in the critical damping coefficient of the system, which increases the damping ratio of the system by 30% that of the initial damping ratio and decreases the displacement response for Model I. Similarly, **Fig. 3-14(d)** shows the relationship between the total damping ratio with the displacement response when the Models are excited by Ojiya. It shows that the decrease in the stiffness of the system leads to decrease in the critical damping coefficient of the system, which increases the damping ratio of the system by 50% that of the initial damping ratio and decreases the displacement response for Model I.

3.5.2 Time history responses subjected to long-period ground motion

The time histories of the isolated object when excited by Shin-Tokai and Tomakomai, respectively are shown in **Figs 3-12** and **3-14**. These figures show that the maximum displacement is 0.675 m and 0.438 m for Shin-Tokai and Tomakomai, respectively, for the conventional base-isolation system because of the resonance of the system. The maximum displacement response decreases by approximately 35% and 63% for Shin-Tokai and

Tomakomai, respectively, in Model II compared to the response of the conventional base isolation system. Particularly, in the case of Shin-Tokai, the system shows a resonance despite the large stiffness of the system as its response spectra (**Fig. 2-3**) show peaks ranging from 2.5 to 4 s. The maximum acceleration response increased remarkably in the case of Shin-Tokai exceeding 0.4g and in Tomakomai about 0.2g. This increase in the acceleration response is due to the decrease in the initial damping ratio of the system (due to the proposed device without damper).

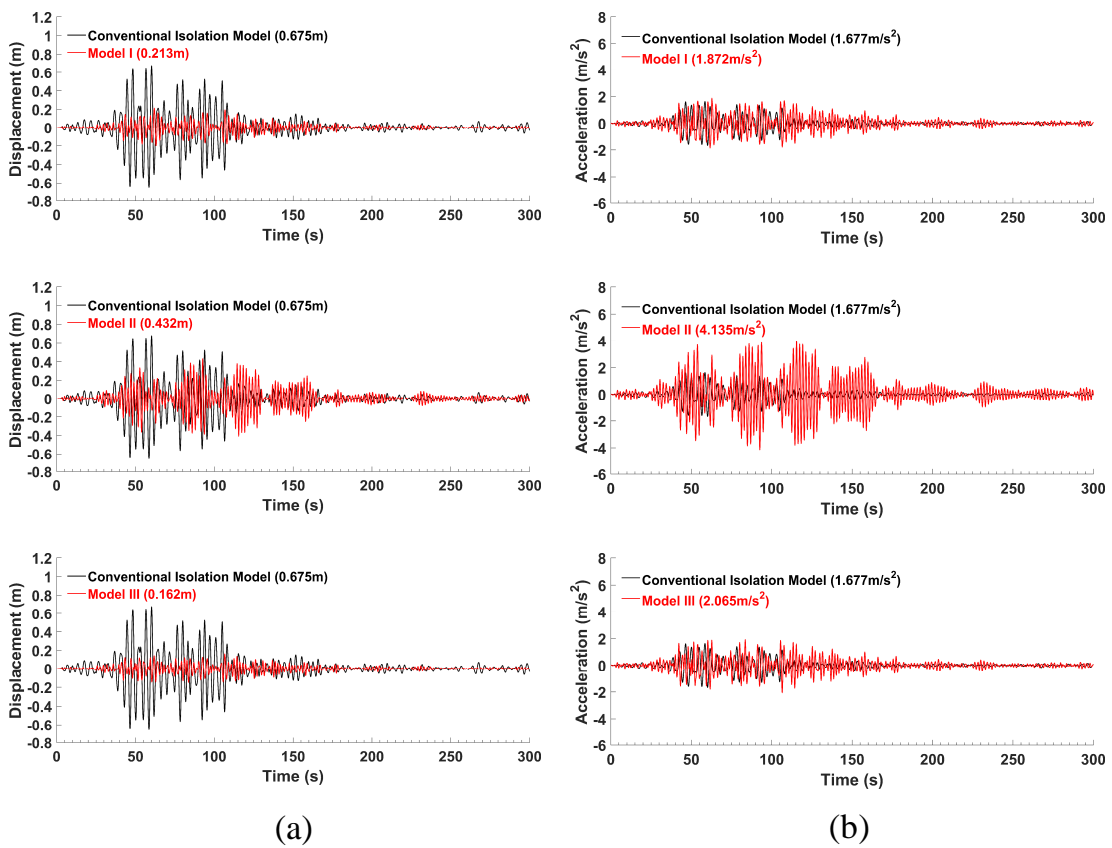


Fig. 3-15: Comparison of time history responses of (a) relative displacements and (b) response accelerations between the conventional base isolation system and the proposed models excited by Shin-Tokai EW.

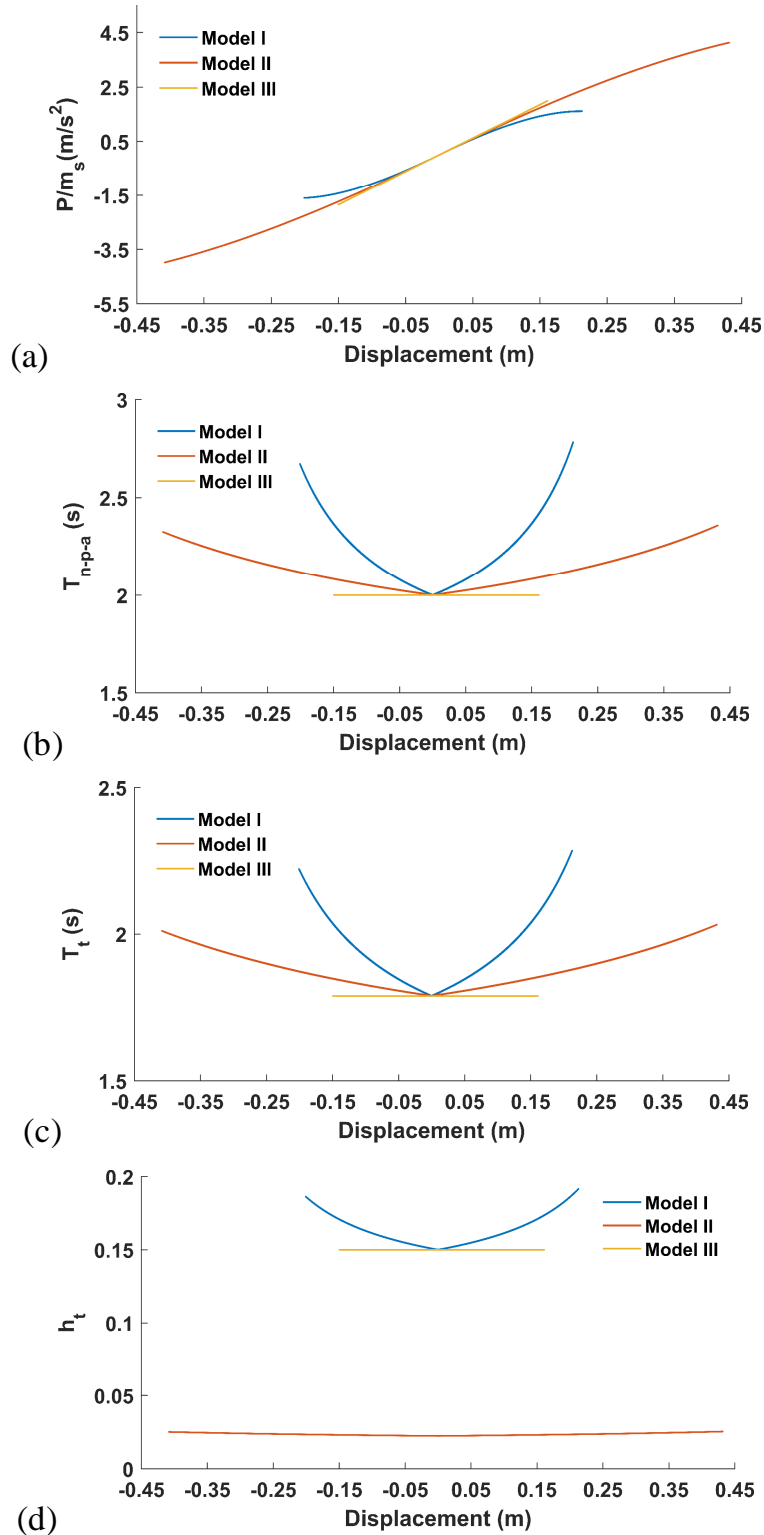


Fig. 3-16: Relationship between (a) restoring force by mass of isolated object, (b) period of the proposed device, (c) period of the system and (d) damping ratio of the system with relative displacement for Model I, Model II and Model III excited by Shin-Tokai.

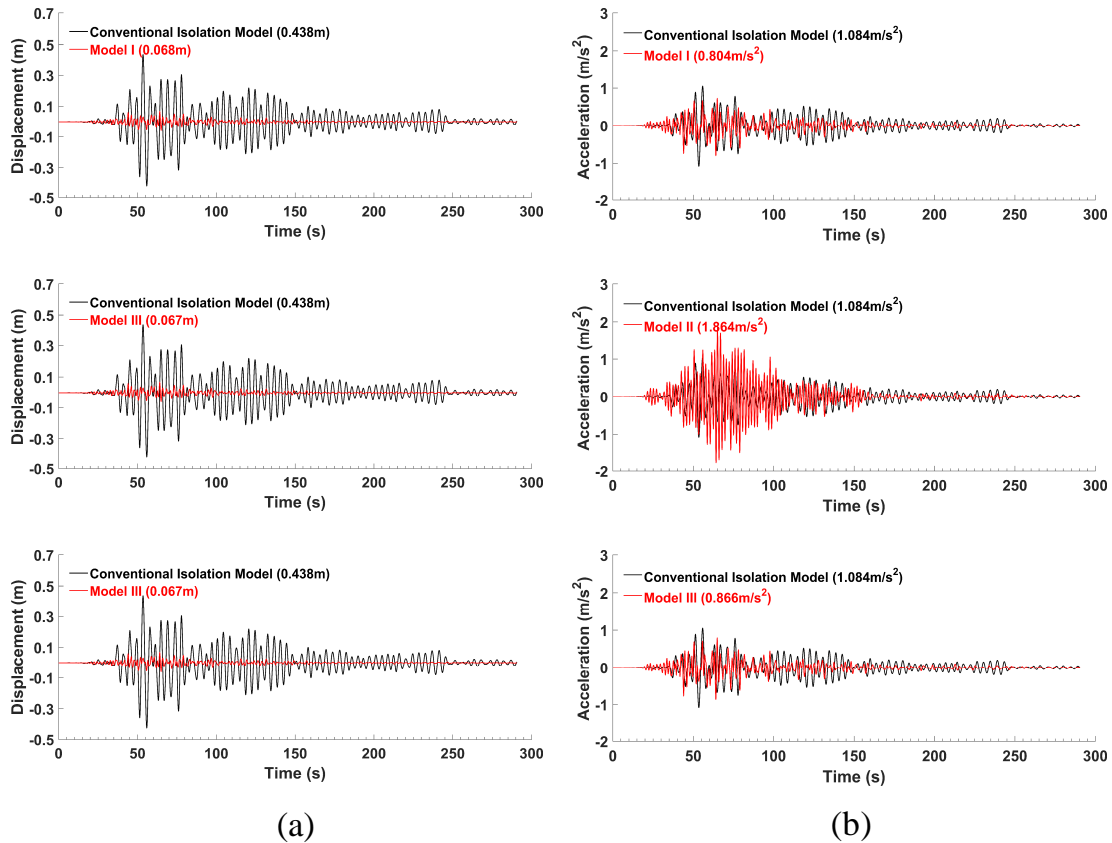


Fig. 3-17: Comparison of time history responses of (a) relative displacements and (b) response accelerations between the conventional base isolation system and the proposed models excited by Tomakomai EW 2003.

Model III shows a further reduction of both the maximum displacement and acceleration responses as compared with Model II. In contrast to the conventional base isolation system, Model III reduces the maximum displacement response by 75% and 85% for Shin-Tokai and Tomakomai, respectively. However, the maximum acceleration response increases slightly in Shin-Tokai and it decreases in Tomakomai. Compared with conventional base isolation system, Model I reduces the maximum displacement response remarkably in both Shin-Tokai and Tomakomai, and the maximum acceleration response increases slightly in Shin-Tokai but it decreases in Tomakomai.

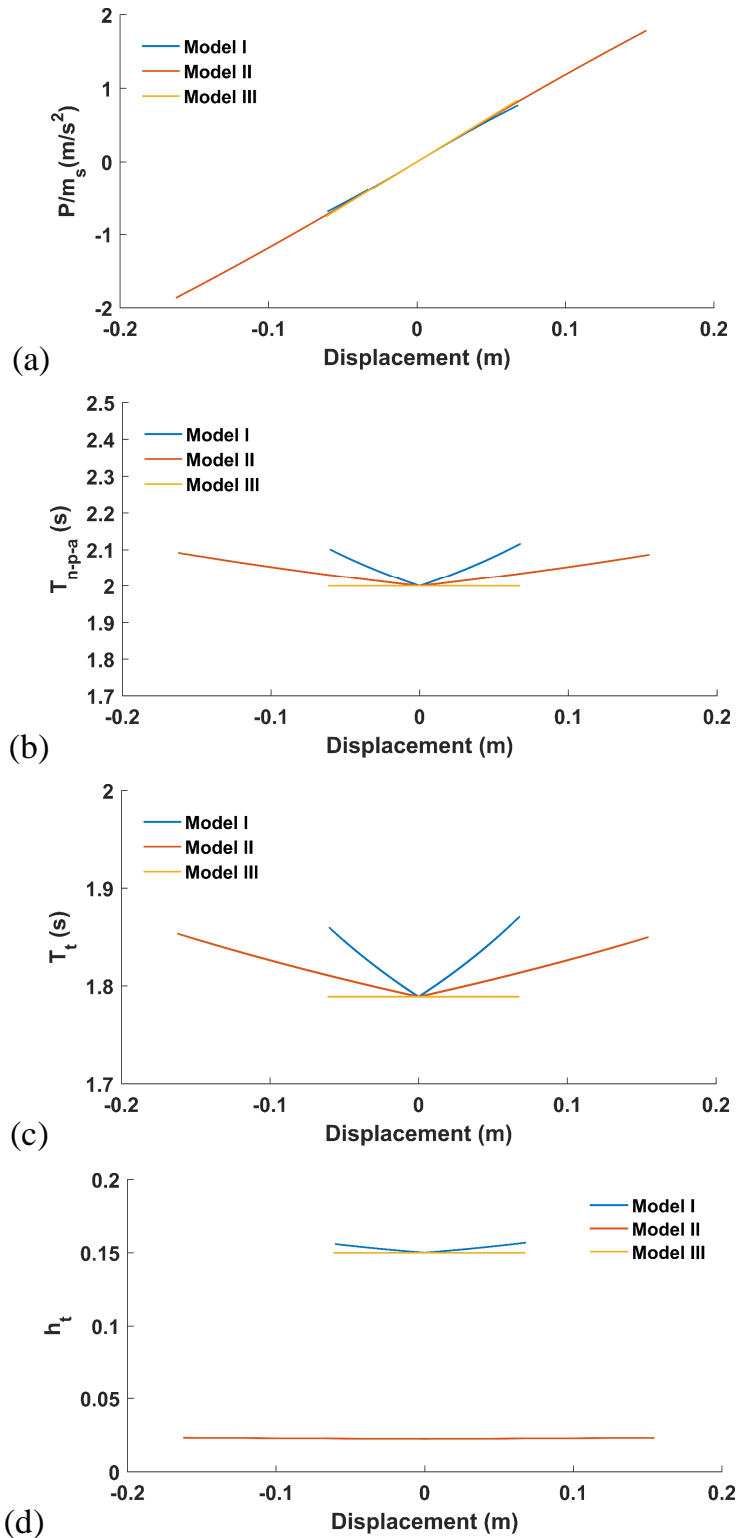


Fig. 3-18: Relationship between (a) restoring force by mass of isolated object, (b) period of the proposed device, (c) period of the system and (d) damping ratio of the system with relative displacement for Model I, Model II and Model III excited by Tomakomai

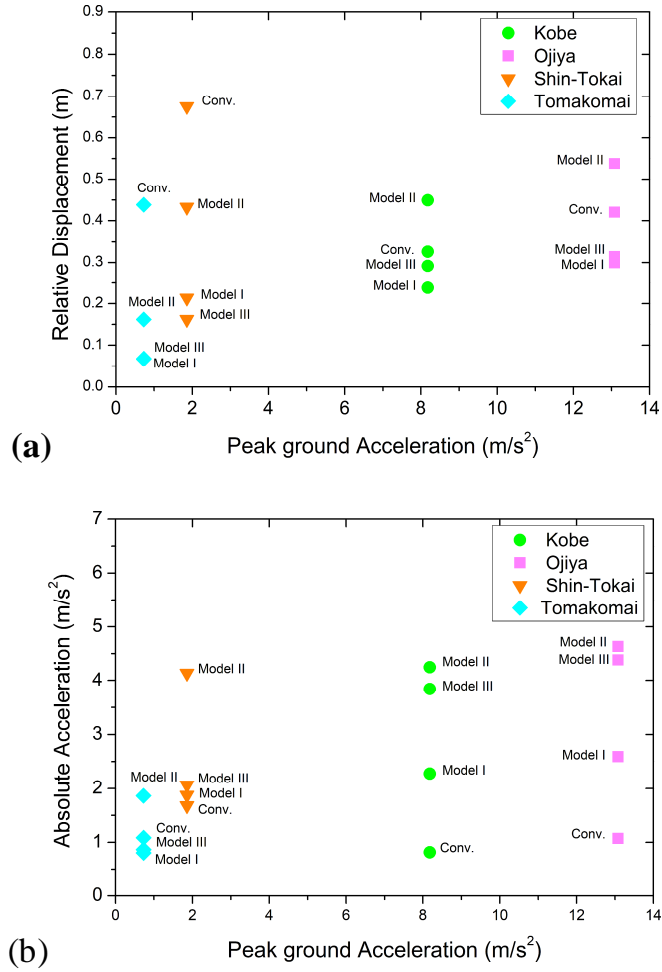


Fig. 3-19: (a) Relative displacement response, (b) Absolute acceleration response for Kobe, Ojiya, Shin-Tokai, and Tomakomai earthquake excitations.

Fig. 3-16 indicates that for Shin-Tokai ground motion, varying the stiffness slightly increases the displacement response with a little reduction in acceleration response (**Fig. 3-16 (a)**) which increase the period of the system to 2.2 s (**Fig. 3-16 15(c)**) for Model I. **Fig. 3-16 (d)** shows that the decrease in the stiffness of the system leads to decrease in the critical damping coefficient which increases the damping ratio of the system about 25% that of the initial damping ratio for Model I. Similarly, **Fig. 3-18** indicates that for Tomakomai ground motion, displacement and acceleration responses increases for Model II (i.e., the proposed model without any damper) as compared to Model I (proposed model

without varying stiffness) and Model III (proposed model). It also shows that for Tomakomai, responses are almost same with and without varying stiffness.

3.5.3 Time history responses for different earthquake ground motions

In the previous section, the time history responses of the proposed models were computed and evaluated in detail for both types of earthquakes. In this section, to enhance the validity of the proposed models, the maximum displacement and acceleration responses of both types of ground motions are discussed.

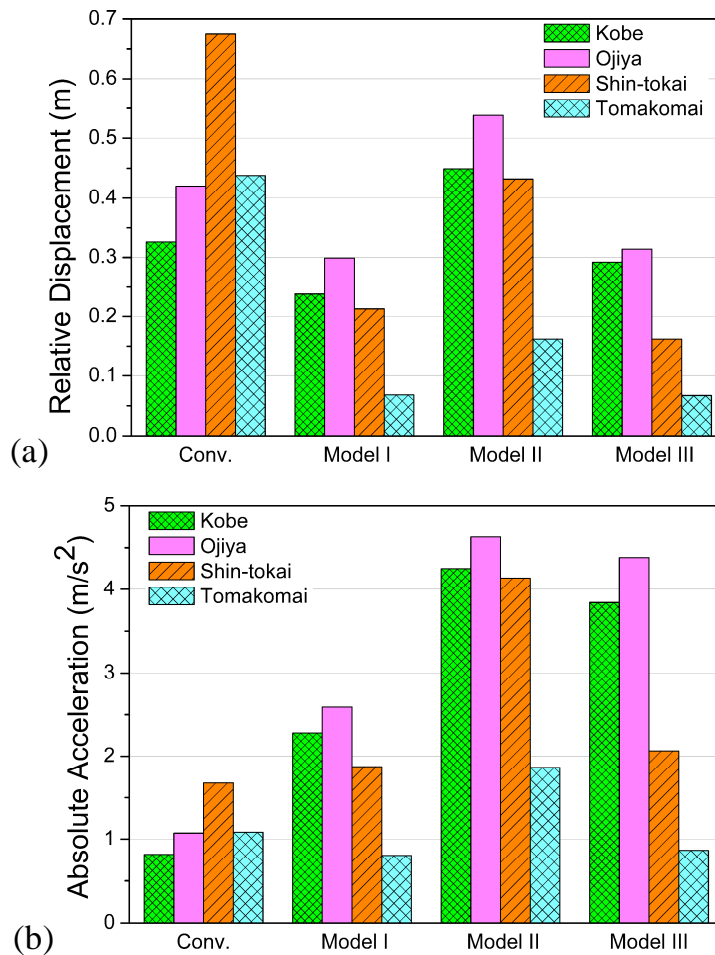


Fig. 3-20: Maximum amplitudes of (a) response of relative displacement, and (b) response of absolute acceleration of the conventional base isolation system (Conv.) and proposed models.

Fig. 3-19(a) shows the maximum displacement response as a function of the peak ground acceleration in a Conventional Model (Conv.), Model I, Model II, Model III for both near-fault and long-period ground motions. The results show that the reductions in the maximum displacement responses for Model I (with the proposed device) compared to the Model III (proposed device without varying stiffness) are 19% for Kobe, 5% for Ojiya, except for Shin-Tokai which increases slightly and for Tomakomai it is the same with Model III. Similarly, **Fig. 3-19(b)** shows that the reductions in the maximum acceleration response for Model I compared to the Model III are 41% for Kobe and Ojiya, 9% for Shin-Tokai and 7% for Tomakomai. From the numerical analysis, it can be concluded that the proposed Model I is able to effectively suppress both the displacement and the acceleration responses to allowable limits for both types of earthquake excitations.

Fig. 3-20 summarizes the maximum displacement and acceleration responses for conventional base isolation system and proposed models. It shows that for both types of ground excitation, Model I shows the good performance although, for long-period ground excitation, both the proposed Model I and III perform well.

3.5.4 Response spectra of proposed model for general ground motions

The near-fault ground motions have a large variation which make a consistent evaluation of near-fault effects difficult. Physical realizable cycloidal pulses have been introduced, and resemblance to the actual near-fault ground motions has been examined in the past studies [50–52]. The cycloidal pulses are also used to approximate the earthquake ground motion with long duration cycles in the displacement history [53]. In the present study, in order to generalize the effectiveness of the proposed device subjected to various ground motions, response spectra are developed using cycloidal pulses. The type-A, type-B and type-C_n cycloidal pulses are selected to develop response spectra of proposed base

isolation system to demonstrate the robustness of NP unit. The acceleration history of the type-A cycloidal pulse is given by,

$$\ddot{u}_g(t) = \omega_p \frac{V_p}{2} \sin(\omega_p t) \quad 0 \leq t \leq T_p \quad (3.16)$$

where, $T_p = 2\pi/\omega_p$ is a predominant period of the pulse and V_p is the amplitude of the velocity pulse. The acceleration history of the type-B cycloidal pulse is given by,

$$\ddot{u}_g(t) = \omega_p V_p \cos(\omega_p t) \quad 0 \leq t \leq T_p \quad (3.17)$$

where, $T_p = 2\pi/\omega_p$ is a predominant period of the pulse and V_p is the amplitude of the velocity pulse. The acceleration history of the type-C_n cycloidal pulse is given by,

$$\ddot{u}_g(t) = \omega_p V_p \cos(\omega_p t + \varphi) \quad 0 \leq t \leq \left(n + \frac{1}{2} - \frac{\varphi}{\pi}\right) T_p \quad (3.18)$$

where, $T_p = 2\pi/\omega_p$ is a predominant period of the pulse and V_p is the amplitude of the velocity pulse. The value of the phase angle, φ , for a type-C₁ pulse ($n = 1$) is $\varphi = 0.0679\pi$, whereas, for a type-C₂ pulse ($n = 2$) is $\varphi = 0.0410\pi$ are taken [52]. In order to exhibit the trend of response spectrum for general ground motions, response spectra for the type-A pulse and type B pulse with amplitude of velocity pulse V_p as 0.5 m/s are presented in the succeeding section.

Fig. 3-21 shows the displacement, velocity and acceleration response spectra plots of Model I, Model III and Conventional (conv.) base isolation system using type-A pulse and type-B pulse and type-C₂. These figures show that the Model I and Model III reduces displacement amplitude of isolated object remarkably in comparison with conventional base isolation system for ground motion with predominant period ranging from 0-10 s. On the other hand, acceleration amplitude increases for Model I and Model III in comparison to the conventional base isolation system. Although, both models reduce acceleration

amplitude, Model III exceeds acceleration amplitude than allowable limit for ground motion with predominant period ranging from 1-2s in case of the type-B and type-C₂, but Model I reduce acceleration amplitude within allowable limit. The spectrum trend for both, type-B and type-C_n pulses are similar. In case of the near-fault ground motion from **Fig. 3-21** it can be seen that the variation of the stiffness is needed to reduce the acceleration response to the allowable limit. Whereas, in case of long-period ground motion, initial stiffness of the system is important for mitigating displacement and acceleration responses. The similar spectrum trend is observed even by increasing the amplitude velocity of pulse. Hence, response spectra are also one of the factors with determines the effectiveness of the NP unit.

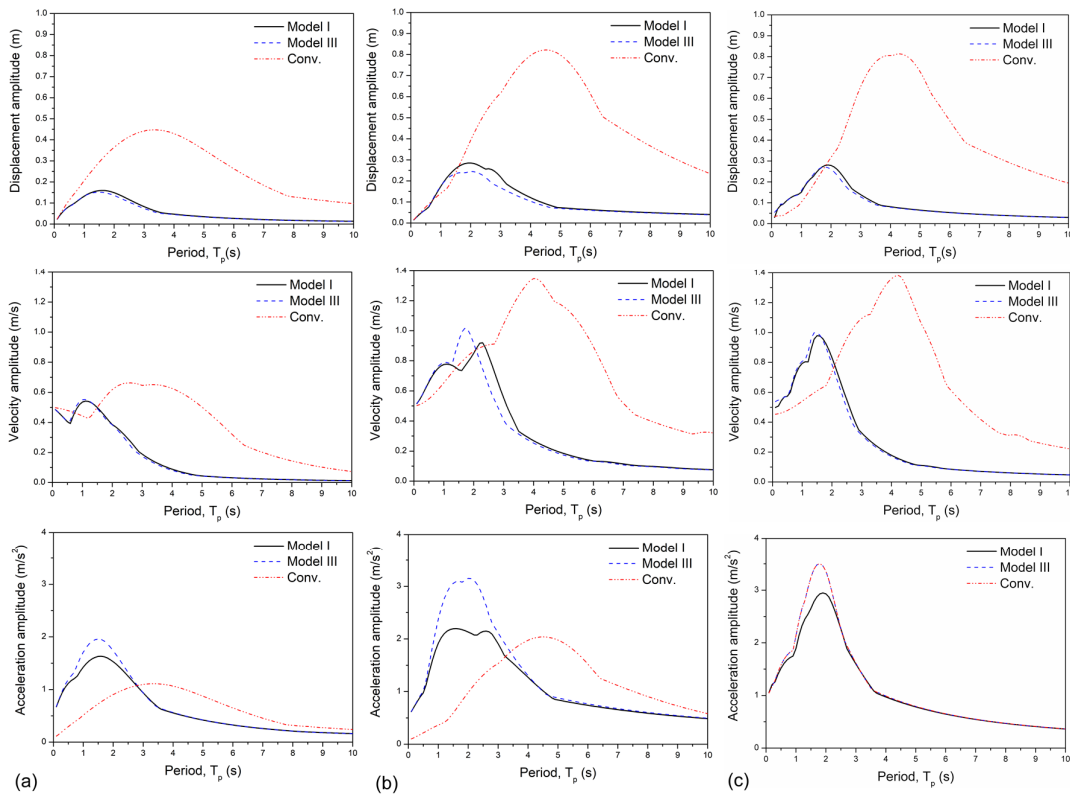


Fig. 3-21: Displacement, velocity and acceleration response spectra of Model I, Model III and Conventional (Conv.) base isolation systems using (a) Type-A, (b) Type-B and (c) Type-C pulse.

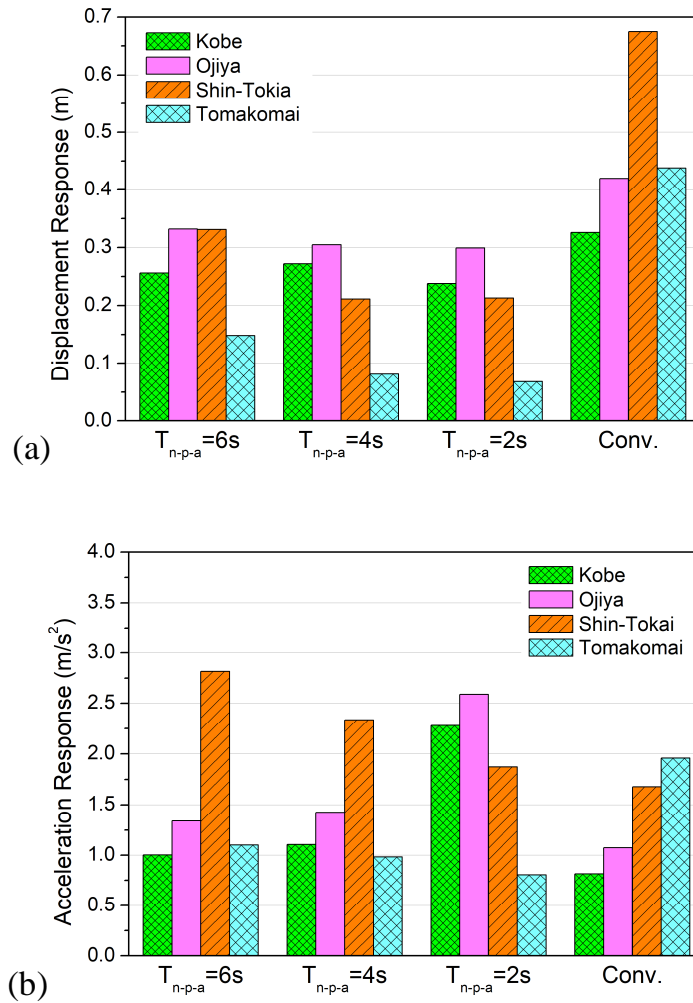


Fig. 3-22: Maximum amplitudes of (a) response of relative displacement, and (b) response of absolute acceleration of the conventional base isolation system (Conv.) and proposed models.

3.6 Discussion

For the effectiveness of the proposed device, appropriate selection of its natural period is of great importance. In the following section, therefore, the effect of the natural period of the external device upon the responses will be discussed. From the numerical analysis and results, it shows that the variation of the stiffness of the NP unit is not compatible with the

variation of α as discussed in the section 3.4.2. Although, the variation of the NP unit stiffness is not significant, the variation of the total stiffness in the system is significant. This mechanism of the system will also be discussed. And the performance of the proposed model (Model I) is compared with the base isolation system with varying negative stiffness and with the previous existing systems.

3.6.1 Setting up of natural period of the system with proposed device

The robustness of the proposed device is verified by selecting the following natural periods i.e., $T_{n-p-a} = 6$ s, 4 s, and 2 s; the corresponding initial period of the system becomes $T_{to} = 3.328$ s, 2.828 s and 1.789 s, respectively. The maximum displacement and acceleration responses are computed for all models and compared against the conventional base isolation system. **Fig. 3-22** shows the maximum amplitude of displacement and acceleration responses for Model I with the various selected natural periods of the device. These figures show that for $T_{n-p-a} = 6$ s ($T_{to} = 3.328$ s), Model I reduces the relative displacement as that of the conventional base isolation system, although for the case of Ojiya and Shin-Tokai it exceeds the allowable limit ($u < 0.3$ m). This is because for Shin-Tokai its response spectra (**Fig. 2-3**) shows peaks ranging from 2.5 to 4 s with a maximum around 3 s and for Ojiya response spectra contains a wide range of frequency components. Varying the stiffness (increasing the period) of the system, thus, attribute to the resonant characteristics of the model. For $T_{n-p-a} = 4$ s ($T_{to} = 2.828$ s), Model I reduces the relative displacement for both near-fault and long-period ground motion (on average, 30% decrease for near-fault and 70% for long-period) to allowable limit, although for Ojiya it exceeds the allowable limit. Similarly, for $T_{n-p-a} = 2$ s ($T_{to} = 1.789$ s), Model I reduces the relative displacement for both near-fault

and long-period ground motion to the allowable limit. These figures also show that the stiffer device ($T_{n-p-a} = 2$ s) increases the acceleration response for near-fault ground motions in comparison to the device with natural periods $T_{n-p-a} = 4$ s and $T_{n-p-a} = 6$ s, displacement response (for Ojiya) decreases to the allowable limit as discussed above. And for long-period ground motions, acceleration response decreases with the stiffer device in comparison to the softer device.

Thus, it can be inferred that the proposed device with the period of $T_{n-p-a} = 2$ s is effective in reducing both the displacement and acceleration responses to allowable limits eluding the system to resonant for both near-fault and long-period earthquakes.

3.6.2 Discussion on the significant change in the total stiffness of the system

As mentioned in section 3.5, the parameters $T_a = 0.5$ s and the initial period of the proposed device $T_{n-p-a} = 2$ s are assumed. Using Eq. (3.7) the period of the NP unit (T_{n-p}) is found to be close to and greater than T_a i.e., stiffnesses $|k^*|$ and k_a are very close to each other with $k_a > |k^*|$. Varying the positive spring stiffness (k_p), the stiffness of NP unit $|k^*|$ approaches to the stiffness k_a i.e., the stiffness of the proposed device approaches zero. The period of the proposed device tends to infinity and thus, the proposed device does not function as resistance force is zero. Hence, the remaining stiffness is close to k_s i.e., 4 s system. Due to this reason, total stiffness of the system decreases significantly although the variation of the stiffness of NP unit is not significant with the variation of α .

Important points to generate the significant change in total stiffness of the system are: - (i) k_a should be greater and closer to the absolute value of the stiffness of the NP unit (k^*),

(ii) the stiffnesses k^* and k_a should be much stiffer than the stiffness k_s because:

- With the stiffer NP unit $|k^*|$ and k_a , the amount of difference in the stiffness ($k_a - |k^*|$) is much more influenceable as compared to the stiffness k_s .
- Varying the stiffness of positive spring of NP unit, the difference ($k_a - |k^*|$) decreases by very small amount. Due to the small amount change in the difference in the stiffness also, the proposed device stiffness varies from stiffer range to softer range of stiffness.
- And, even with a small amount of difference in the stiffness of the proposed device very large change in total stiffness is generated.

3.6.3 Comparison of Model I with variable negative stiffness system

In a comparison between Model I and variable negative stiffness with power function ($u^{1.5}$), displacement and acceleration responses due to both the systems show a good match. **Table 3-1** Maximum amplitudes of displacement and acceleration responses of base isolation systems (Conv., Model I and Model with variable negative stiffness) shows the comparison maximum relative displacement and maximum acceleration responses of Model I, variable negative stiffness with power function ($u^{1.5}$) and Conventional base isolation system (Conv.). **Figs. 3-19, 3-20, 3-21 and 3-22** shows the relationship of total stiffness (k_t), negative stiffness (k_n) and the total period of the system (T_t) with relative displacement (u) of the isolated object for Model I and variable negative stiffness system with power function ($u^{1.5}$) for Kobe, Ojiya, Shin-Tokai and Tomakomai respectively.

These figures show that the total stiffness (k_t), negative stiffness (k_n) and the total period of the system (T_t) of both the base isolation systems are almost similar to each other. The proposed base isolation system (Model I) subjected to Kobe, Ojiya and Shin-Tokai

earthquakes shows a good match with the base isolation system with variable negative stiffness using Eq. (2.5).

Hence, it can be concluded that the base isolation system with the proposed external device (with varying the positive stiffness of NP unit) is able to obtain similar results in comparison to the base isolation system with variable negative stiffness using Eq. (2.5).

Table 3-1 Maximum amplitudes of displacement and acceleration responses of base isolation systems (Conv., Model I and Model with variable negative stiffness)

| | Relative Displacement (m) | | | |
|--------------------------|--|--------------|-------------------|------------------|
| | Kobe | Ojiya | Shin-Tokai | Tomakomai |
| Conv. | 0.326 | 0.420 | 0.675 | 0.438 |
| Proposed Model (Model I) | 0.238 | 0.299 | 0.213 | 0.068 |
| Power function $u^{1.5}$ | 0.246 | 0.294 | 0.230 | 0.068 |
| | Absolute Acceleration (m/s²) | | | |
| | Kobe | Ojiya | Shin-Tokai | Tomakomai |
| Conv. | 0.815 | 1.073 | 1.677 | 1.084 |
| Proposed Model (Model I) | 2.279 | 2.591 | 1.872 | 0.804 |
| Power function $u^{1.5}$ | 2.128 | 2.530 | 1.835 | 0.812 |

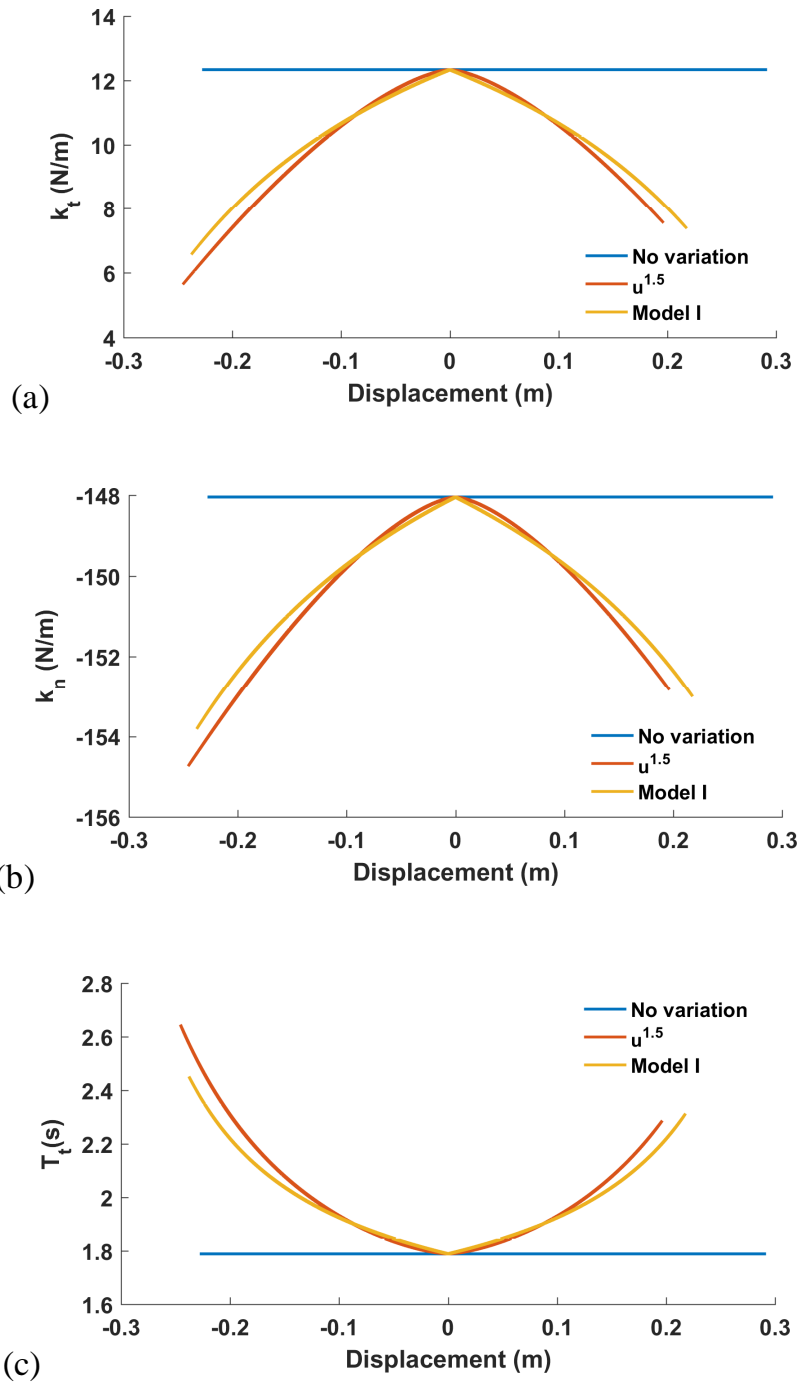


Fig. 3-23: Relationship between (a) total stiffness, (b) negative stiffness, and (c) period of the system with relative displacement Model I and variable negative stiffness system with power function ($u^{1.5}$) when excited by Kobe.

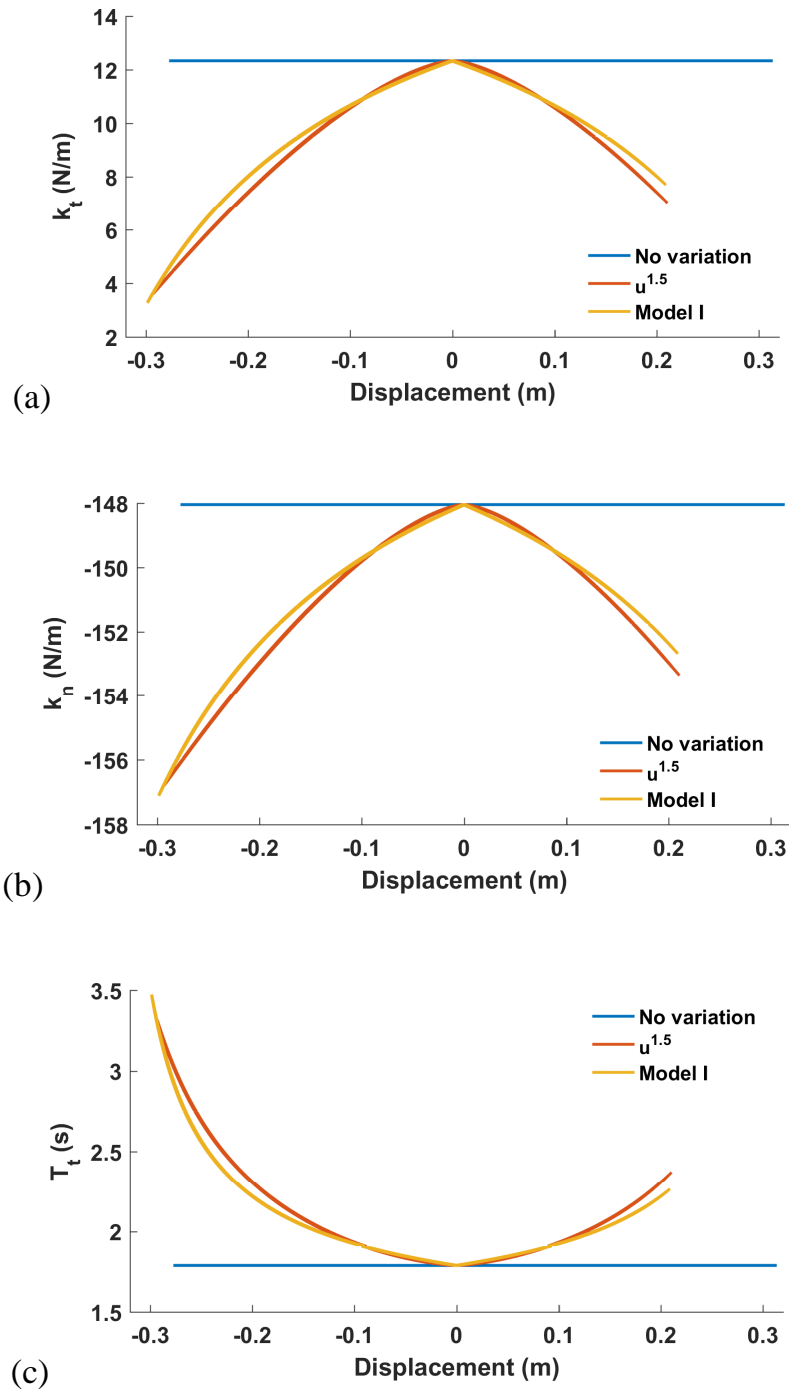


Fig. 3-24: Relationship between (a) total stiffness, (b) negative stiffness, and (c) period of the system with relative displacement Model I and variable negative stiffness system with power function ($u^{1.5}$) when excited by Ojiya.

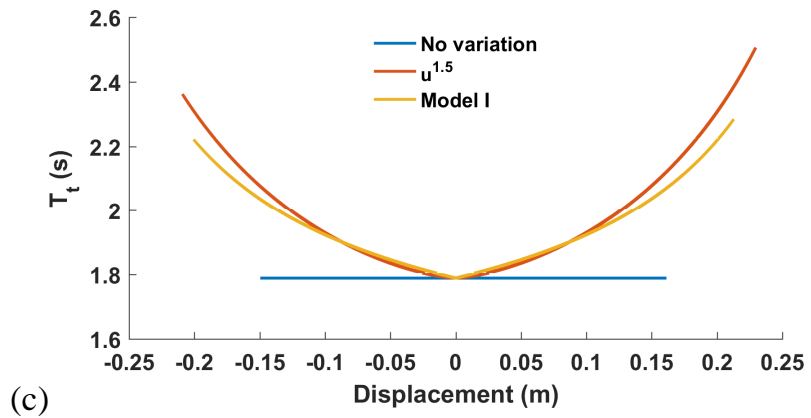
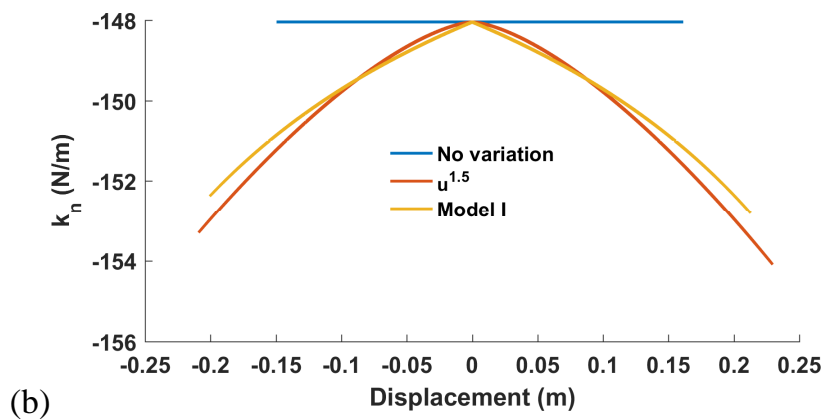
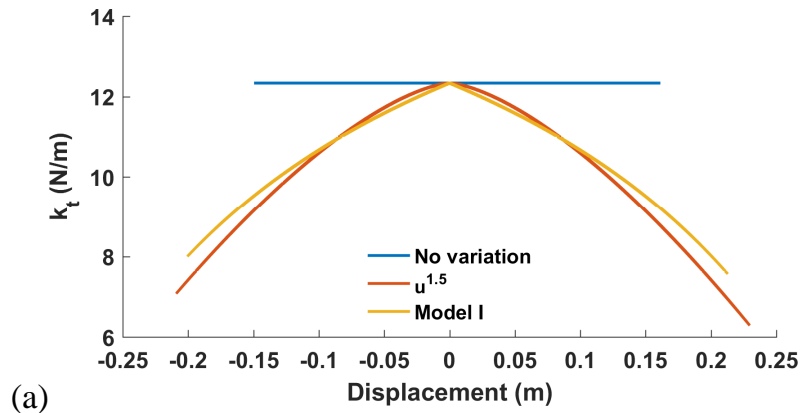


Fig. 3-25: Relationship between (a) total stiffness, (b) negative stiffness, and (c) period of the system with relative displacement Model I and variable negative stiffness system with power function ($u^{1.5}$) when excited by Shin-Tokai.

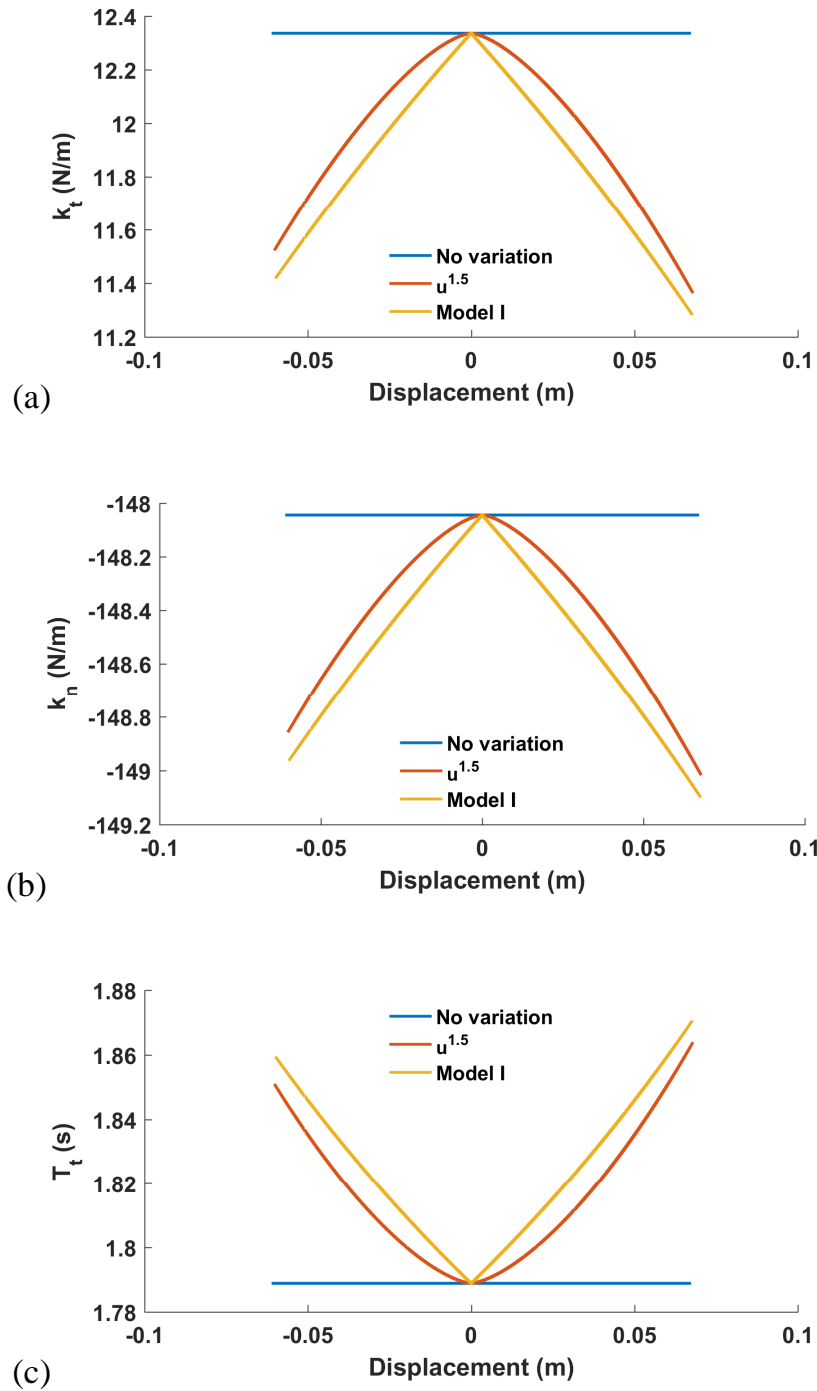


Fig. 3-26: Relationship between (a) total stiffness, (b) negative stiffness, and (c) period of the system with relative displacement Model I and variable negative stiffness system with power function ($u^{1.5}$) when excited by Tomakomai.

3.7 Conclusions

The current work can be concluded as:

- Study proposes the base isolation systems incorporating a new external proposed device for reducing the lateral displacement. The proposed device consists of a negative-positive spring unit (NP unit) arranged in parallel with a positive spring and a damper. The advantage of the NP unit is that it can generate a rapid and a wide change in the stiffness.
- for varying the total stiffness of the system using proposed device, engineers dealing with the production of the proposed device needs to account following points:- (i) k_a should be greater and closer to the absolute value of the stiffness of NP unit (k^*), (ii) the stiffnesses $|k^*|$ and k_a should be much stiffer than the stiffness k_s .
- parametric studies for various α_o , h_t and κ are performed and the maximum displacement and acceleration responses are computed for varying the robustness of Model I and Model II.
- parametric studies conclude that in case of the small value of α_o with various κ values, node displacement (NP unit node) is found to be large than for the greater value of α_o . Although, the parameters α_o and κ have many combinations satisfying the performance of the proposed model, in this study performance of base isolated object are enhanced using $\alpha_o = 20$, $\kappa = 35$.
- Equilibrium equations of motion for the systems are presented, and the time history of displacement and acceleration responses of the systems subjected to near-fault and long-period ground motions are shown.
- Model II reduces the displacement response of the isolated object for long-period

ground motion but for near-fault it increases and the acceleration response increases for both types of earthquake excitations. This is due to the decrease in the initial damping ratio with an increase in the stiffness when the proposed device without any damper is linked to the conventional base isolation system.

- Model III reduces displacement response markedly for both near-fault and long-period ground motions. On the other hand, acceleration response increases remarkably for near-fault as compared to conventional base isolation.
- the proposed model I exhibits a significant decrease in the relative displacement of the object with respect to the base for both types earthquake excitations. The maximum displacement of the isolated object decreases by almost 30% and more than 70% when subjected to near-fault and long-period ground motions respectively in comparison with conventional base isolation system.
- the effect of the natural period of the external device is discussed and found that stiffer device (i.e., $T_{n-p-a} = 2$ s) can effectively reduce displacement and acceleration responses to the allowable limits.
- the displacement mitigation is usually achieved at the expense of losing efficacy in filtering acceleration and the point is the degree of the loss of efficacy. The results of this study show that the achieved maximum absolute acceleration of the base-isolated object with the proposed model I is almost 2.5 m/s^2 , while the maximum relative displacement is less than 0.3 m for both types of earthquake ground motions. Hence, the results of this work devote toward improving the displacement reduction with the allowable accelerations for structural safety.
- all the springs comprising the system are elastic linear, so it does not have any residual displacement.

As a final note, the earthquakes (both near-fault and long-period ground motions) having the extreme characteristics (such as large acceleration amplitudes, large velocity amplitudes, and long fundamental natural period etc.) are used in numerical study of the current work. Further, the current study focuses on the development of the base isolation system considering the general location. The stability of the external device has also been considered by potential energy function. Furthermore, to consider the effect of near-fault ground motion, the response spectrum for the proposed model (Model I) is developed using cycloidal pulses and is compared with Model III and the conventional base isolation system. These response spectra exhibit the effectiveness of the proposed model by showing its applicability for wide range of ground motions.

CHAPTER 4

APPROXIMATION OF NEGATIVE-POSITIVE VARIABLE STIFFNESS IN PRACTICE

In order to realize the system practically, first we need to realize the variable positive spring of NP unit. As discussed in Chapter 3, variable positive spring of NP unit is function of relative displacement of the isolated object with respect to the ground. Hence, in this chapter, influence of approximate system with negative-positive variable stiffness in practice has been discussed.

4.1 Approximation of the system using step function for varying stiffness

Generally, it is difficult to obtain smooth line stiffness-displacement curve (K-D curve) as shown in **Fig. 4-1** (red color line) from the mechanical device. Usually, a mechanical device is a combination of springs and one spring have one spring constant and the multiple springs show a kind of a line so in this chapter to realize the system for practical use, discontinuous stiffness-displacement (K-D) curve (**Fig. 4-1** (black color line)) is analyzed. Hence, model to obtain discontinuous stiffness-displacement (K-D) relationships is considered and numerical simulation is performed. As positive spring of N-P unit is variable stiffness spring, to obtain discontinuous K-D curve, positive spring of N-P unit is considered as the group of springs arrange in parallel. For this analysis group of two and three springs are considered in parallel.

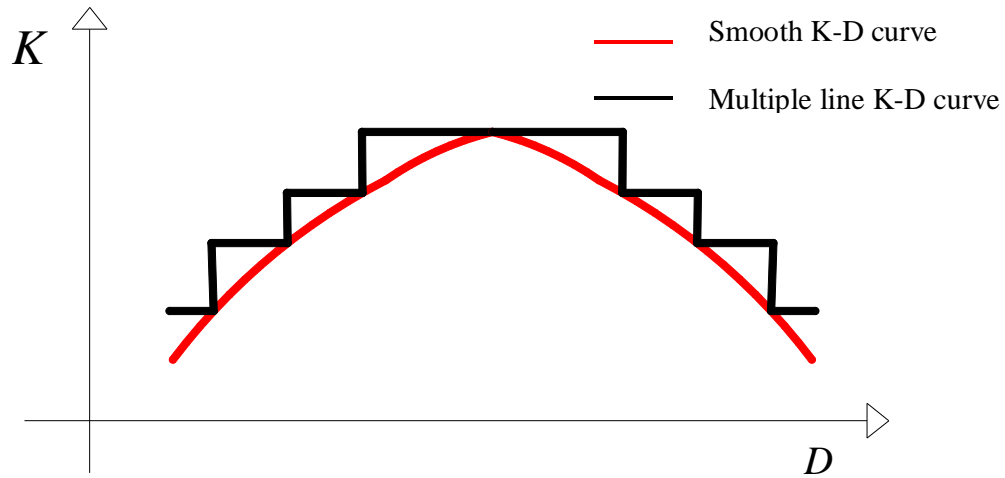


Fig. 4-1: Stiffness-displacement relationship

Table 4-1 Comparison of relative displacement and absolute acceleration of base isolation systems (Model I (smooth line K-D curve) and isolation system with a discontinuous K-D curve) using two springs and conventional base isolation system

| | Relative Displacement (m) | | | |
|---|---|-------|------------|-----------|
| | Kobe | Ojiya | Shin-Tokai | Tomakomai |
| Conv. | 0.326 | 0.420 | 0.675 | 0.438 |
| Model I (Smooth line K-D curve) | 0.238 | 0.299 | 0.213 | 0.068 |
| Step function (discontinuous K-D curve) | 0.270 | 0.298 | 0.166 | 0.067 |
| | Absolute Acceleration (m/s ²) | | | |
| | Kobe | Ojiya | Shin-Tokai | Tomakomai |
| Conv. | 0.815 | 1.073 | 1.677 | 1.084 |
| Model I (Smooth line K-D curve) | 2.279 | 2.591 | 1.872 | 0.804 |
| Step function (discontinuous K-D curve) | 2.842 | 3.100 | 2.049 | 0.866 |

4.1.1 Numerical Analysis and Result

The time history responses of the base isolation system with discontinuous K-D curve is calculated for the various earthquakes discussed in Chapter 2, Section 2.2.3. The performance of the base isolation system with discontinuous K-D relationship is compared with the conventional base isolation system. The other parameter of the system is same as the pervious study.

Table 4-1 shows the summary of relative displacement and absolute acceleration of base isolation systems with a smooth K-D curve and discontinuous K-D curve using two springs which are compared against conventional base isolation system. Table shows that both the obtained displacement and acceleration responses are within the allowable limits for all ground motion except for the Ojiya with exceeds the acceleration response. **Figs 4-2, 4-3, 4-4 and 4-5** show the relationship between positive stiffness, total stiffness of the system, total period of the system and restoring force by mass of the isolated object with the relative displacement for Model I and Model with Step function variation of stiffness using two springs excited by various earthquakes. For varying stiffness using step function with two springs in parallel particularly for Ojiya, acceleration response exceeds the allowable limits. Therefore, using two positive springs desired responses of the isolated objects subjected to near-fault and long-period ground motion cannot be accomplished.

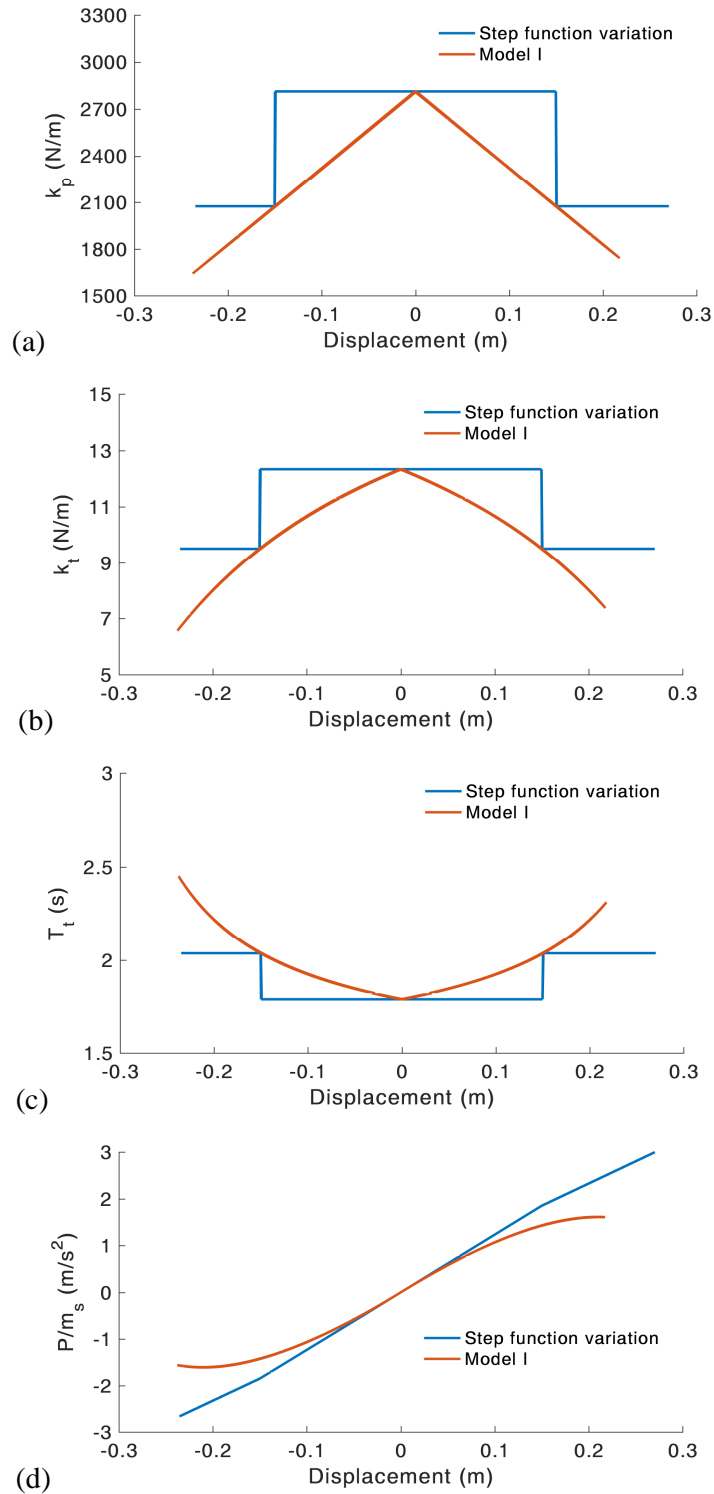


Fig. 4-2: Relationship between (a) positive stiffness, (b) total stiffness of the system, (c) total period of the system and (d) restoring force by mass of the isolated object with relative displacement for Model I, Model with Step function variation of stiffness using two springs excited by Kobe.

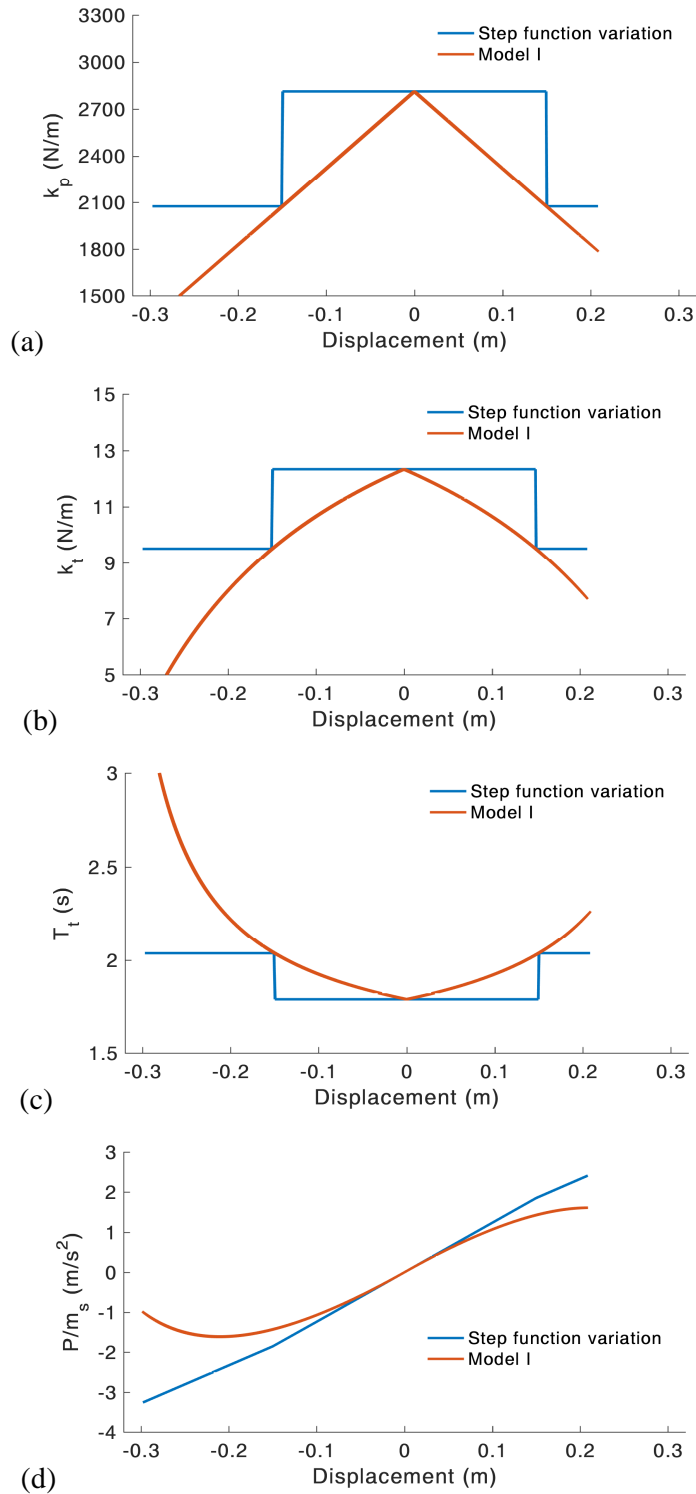


Fig. 4-3: Relationship between **a)** positive stiffness, **(b)** total stiffness of the system, **(c)** total period of the system and **(d)** restoring force by mass of the isolated object with relative displacement for Model I, Model with Step function variation of stiffness using two springs excited by Ojjiya.

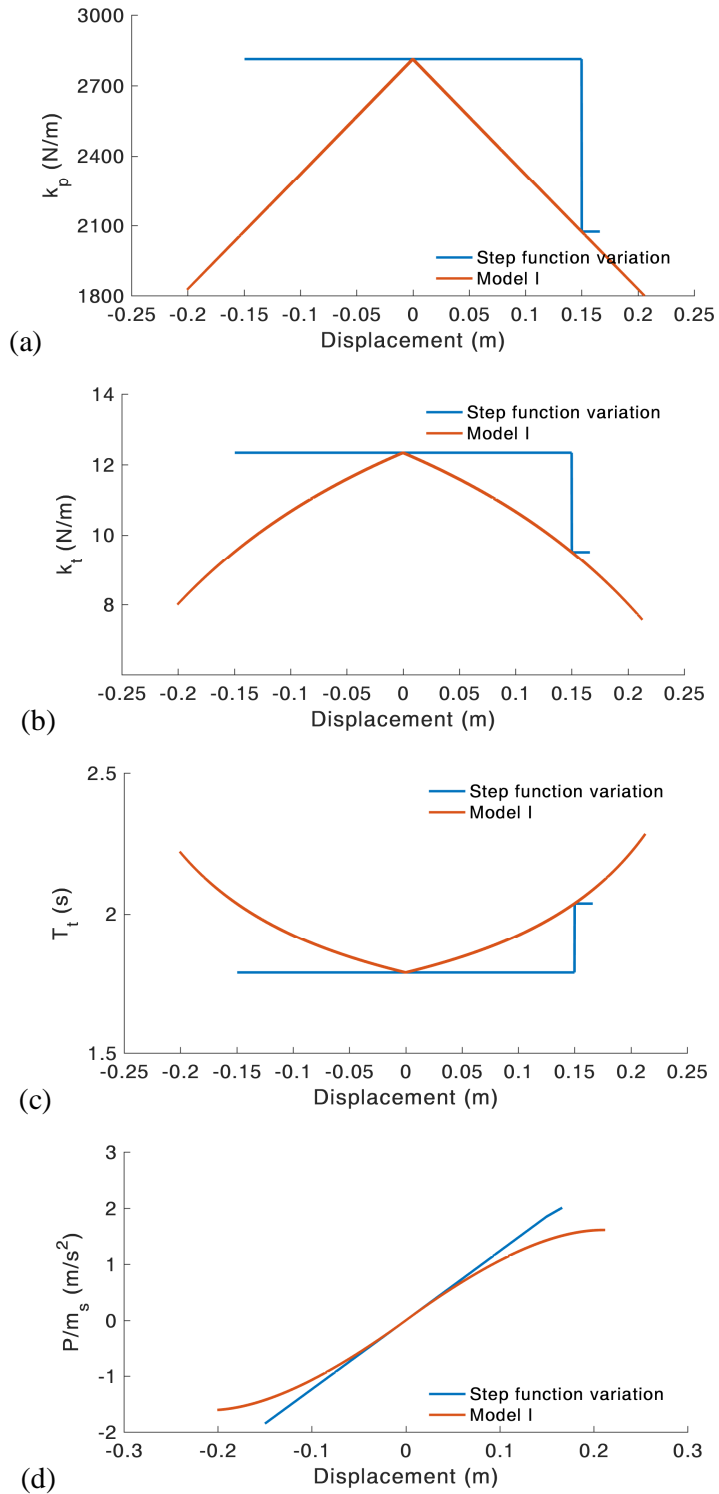


Fig. 4-4: Relationship between **a)** positive stiffness, **(b)** total stiffness of the system, **(c)** total period of the system and **(d)** restoring force by mass of the isolated object with relative displacement for Model I, Model with Step function variation of stiffness using two springs excited by Shin-Tokai

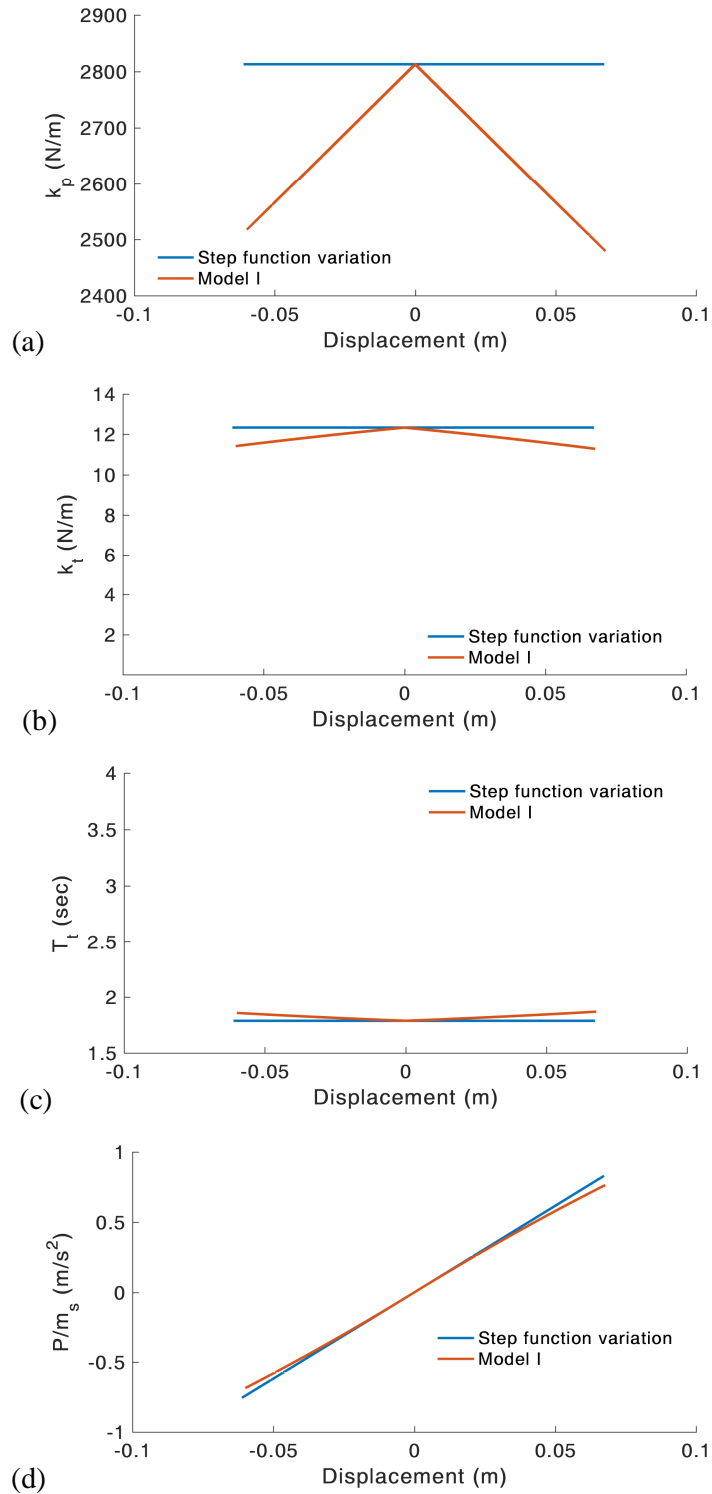


Fig. 4-5: Relationship between (a) positive stiffness, (b) total stiffness of the system, (c) total period of the system and (d) restoring force by mass of the isolated object with relative displacement for Model I, Model with Step function variation of stiffness using two springs excited by Tomakomai

Table 4-2 shows the summary of relative displacement and absolute acceleration of base isolation systems with a smooth K-D curve and discontinuous K-D curve using three springs which are compared against conventional base isolation system. Table shows that both the obtained displacement and acceleration responses are within the allowable limits. **Figs 4-6, 4-7, 4-8 and 4-9** show the relationship between positive stiffness, total stiffness of the system, total period of the system and restoring force by mass of the isolated object with the relative displacement for Model I and Model with Step function variation of stiffness using three springs excited by various earthquakes. Although, these result does not show the good match between Model I (smooth K-D relationship) and Model with step-function variation (multiple lines discontinuous K-D relationship) using three springs, both the displacement and the acceleration responses are still within the allowable limits. Therefore, to achieve the desired responses, in order to realize the variable positive spring, at least three springs in parallel are required.

Table 4-2 Comparison of relative displacement and absolute acceleration of base isolation systems (Model I (smooth line K-D curve) and isolation system with a discontinuous K-D curve) using three springs and conventional base isolation system

| | Relative Displacement (m) | | | |
|---|--|--------------|-------------------|------------------|
| | Kobe | Ojiya | Shin-Tokai | Tomakomai |
| Conv. | 0.326 | 0.420 | 0.675 | 0.438 |
| Model I (Smooth line K-D curve) | 0.238 | 0.299 | 0.213 | 0.068 |
| Step function (discontinuous K-D curve) | 0.260 | 0.288 | 0.187 | 0.067 |
| | Absolute Acceleration (m/s²) | | | |
| | Kobe | Ojiya | Shin-Tokai | Tomakomai |
| Conv. | 0.815 | 1.073 | 1.677 | 1.084 |
| Model I (Smooth line curve) | 2.279 | 2.591 | 1.872 | 0.804 |
| Step function (discontinuous K-D curve) | 2.806 | 2.844 | 2.003 | 0.866 |

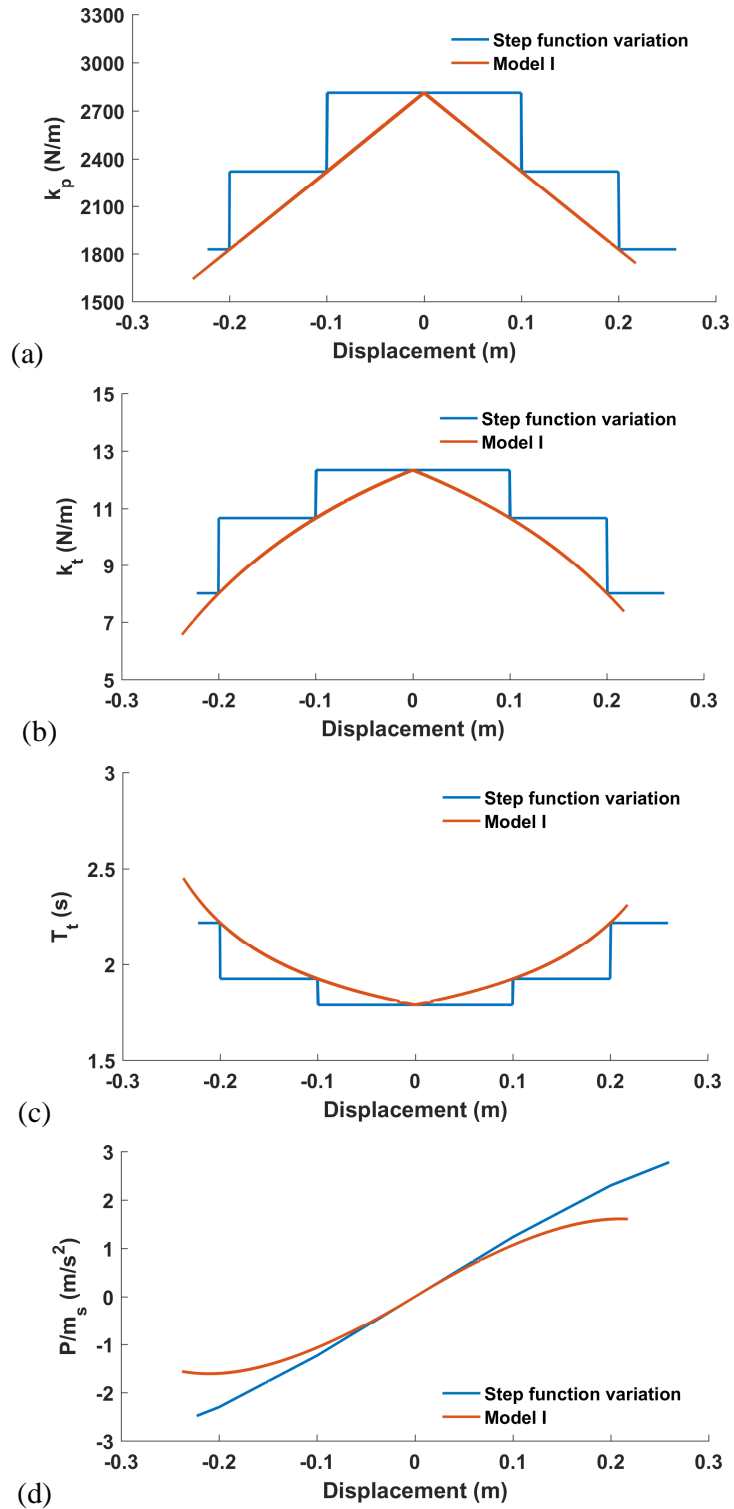


Fig. 4-6: Relationship between (a) positive stiffness, (b) total stiffness of the system, (c) total period of the system and (d) restoring force by mass of the isolated object with relative displacement for Model I, Model with Step function variation of stiffness using three springs excited by Kobe.

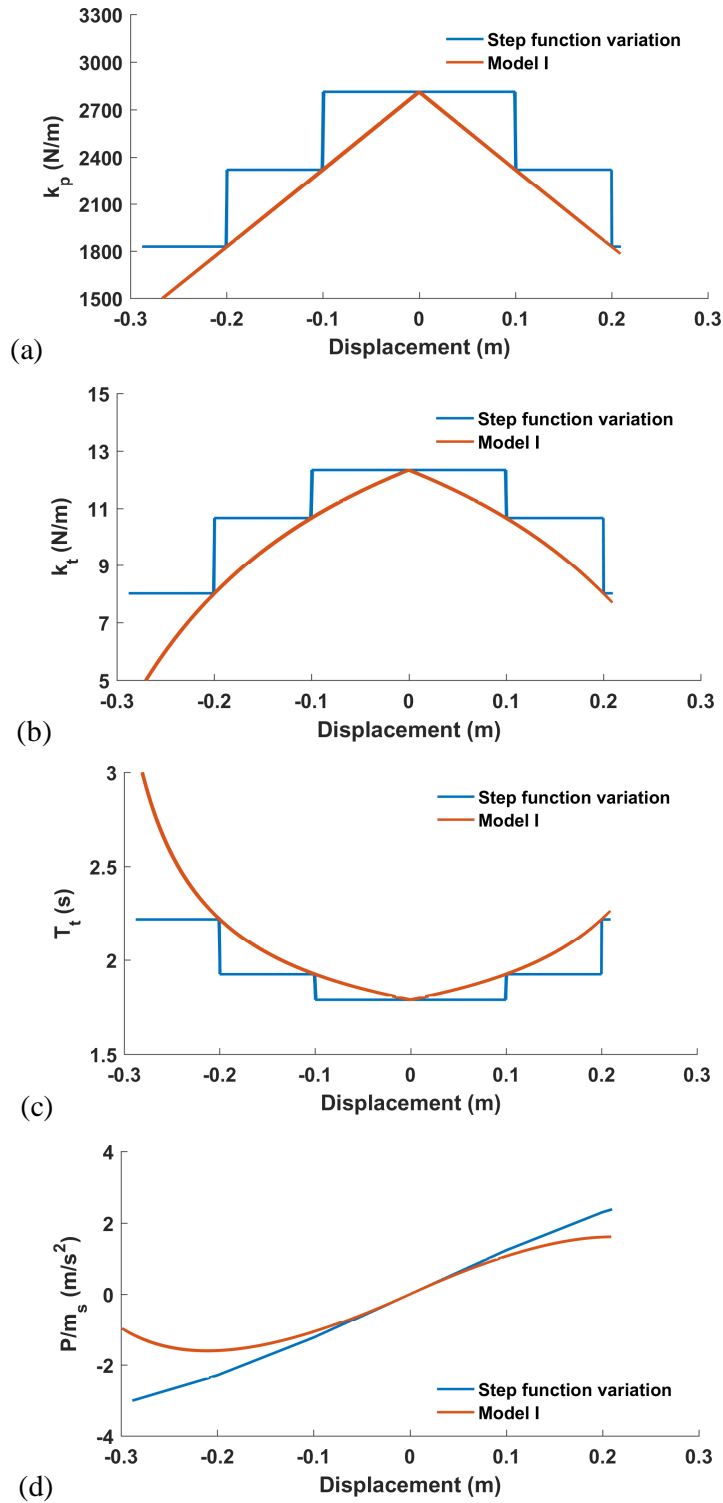


Fig. 4-7: Relationship between (a) positive stiffness, (b) total stiffness of the system, (c) total period of the system and (d) restoring force by mass of the isolated object with relative displacement for Model I, Model with Step function variation of stiffness using three springs excited by Ojiya.

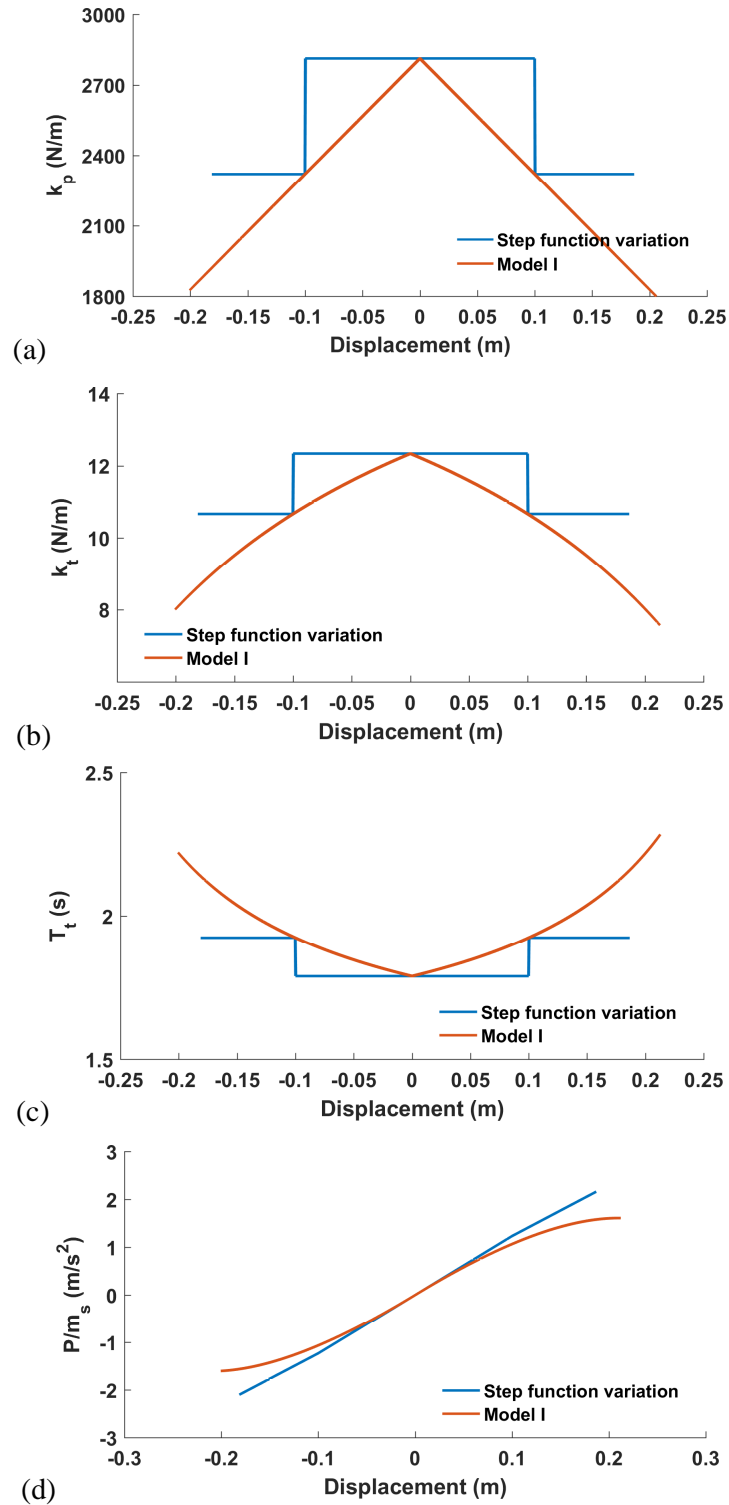


Fig. 4-8: Relationship between (a) positive stiffness, (b) total stiffness of the system, (c) total period of the system and (d) restoring force by mass of the isolated object with relative displacement for Model I, Model with Step function variation of stiffness using three springs excited by Shin-Tokai

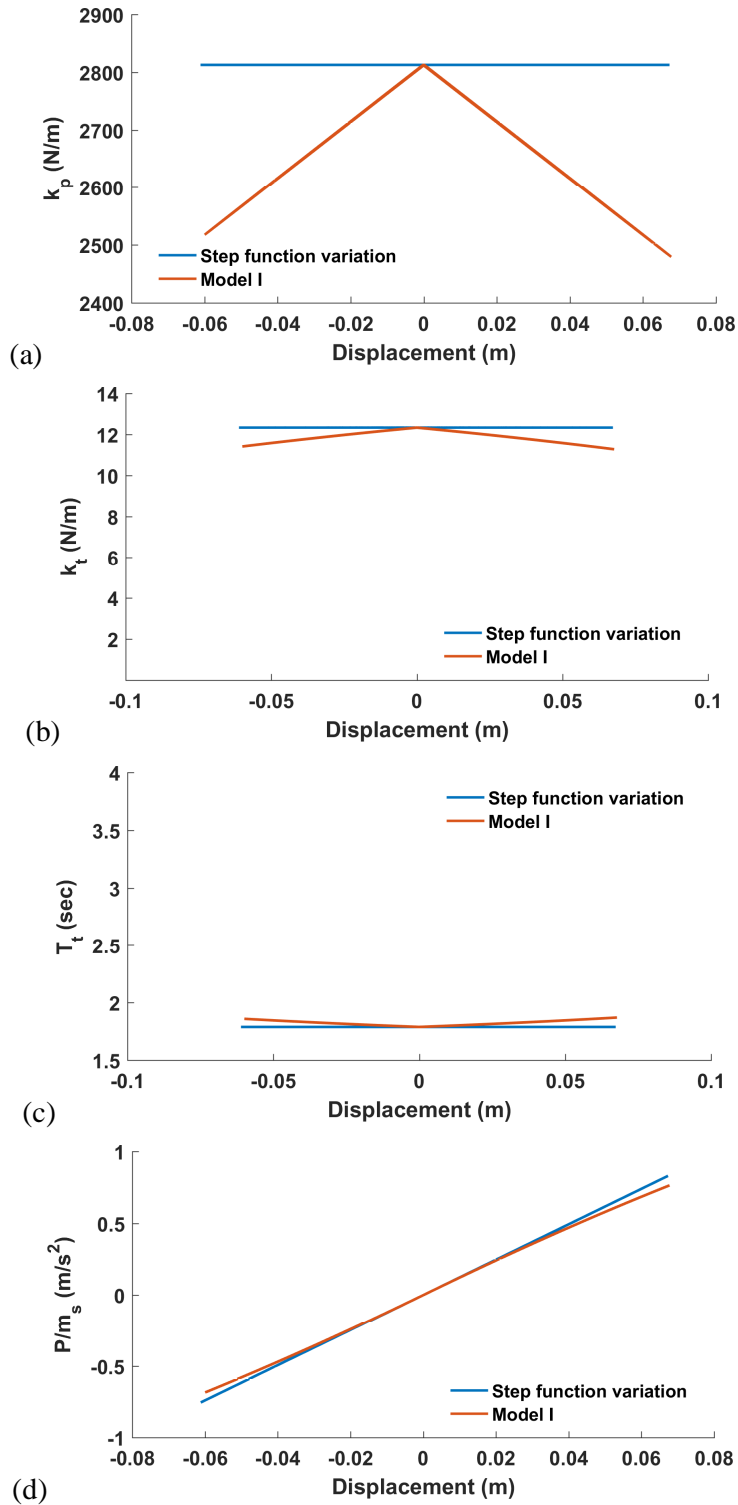


Fig. 4-9: Relationship between (a) positive stiffness, (b) total stiffness of the system, (c) total period of the system and (d) restoring force by mass of the isolated object with relative displacement for Model I, Model with Step function variation of stiffness using three springs excited by Tomakomai

4.1.2 Practical Implementations

One of the possible options for practical realization of variable positive stiffness with step function (discontinuous K-D relationship) for varying stiffness might be using the mechanical system and coil springs either actively or passively. Although passive systems are more resilient over the active systems, passive systems are difficult to realize to control the stiffness of the positive spring of NP unit as a function of the relative displacement of the base isolated object with respect to the ground practically. But the active system might be easy that passive system as the power supply can be used to switch the stiffness of the positive spring with the relative displacement of the base isolated object. For emergency due to power blackout during an earthquake, the generator can be used as a backup source of electricity to control active systems.

CHAPTER 5

CONCLUSIONS AND RECOMMENDATIONS FOR FUTURE RESEARCH

Seismic isolation is one of the effective methods for protecting structures as well as equipments such as critical computer servers, cultural assets, and machinery. Understanding the behavior of base isolation systems under different types of ground motion is important from the viewpoint of earthquake resistance design. Previous studies show that the base isolation systems under near-fault ground motions generate large lateral displacement. Very few studies have been reported for base isolation system under both near-fault and long-period ground motions. But due to the presence of friction device, the system always shows the residual displacement after an earthquake. Development of base isolation system comprising the elastic linear springs, does not have the residual displacement after an earthquake. These issues have been considered as the objective of this study.

Base isolation system with various function (power functions, exponential function and elliptical function) for varying negative stiffness is considered and performance of base isolation system is investigated under both long-period and near-fault ground motions. Negative stiffness itself is negative so varying negative stiffness is quite difficult hence new base isolation system with the negative variable positive mechanical unit for varying total negative stiffness was considered for the practical viewpoint of the system. Time history analysis is performed by Newmark's beta method with $\beta = 1/6$ and Newton Rapson method is implemented for obtaining conversed responses.

5.1 General conclusions

The following are the main conclusions drawn from this thesis.

In **chapter 2**, a new base isolation system employing variable negative stiffness with different power functions in terms of the displacement responses of the isolated objects is proposed. The performance of the proposed system is verified analytically by comparing against the conventional base isolation systems. An optimal order of the power function to satisfy the acceptable limits of both the displacement and the acceleration responses of an isolated object subjected to near-fault and long-period ground motions is proposed. It is concluded that:

- proposed model with high order power of u ($u^{1.5}$), elliptical and exponential functions, the maximum displacement of the isolated object was reduced by 25% under the near-fault ground motion and by 65% under the long-period ground motion while compared to conventional base isolation system.
- the maximum achieved absolute acceleration of the base-isolated object with the proposed system is less than 3.0 m/s^2 and the relative displacement is less than 0.3 m for both types of the earthquake ground motions.

In **chapter 3**, a negative-variable positive mechanical unit to vary the total negative stiffness is proposed and its performance is verified. Practical range of different parameters such as damping ratio and slope of the linear function is optimized to satisfy the allowable limits of both the displacement and acceleration responses. The main conclusions of this chapter are:

- Model II reduces the displacement response of the isolated object for long-period ground motion but for near-fault it increases and the acceleration response increases for both types of earthquake excitations.

- Model III reduces displacement response markedly for both near-fault and long-period ground motions. On the other hand, acceleration response increases remarkably for near-fault as compared to conventional base isolation.
- the proposed model (Model I) exhibits a significant decrease in the relative displacement of the object with respect to the base for both types earthquake excitations. The maximum displacement of the isolated object decreases by almost 30% and more than 70% when subjected to near-fault and long-period ground motions respectively in comparison with conventional base isolation system.
- the achieved maximum absolute acceleration of the base-isolated object with Model I is almost 2.5 m/s^2 , and the maximum relative displacement is less than 0.3 m for both types of earthquake ground motions.
- all the springs comprising the system are elastic linear, so it does not have any residual displacement.

The performance of the proposed model (Model I) is compared against isolation system with variable negative stiffness and with existing previous work. It is found that the proposed model (Model I) is effective in mitigating displacement with the allowable range of acceleration and moreover, all the springs comprising the unit are elastic linear, so it does not have any residual displacement.

In **chapter 4**, the discussion on the approximation of negative-positive variable stiffness in practice is presented. The influence of approximation of the systems using discontinuous stiffness-displacement relationship has been discussed and numerical analysis of the system with a discontinuous stiffness-displacement has been conducted to verify the performance of the base isolation system.

5.2 Recommendations for future research

Recommendations for future research include: (i) development of the prototype model of the proposed device with NP unit for the realization of the system, (ii) verification of the model by shaking table test or the computer simulation.

REFERENCES

- [1] J. M. Kelly, Aseismic base isolation: review and bibliography, *Soil Dyn. Earthq. Eng.*, 5 (4) (1986) 202–216.
- [2] I. G. Buckle and R. L. Mayes, Seismic isolation: history, application, and performance—a world view, *Earthq. spectra*, 6 (2) (1990) 161–201.
- [3] M. Constantinou, A. Mokha, and A. Reinhorn, Teflon Bearings in Base Isolation II: Modeling, *J. Struct. Eng.*, 116 (2) (1990) 455–474.
- [4] S. Nagarajaiah, A. M. Reinhorn, and M. C. Constantinou, Torsional coupling in sliding base-isolated structures, *J. Struct. Eng. (United States)*, 119 (1) (1993) 130–149.
- [5] J. N. Yang, J. C. Wu, A. M. Reinhorn, and M. Riley, Control of sliding-isolated buildings using sliding-mode control, *J. Struct. Eng.*, 122 (2) (1996) 179–186.
- [6] D. H. Turkington, A. J. Carr, N. Cooke, and P. J. Moss, Seismic design of bridges on lead-rubber bearings, *J. Struct. Eng.*, 115 (12) (1989) 3000–3016.
- [7] W. Robinson, Lead-rubber hysteretic bearings suitable for protecting structures during earthquakes, *Seism. Isol. Prot. Syst.*, 2 (1) (2011) 5–19.
- [8] R. S. Jangid and J. M. Kelly, Base isolation for near-fault motions, *Earthq. Eng. Struct. Dyn.*, 30 (5) (2001) 691–707.
- [9] M. Dicleli, Supplemental elastic stiffness to reduce isolator displacements for seismic-isolated bridges in near-fault zones, *Eng. Struct.*, 29 (5) (2007) 763–775.
- [10] R. S. Jangid, Optimum friction pendulum system for near-fault motions, *Eng. Struct.*, 27 (3) (2005) 349–359.
- [11] R. S. Jangid, Optimum lead-rubber isolation bearings for near-fault motions, *Eng. Struct.*, 29 (10) (2007) 2503–2513.
- [12] C. P. Providakis, Effect of LRB isolators and supplemental viscous dampers on seismic isolated buildings under near-fault excitations, *Eng. Struct.*, 30 (5) (2008)

1187–1198.

- [13] C. P.-S. D. and E. Engineering and undefined 2009, Effect of supplemental damping on LRB and FPS seismic isolators under near-fault ground motions, *Elsevier*,.
- [14] C. S. Tsai, T.-C. Chiang, and B.-J. Chen, Finite element formulations and theoretical study for variable curvature friction pendulum system, *Eng. Struct.*, 25 (14) (2003) 1719–1730.
- [15] L. Lu, M. Shih, and C. Wu, Near-Fault Seismic Isolation Using Sliding Bearings With Variable Curvatures, *Construction*, (3264) (2004).
- [16] T. Ariga, Y. Kanno, and I. Takewaki, Resonant behaviour of base-isolated high-rise buildings under long-period ground motions, *Struct. Des. Tall Spec. Build.*, 15 (3) (2006) 325–338.
- [17] T. Saito, Response of High-Rise Buildings under Long Period Earthquake Ground Motions, *Int. J. Struct. Civ. Eng. Res.*, 5 (4) (2016) 308–314.
- [18] K. Koketsu, K. Hatayama, T. Furumura, Y. Ikegami, and S. Akiyama, Damaging Long-period Ground Motions from the 2003 Mw 8.3 Tokachi-oki, Japan Earthquake, *Seismol. Res. Lett.*, 76 (1) (2009) 67–73.
- [19] S. Zama, H. Nishi, M. Yamada, and K. Hatayama, Damage of Oil Storage Tanks Caused by Liquid Sloshing in the 2003 Tokachi Oki Earthquake and Revision of Design Spectra in the Long-Period Range, *Proc. Fourteenth World Conf. Earthq. Eng.*, (2008).
- [20] T. Kobori, M. Takahashi, T. Nasu, N. Niwa, and K. Ogasawara, Seismic response controlled structure with Active Variable Stiffness system, *Earthq. Eng. Struct. Dyn.*, 22 (11) (1993) 925–941.
- [21] S. Narasimhan and S. Nagarajaiah, A STFT semiactive controller for base isolated buildings with variable stiffness isolation systems, *Eng. Struct.*, 27 (4) (2005) 514–523.
- [22] S. Nagarajaiah and S. Sahasrabudhe, Seismic response control of smart sliding

- isolated buildings using variable stiffness systems: An experimental and numerical study, *Earthq. Eng. Struct. Dyn.*, 35 (2) (2006) 177–197.
- [23] L. Y. Lu, G. L. Lin, and T. C. Kuo, Stiffness controllable isolation system for near-fault seismic isolation, *Eng. Struct.*, 30 (3) (2008) 747–765.
- [24] Y. Liu, H. Matsuhisa, and H. Utsuno, Semi-active vibration isolation system with variable stiffness and damping control, *J. Sound Vib.*, 313 (1–2) (2008) 16–28.
- [25] T. K. Lin, L. Y. Lu, and H. Chang, Fuzzy logic control of a stiffness-adaptable seismic isolation system, *Struct. Control Heal. Monit.*, 22 (1) (2015) 177–195.
- [26] D. M. Fenz and M. C. Constantinou, Spherical sliding isolation bearings with adaptive behavior: Theory, *Earthq. Eng. Struct. Dyn.*, 37 (2) (2008) 163–183.
- [27] S. Nagarajaiah, Adaptive passive, semiactive, smart tuned mass dampers: Identification and control using empirical mode decomposition, hilbert transform, and short-term fourier transform, *Struct. Control Heal. Monit.*, 16 (7–8) (2009) 800–841.
- [28] H. Iemura, A. Igarashi, M. H. Pradono, and A. Kalantari, Negative stiffness friction damping for seismically isolated structures, *Struct. Control Heal. Monit.*, 13 (2–3) (2006) 775–791.
- [29] H. Iemura and M. H. Pradono, Advances in the development of pseudo-negative-stiffness dampers for seismic response control, *Struct. Control Heal. Monit.*, 16 (7–8) (2009) 784–799.
- [30] A. A. Sarlis, D. T. R. Pasala, M. C. Constantinou, A. M. Reinhorn, S. Nagarajaiah, and D. P. Taylor, Negative stiffness device for seismic protection of structures, *J. Struct. Eng.*, 139 (7) (2012) 1124–1133.
- [31] T. Sun, Z. Lai, S. Nagarajaiah, and H. N. Li, Negative stiffness device for seismic protection of smart base isolated benchmark building, *Struct. Control Heal. Monit.*, 24 (11) (2017).
- [32] D. T. R. Pasala, A. A. Sarlis, S. Nagarajaiah, A. M. Reinhorn, M. C. Constantinou, and D. Taylor, Adaptive Negative Stiffness: New Structural Modification Approach

- for Seismic Protection, *J. Struct. Eng.*, 139 (7) (2012) 1112–1123.
- [33] I. Takewaki, Earthquake Input Energy to Two Buildings Connected by Viscous Dampers, *J. Struct. Eng.*, 133 (5) (2007) 620–628.
- [34] I. Takewaki, S. Murakami, K. Fujita, S. Yoshitomi, and M. Tsuji, The 2011 off the Pacific coast of Tohoku earthquake and response of high-rise buildings under long-period ground motions, *Soil Dyn. Earthq. Eng.*, 31 (11) (2011) 1511–1528.
- [35] Z. Xu, A. Agrawal, W. He, and P. Tan, Performance of passive energy dissipation systems during near-field ground motion type pulses, *Eng. Struct.*, 29 (2) (2007) 224–236.
- [36] P. Xiang and A. Nishitani, Optimum design for more effective tuned mass damper system and its application to base-isolated buildings, *Struct. Control Heal. Monit.*, 21 (1) (2014) 98–114.
- [37] K. Kamae, H. Kawabe, and K. Irikura, Strong ground motion prediction for huge subduction earthquakes using a characterized source model and several simulation techniques, *Proc. Thirteen. World Conf. Earthq. Eng.*, (2004).
- [38] F. Fadi and M. C. Constantinou, Evaluation of simplified methods of analysis for structures with triple friction pendulum isolators, *Earthq. Eng. Struct. Dyn.*, 39 (1) (2010) 5–22.
- [39] A. A. Sarlis and M. C. Constantinou, A model of triple friction pendulum bearing for general geometric and frictional parameters, *Earthq. Eng. Struct. Dyn.*, 45 (11) (2016) 1837–1853.
- [40] M. Saitoh, An external rotary friction device for displacement mitigation in base isolation systems, *Struct. Control Heal. Monit.*, 21 (2) (2014) 173–188.
- [41] R. S. Lakes, Extreme damping in composite materials with a negative stiffness phase, *Phys. Rev. Lett.*, 86 (13) (2001) 2897.
- [42] R. S. Lakes, Extreme damping in compliant composites with a negative-stiffness phase, *Philos. Mag. Lett.*, 81 (2) (2001) 95–100.
- [43] Y. C. Wang and R. Lakes, Stability of negative stiffness viscoelastic systems, *Q.*

Appl. Math., 63 (1) (2005) 34–55.

- [44] Y. C. Wang and R. Lakes, Negative stiffness-induced extreme viscoelastic mechanical properties: Stability and dynamics, *Philos. Mag.*, 84 (35) (2004) 3785–3801.
- [45] W. G. Molyneux, *Supports for vibration isolation*. HM Stationery Office, (1957).
- [46] T. Mizuno, Vibration isolation system using zero-power magnetic suspension, 955 (2002).
- [47] H. Iemura and M. H. Pradono, Application of pseudo-negative stiffness control to the benchmark cable-stayed bridge, *J. Struct. Control*, 10 (3–4) (2003) 187–203.
- [48] N. Nakagawa, T. Okuno, and Y. Sekiguchi, A study on improvement of constant repulsive force characteristic, *Trans. JSME Ser. C (in Japanese)*, 74 (739) (2008) 536–541.
- [49] T. Nakata *et al.*, Strong motion prediction for retrofit of buildings in the Sannomaru district of Nagoya City: part 1: project summary, *Summ. Tech. Pap. Annu. Meet. Archit. Inst. Japan B-2, Struct. II, Struct. Dyn. Nucl. power plants (in Japanese)*, *AIJ*, (2004).
- [50] N. Makris, Rigidity - plasticity - viscosity: Can electrorheological dampers protect base-isolated structures from near-source ground motions?, *Earthq. Eng. Struct. Dyn.*, 26 (5) (1997) 571–591.
- [51] N. Makris and S. P. Chang, Response of damped oscillators to cycloidal pulses, *J. Eng. Mech.*, 126 (February) (2000) 123.
- [52] N. Makris and S. P. Chang, Effect of viscous, viscoplastic and friction damping on the response of seismic isolated structures, *Earthq. Eng. Struct. Dyn.*, 29 (1) (2000) 85–107.
- [53] V. R. Panchal and R. S. Jangid, Variable friction pendulum system for seismic isolation of liquid storage tanks, *Nucl. Eng. Des.*, 238 (6) (2008) 1304–1315.